The Pennsylvania State University

The Graduate School

Department of Pharmacology

# NOVEL APPROACHES TO MODULATE ORNITHINE DECARBOXYLASE ACTIVITY AND TO DETERMINE A ROLE FOR ORNITHINE DECARBOXYLASE IN CELL TRANSFORMATION

A Thesis in

Pharmacology

by

Joseph M. Ackermann



Submitted in Partial Fulfillment
of the Requirements
for the Degree of

Doctor of Philosophy

May 2005

The thesis of Joseph M. Ackermann was reviewed and approved* by the following:

Anthony E. Pegg
Evan Pugh Professor of Cellular and Molecular Physiology and Pharmacology
J. Lloyd Huck Professor of Cell and Molecular Biology
Thesis Advisor
Chair of Committee

Melvin L. Billingsley
Professor of Pharmacology

Mark Kester
Professor of Pharmacology

Lisa M. Shantz
Associate Professor of Cellular and Molecular Physiology

Charles D. Smith
Professor of Pharmacology

Kent E. Vrana
Elliot S. Vesell Professor of Pharmacology
Head of the Department of Pharmacology

*Signatures are on file in the Graduate School

## ABSTRACT

Ornithine decarboxylase (ODC) is known to have an important role in cell transformation, but that role is not well understood. The scientific and clinical value of reducing the activity of ODC, a key enzyme in the biosynthesis of polyamines, is well appreciated. Polyamines are necessary components for cell growth and manipulation of polyamine homeostasis may be an effective strategy for the treatment of a number of disorders, including neoplastic diseases. Indeed, α-difluoromethylornithine (DFMO), a specific enzyme-activated irreversible inhibitor of ODC is currently in clinical trials as a potential chemopreventative/therapeutic agent and is clinically used for other disorders. However, the effectiveness of DFMO is limited by the pharmacokinetic profile of the drug and the unique regulation of ODC.

Targeting ODC mRNA may be an effective method to reduce ODC activity due to the extensive regulation of the enzyme at the translational and protein levels. The half-life of ODC is among the shortest of any known protein. Due to the rapid turnover of ODC protein, cells are reliant on translation of new protein to maintain or elevate ODC activity. A number of reports have indicated that little to no change in ODC mRNA content is often detected upon substantial increases or decreases in ODC protein content and activity. Reversible inhibitors of ODC protein have a disadvantage because they can stabilize ODC from degradation. The initial inhibition of ODC leads to increased ODC transcription and active ODC can accumulate in the cells. Conversely, the efficacy of irreversible inhibitors may be limited by the short half-life of ODC. Therefore targeting ODC mRNA, rather than protein, may be a better strategy.

An approach to develop an effective 10-23 DNAzyme and hammerhead ribozyme against ODC is described in these studies. DNAzymes and ribozymes bind to a cognate RNA substrate via Watson-Crick base pairing hybridization arms and subsequently catalyze cleavage of a phosphodiester bond of the RNA. The major difference between the two is the base composition; DNAzymes are composed of DNA, ribozymes of RNA. DNAzymes capable of cleaving the target ODC RNA were identified *in vitro* and further characterized by the effect each had on ODC protein and activity levels using *in vitro* translated ODC RNA. ODC protein levels and activity correlated well with the RNA cleavage activity of the DNAzyme. A DNAzymes that exhibited good activity was optimized for use in cell culture studies. The length of the DNAzyme hybridization arms was altered and kinetics were performed to identify the most catalytically efficient configuration. One DNAzyme, DZ IV, with equal length arms of nine nucleotides proved to be the most catalytically efficient. In HEK 293 cells, DZ IV was able to reduce the amount of translated ODC protein resulting in ~80% reduction in ODC activity—a statistically significant enhancement over the antisense effect of a catalytically inactive DNAzyme.

The effectiveness of DZ IV was evaluated in an *in vivo* model with clinical significance. DFMO is currently undergoing clinical trials for chemoprevention in skin cancer and topical application of DFMO is FDA-approved for the treatment of unwanted facial hair. ODC activity is induced in the skin in response to tumor promoters, including 12-*O*-tetradecanoylphorbol-13-acetate (TPA). Topical DZ IV reduced TPA-induced ODC activity by ~50 % over vehicle control in the dermis of mice. The result is more

impressive considering that TPA treatment induces ODC activity ~1000-fold over basal levels.

Hammerhead ribozymes targeted against ODC were designed to sites identified by a ribozyme site selection screen. Two of the identified sites cleaved ODC mRNA within 5 nucleotides from the DZ IV cleavage site indicating that this is an accessible site within the mRNA. Four of the ribozymes that most effectively cleaved *in vitro* transcribed RNA were cloned into a novel expression vector. The ribozymes were evaluated in cell culture, however an accurate assessment could not be made due to non-specific silencing from the expression vector. The ribozymes may be active but must be evaluated with a different expression system.

ODC is known to have an important role in cell transformation, but that role is not well understood. A better understanding of the role of ODC in transformation may identify effectors downstream of ODC that are better drug targets. NIH/3T3 cells transfected with an activated Ras mutant [3T3+HRas(61L) cells] display a transformed phenotype, but the transformed phenotype can be reversed by co-expression of a dominant-negative ODC [3T3+HRas(61L)+ODC-dn cells]. Microarray analysis was performed on the 3T3, 3T3+HRas (61L) and 3T3+HRas(61L)+ODC-dn cells and genes potentially downstream of ODC that are essential for Ras transformation in 3T3 cells were identified.

In conclusion, these results indicate that targeting ODC at the mRNA level is an effective way to modulate ODC activity. An effective DNAzyme has been demonstrated to be active *in vitro* and *in vivo* and can be used as a tool to study the function and translational regulation of ODC and the potential of DNAzymes for therapeutic uses.

Identification of effectors downstream of ODC that cooperate in transformation may provide better chemopreventative/therapeutic drug targets than ODC.

# TABLE OF CONTENTS

# LIST OF FIGURES

# LIST OF TABLES

## ACKNOWLEDGEMENTS

I thank Drs. Wei-Hua Pan and Gary Clawson (Penn State College of Medicine) for their collaboration on the ribozyme project (Chapter 5). Dr. Pan performed the site SELEX screen and confirmed the ribozyme activity *in vitro*.

I am very grateful to many people for their help during my time at Penn State. I would like to thank all the members of the Pegg lab. They have always offered help at any time. I especially extend my thanks to Dave Feith, Lisa Shantz and Sreenivas Kanugula. It is not possible for them to know how much I appreciate all that they have done. I am grateful to my committee members for their valuable insight and different scientific perspectives. I am most grateful to Dr. Pegg, a wonderful mentor. He provided me with freedom to direct my projects tempered with guidance to keep me on track. I will always fondly remember my time in his lab as an instrumental part of my career.

# Chapter 1

# Introduction

## Overview of the Polyamine Pathway

The first reported observation of polyamines dates back to the late 17$^{th}$ century and since this time research has produced a vast base of literature leading to numerous important advances to understanding polyamine biosynthesis, regulation and the roles of polyamines in physiological processes. Despite these significant advances, much work still lies ahead to more fully understand the polyamine field. Polyamine biosynthesis and catabolism is marked by complex interactions of enzymes that work in concert to maintain polyamine homeostasis within the cell. Polyamine transporters, compensatory changes in enzyme levels and multiple modes of regulating enzymes involved in polyamine biosynthesis confound the complexity.

The general term "polyamines" specifically refers to three aliphatic organic cations: the diamine putrescine, tri-amine spermidine and tetra-amine spermine. The common names recall the origin of their discoveries in putrefied meat and seminal fluid (*1*). Conversion of arginine to ornithine by the action of arginase is often considered to be the initial step in polyamine biosynthesis (Figure 1.1). Arginine is also a precursor to other important molecules including nitric oxide (NO), citrulline, agmatine (plants and

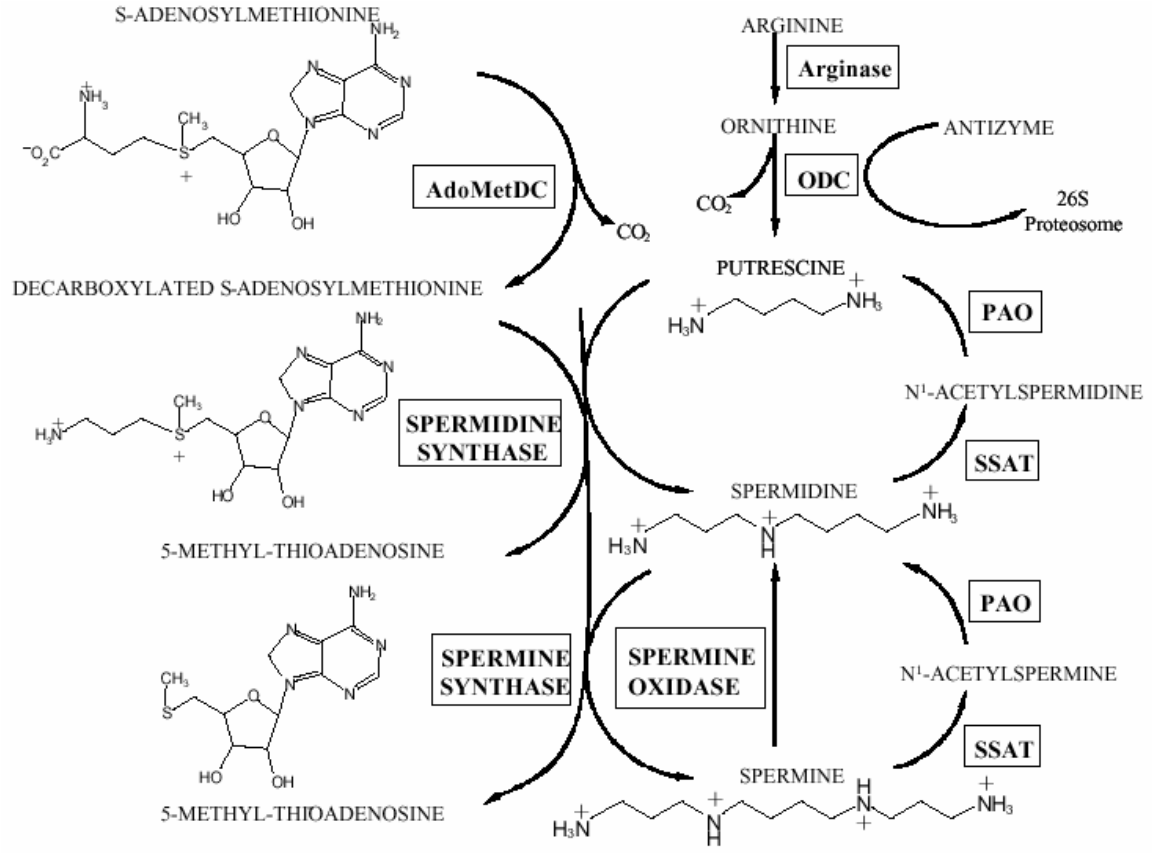


**Figure 1.1**: *Polyamine Biosynthetic and Catabolism Pathway*

See text for details.

prokaryotes) and urea, as well as an essential amino acid. Therefore, through this common precursor, polyamine biosynthesis is linked to a number of other pathways. Ornithine, the precursor to putrescine, is formed by the action of arginase on arginine. Ornithine decarboxylase (ODC) removes the carboxyl group from L-ornithine to form putrescine—often a rate-limiting step in the biosynthesis of polyamines.

The synthesis of the higher polyamines is dependent upon availability of decarboxylated *S*-adenosylmethionine (dcAdoMet). *S*-adenosylmethionine decarboxylase (AdoMetDC) decarboxylates *S*-adenosylmethionine (AdoMet) to form dcAdoMet, and this reaction can replace ODC as the rate-limiting step in the biosynthesis of the higher polyamines depending on the physiological situation. AdoMet is the major methyl-donor source for methylation reactions in living organisms and subsequently the second most widely used enzyme substrate behind ATP (*2*). Once decarboxylated by AdoMetDC, AdoMet is committed for use in polyamine biosynthesis (although it can undergo a reverse acetylation reaction) (*3*). Spermidine synthase transfers the aminopropyl group from dcAdoMet to putrescine to form spermidine. Spermine synthase converts spermidine into spermine through a similar transfer of the aminopropyl group from dcAdoMet to spermidine. 5'-methyl thioadenosine (MTA), the byproduct of the spermidine and spermine synthase reactions, is metabolized by MTA-phosphorylase to 5-methylthioribose-1-phosphate and adenine—an important step in the methionine and purine salvage pathways, respectively (*4*). While both ODC and AdoMetDC are inducible, the two synthase enzymes are stably expressed and appear to be regulated by the availability of their substrate (*5*).

Polyamines and the enzymes involved in polyamine biosynthesis are controlled by numerous regulatory mechanisms. One important means of regulating polyamines is through catabolism. Spermine can be converted back to spermidine and spermidine to putrescine through the sequential action of spermidine-spermine $N^1$-acetyltransferase (SSAT) and acetylated polyamine oxidase (PAO), a FAD-dependent enzyme. SSAT is a highly inducible enzyme and the rate-limiting enzyme for polyamine catabolism (*6*). SSAT acetylates spermine and spermidine to $N^1$-acetylspermine (AcSpm) and $N^1$-acetylspermidine (AcSpd) respectively, the preferred substrates for PAO. PAO cleaves acetylated spermine and spermidine to spermidine and putrescine respectively, reactions that occur much slower with the unacetylated polyamines (*7*). Acetylation of the polyamines removes the charge of the terminal aminopropyl group, thereby greatly enhancing the reactivity of these substrates with PAO (*8*). The activity of PAO is constitutive and stable, therefore its activity is dependent upon the availability of AcSpm and AcSpd. The reaction of PAO with the acetylated polyamines produces two by-products, $H_2O_2$ and 3-acetamido propanol, which both have been demonstrated to be toxic to cells (*6*). $H_2O_2$ also induces SSAT activity completing a positive feedback loop that can lead to concentrations of $H_2O_2$ that result in oxidative stress and cell death (*9*).

It was believed that the biosynthetic reactions were essentially irreversible and that the retroconversion pathway was the only means to convert spermine to spermidine and spermidine to putrescine. However, another layer of complexity was added to the polyamine field with the recent cloning of an enzyme that directly converts spermine to spermidine (*10, 11*). This enzyme, referred to as spermine oxidase (SMO) or polyamine oxidase human 1 (PAOh1), preferentially metabolizes spermine over $N^1$-acetylspermine

and does not react with $N^1$,$N^{12}$-diacetylspermine (the preferred PAO substrate), spermidine or $N^1$-acetylspermidine (*11*). The significance of having two different catabolic pathways is not yet understood, nor has an oxidase that directly converts spermidine to putrescine been identified. The activity of SMO on spermine also produces the reactive oxygen species $H_2O_2$ (*10*, *11*), thereby dispelling the hypothesis that back conversion of spermine through SMO is a nontoxic alternative to the actions of SSAT/PAO. AcSpm and AcSpd are the major forms of polyamines excreted from the cell (*12*), so one could speculate that this provides another means to regulate polyamine levels.

Polyamine biosynthesis is uniquely regulated by a protein termed antizyme. Antizyme alters polyamine pools by at least three ways. Antizyme can also bind to an ODC monomer thereby inactivating ODC which is an obligate homodimer. Antizyme heterodimerization with ODC increases the efficiency in which ODC is degraded by the 26 S proteasome (*13*). Antizyme inhibits the cellular uptake of polyamines through its interaction with ill-characterized polyamine transporters (*14, 15*). Reportedly, antizyme also stimulates polyamine excretion (*16*).

All known living organisms require polyamines, with the exception of two orders of Archaea, *Methanobacteriales* and *Halobacteriales* , whose growth appears to be independent of measurable polyamine levels (although *Halobacteriales* produce agmatine which can be a precursor to polyamine synthesis in plants and some prokaryotes) (*7*). Many organisms are able to synthesize polyamines endogenously, but also utilize polyamines synthesized by intestinal flora or obtained from the diet through the uptake of polyamine transporters. However, some organisms that lack the ability to synthesize

polyamines and subsist on exogenous polyamines alone have been identified, such as *Trypanosoma cruzi* (*7*). It is widely accepted that polyamines are essential for cell growth in humans and other mammals, but the reason for this is less well-understood.

At the most basic level, the function of polyamines is often attributed to the positive charge of the molecules. The N atoms of the polyamines are positively charged at physiological pH. Unlike organic cations, the charges are spaced out across the polyamine backbone at fixed distances. This difference may cause polyamines to have very different effects compared to other positively charged molecules. Polyamines have been found to interact with a number of polyanionic macromolecules within the cell including DNA and RNA (reviewed in (*17*)). Spermidine and spermine can bridge the minor and major grooves of DNA thus linking molecules of DNA or different regions of the same DNA and, in fact, have been shown to drive DNA in the B conformation into to Z conformation. The higher polyamines promote the translation of full-length antizyme through a +1 frameshift mechanism which may be induced by polyamine interaction with the mRNA (*18*). Polyamine depletion leads to partial unwinding of DNA in the nucleosome exposing previously buried sequences. It has been proposed that these newly exposed sequences may be binding sites for transcription regulatory factors and this may represent a mechanism by which polyamines regulate transcription of growth related genes, such as c-*myc* (*17*). Polyamines have been reported to interact with membrane-bound proteins (e.g. adenylate cyclase) and acidic phospholipids, as well as regulate ion channels, including KIR (inwardly rectifying $K^+$), NMDA (*N*-methyl-D-aspartate) and voltage-activated $Ca^{2+}$ channels (*17*). However, it is not known whether these

interactions mediate the primary functions of polyamines or are merely by-products of their charge.

It is quite difficult to determine physiological roles of polyamines by directly studying the polyamines themselves. Not the least problem being that the free intracellular polyamine content in living cells is unknown and is very difficult to determine because a large portion of the polyamines are likely to be bound to cellular components. The most useful studies to shed light on the role of polyamines have examined the enzymes involved in polyamine regulation.

The studies in this thesis focus on ODC, thus the discussion on the polyamine pathway will be narrowed to ODC from herein. However, it is important to appreciate that ODC does not function in an isolated environment, but works in concert with other factors to maintain polyamine homeostasis through unique and dynamic mechanisms.

**ODC Structure**

ODC is a pyridoxal-5'-phosphate (vitamin $B_6$) dependent obligate homodimer. Pyridoxal-5'-phosphate (PLP) is a common cofactor in enzymes that metabolize amino acids into amines (*19*). PLP binds to lysine-69 within the active site of ODC via a Schiff-base. Ornithine reacts with the bound PLP through a transaldimination reaction to form an external aldimine. At this point any of the three free bonds around the Cα atom may be cleaved to enable one of several reactions including, decarboxylation, transamination, deamination, racemization, retro-also cleavage and replacement reactions. Subsites within ODC are believed to interact with the groups surrounding the Cα atom so that the

α carboxylate is perpendicular to the pyridine ring, thereby specifying decarboxylation of ornithine to putrescine.

The ODC homodimer is necessary for ODC activity because each monomer contributes residues essential for the two active sites formed in one dimer. Each 51 kD ODC monomer is composed of two domains, a barrel and a sheet domain, which are linked by two neighboring loops. The monomers bind in a head-to-tail (N to C terminus) orientation so that the barrel domain of one monomer interacts with the sheet domain of the other. The monomers have been shown to rapidly exchange—homodimerization is reversible (*20*). This has important consequences for ODC activity because heterodimerization with antizyme can regulate ODC activity. In the crystal structure of mouse ODC, only 655 $Å^2$ of the solvent-accessible surface area per monomer is buried upon dimer formation compared to 6450 $Å^2$ for the very stable ODC homodimer from the bacteria *Lactobacillus 30a* (*19*). Any mutation to G387, which is located between the barrel and sheet domains, prevents dimerization (*21*). The dimer is stabilized by two salt bridges (K169-D364' and D134-K294', where the symbol prime represent residues of the other monomer) and a stack of aromatic amino acids (F397Y'/Y323'/Y331 and Y331'/Y323/F397).

Two shallow active sites per homodimer are formed near the subunit interface. Each active site is formed from residues donated by the loops near the C-terminal end of the α/β domain, one loop from the sheet domain and two additional loops (357'-364', 398'-403') from the sheet domain of the second monomer. One of the salt bridges stabilizes the dimer (K169-D364') is important in fixing the loop (containing residues C360', D361' and D364) from the sheet domain of the second monomer in place to

complete the active site (*21*). A dominant-negative form of ODC in which K69 and C360 are mutated to alanines is commonly used to study ODC. The K69 is important in PLP binding and C360 plays a role in forming the active site as previously mentioned.

**Regulation of ODC**

Proteins with critical role(s) in cellular functions are often highly controlled by multiple mechanisms. ODC is no exception, and is in fact one of the most highly regulated eukaryotic enzymes known. It is controlled at the transcriptional, translational and post-translation levels by a number of different mechanisms. At the transcriptional level, *Odc* is considered an immediate early gene and increased transcription of the ODC gene, as well as activity, is associated with cell transformation by c-*myc*, *ras* and v-*src* (*22*). The ODC gene contains response elements for cAMP, a putative insulin response element, Sp1 binding sites and *c-myc* binding sites, which are the best characterized. Myc is a basic helix-loop-helix-leucine zipper (b-HLH-Zip) transcription factor involved in the regulation of cell proliferation, apoptosis and differentiation. Myc heterodimerizes with Max, another b-HLH-Zip protein, and binds to its recognition element, a CACGTG E-box, on the target gene to induce transcription. *Odc* has three c-Myc response elements; two CACGTG E-binding sites in the first intron and a CATGTG sequence in the 5'-flanking region of mouse *Odc* which has been demonstrated to be a functional c-Myc response element (*23*). Until recently it was believed that Myc-Max binding to the response elements lead to transcription of the ODC gene. Interestingly, recent evidence suggests that it is not the binding of Myc-Max to the response elements that leads to

transcription, but the displacement of Mnt from binding to *Odc* (*24*). Knockdown of *Mnt* shows many of the same phenotype traits as overexpression of Myc (*24, 25*). However, knockdown of *Mnt* in fibroblasts in cell culture leads to accelerated proliferation and apoptosis similar to the "Myc" response. Unexpectedly, this response to *Mnt* knockdown occurs even in cells lacking c-*myc*. Therefore, c-Myc may act as a oncogene by displacing or preventing the putative tumor suppressor Mnt from binding to the ODC gene.

ODC mRNA has many characteristics of translationally repressed mRNAs, which are generally associated with mRNAs that encode factors related to cell proliferation, such as growth factors and proto-oncogenes (reviewed in (*26*)): a long 5' untranslated region (UTR) that contains a GC-rich region that has been shown to repress translation, a small internal open reading frame (ORF) in the 5' UTR (*22*) and an internal ribosome entry site (IRES) for cap-independent translation (*27*). Little to no change in ODC mRNA content is often detected upon substantial increases or decreases in ODC protein content and activity (*28-32*). Indeed, NIH-3T3 cells that overexpress eIF-4E, the limiting component of the eIF4F complex needed for cap-dependent translation, exhibit elevated ODC levels up to 30 times higher than wild-type NIH-3T3 cells with no significant change in ODC mRNA (*30*). Polyamines themselves are also known to regulate the translation of ODC through a putative polyamine response element in the 5' UTR, with low levels of polyamines stimulating ODC translation and higher levels reducing it (reviewed in (*22*)).

ODC is controlled at the post-translation level by several mechanisms. ODC protein has one of the shortest $t_{1/2}$ (half-life) of any known protein—measured as short as

10-60 min (*33, 34*). A protein termed antizyme binds to ODC and directly regulates ODC in two ways (*13*). By virtue of heterodimerizing with an ODC monomer, antizyme can reduce the pool of active ODC which is an obligate homodimer. Antizyme binding to ODC also accelerates ODC degradation via the 26 S proteasome. Polyamines themselves control the antizyme expression through a unique feedback mechanism based on translation frameshifting (*18*). Elevated polyamine levels signal the translation of full-length antizyme which in return inactivates and degrades ODC and can also block the uptake of polyamines by an ill-defined polyamine transport system. Evidence also suggests that antizyme increases polyamine export (*16*). As mentioned previously, the use of the common precursor arginine invariably links the polyamine pathway to other pathways including the citrulline-NO cycle and agmatine production. NO has been shown to inhibit ODC via *S*-nitrosylation of cysteine 360, a residue within the active site critical for ODC activity (*35*). Arginine can be decarboxylated by arginine decarboxylase to agmatine, which is structurally analogous to polyamines. It has been reported that agmatine can affect polyamine biosynthesis by also promoting translational frameshifting of antizyme (*36*). Agmatine is taken up from the diet and is present in mammalians cells, however arginine decarboxylase has not yet been found in mammals (*37*). Therefore, the significance of the proposed action of agmatine on antizyme in mammalian cells is uncertain.

**Antizyme**

Antizyme is uniquely involved and an important mediator of polyamine homeostasis and thereby merits a more in depth discussion. Monomers of ODC interact weakly with one another and continuously cycle between the monomeric and dimeric species. In contrast, antizyme has a high affinity for the ODC monomer favoring inactive antizyme:ODC heterodimers (*13*). Antizyme, a 23 kD protein, binds to ODC at a site that obstructs the ODC homodimer interface. Two molecules of antizyme inactivate one ODC dimer—one molecule of antizyme binds to each of the ODC monomers. Antizyme further regulates ODC activity by targeting it for degradation via the 26 S proteasome. ODC is degraded by the proteasome even in the absence of antizyme; antizyme expedites the process reducing the $t_{1/2}$ of ODC to minutes.

Proteins are generally targeted to proteasomal degradation by the covalent attachment of ubiquitin to lysines in the substrate protein (ubiquitination). However, antizyme directs ODC to be degraded by the 26 S proteasome by a ubiquitin-independent mechanism. ODC is one of a few known proteins that is degraded by the proteasome in a ubiquitin-independent manner (*38*). It is not exactly clear how antizyme binding to ODC promotes ODC degradation, but it is believed that the antizyme-ODC heterodimer exposes the C-terminus of ODC which was previously inaccessible. Truncation of the last five C-terminal amino acids from ODC prevents it from being degraded by the proteasome. All of the ODC constructs used in this thesis encode a C-terminally truncated ODC (425 of 461 amino acids) because the protein is more stable (degradation is not accelerated by antizyme), yet the truncation does not affect ODC activity. In the

process of targeting ODC for degradation, antizyme is spared and can inactivate and increase the rate of degradation of more molecules of ODC.

Polyamines are able to regulate their levels through a unique feedback mechanism involving antizyme (*18*). The antizyme mRNA consists of two open reading frames. ORF1 contains two potential start codons to initiate translation . ORF2 has no meaningful start codon but contains most of the coding sequence for antizyme. For functional antizyme to be translated, translation must begin at the start of ORF1 and frameshift forward one base before the stop codon in ORF1 and continue to translate ORF2 in the +1 frame. Sequences near the frameshift site and the mRNA secondary structure direct the frameshift. Elevated polyamine levels greatly enhance the +1 frameshifting, but it is not known whether the polyamines directly influence the frameshift by interacting with the mRNA or affect it by another means.

Antizyme itself can be inhibited by a protein termed antizyme inhibitor (*39-41*). Although the sequence of antizyme inhibitor is closely related to ODC, it is unique and has no ODC activity even as a homodimer. Antizyme inhibitor heterodimerizes with antizyme to prevent it from dimerizing with ODC, but antizyme inhibitor is not known to heterodimerize with ODC.

Three isoforms of antizyme are now recognized (*13*). The discussion on antizyme thus far has been restricted to the antizyme 1 isoform. Antizyme 1 and 2 are distributed in a wide variety of tissues, but the mRNA levels of antizyme 1 are much more abundant. Antizyme 2 can bind and inactivate ODC and has been reported to block polyamine uptake, but it is not known to target ODC for proteasomal degradation and thereby may act as a reversible inhibitor of ODC (*42*). Antizyme 3 is specifically expressed in the

testes in the late stage of spermatogenesis (*43*). Because of its specific temporal expression, it may play a critical role at this stage. Indeed, overexpression of ODC in transgenic mice has been shown to have deleterious effects on the germ cells in the testes and cause sterility (*44*).

Antizyme may not exert all of its growth inhibitory effects through polyamines however. Recently it has been reported that antizyme non-covalently binds to cyclin D1 and accelerates its degradation rate (*45*). Similar to ODC, antizyme targets cyclin D1 for degradation independent of ubiquitination.

**Physiological and Molecular Roles of Ornithine Decarboxylase**

ODC was speculated to be a proto-oncogene because overexpression of ODC in NIH/3T3 cells was shown to convert the cells to a transformed phenotype which could be reverted by an expression vector coding for the complementary ODC DNA sequence (*46, 47*). ODC has been shown to have a key role in transformation, however overexpression of ODC alone is not sufficient for transformation in many animal models. Therefore it is unlikely that ODC is a true oncogene. Numerous studies have shown that ODC can cooperate with other factors to transform cells and that ODC is essential to Ras transformation. Ras proteins are GTPases that play key functions in oncogenesis and regulation of cytoplasmic signaling networks (reviewed in (*48*)). The involvement of ODC in Ras transformation will be expanded upon in Chapter 7.

A number of mouse models have helped to better understand the physiological roles of ODC. ODC is essential during mouse development; ODC knockout mice are not

viable past the earliest stages of embryonic development (*49*). ODC, a dominant negative ODC and antizyme have been overexpressed in transgenic mouse models to study ODC regulation of polyamines (*50, 51*). Overexpression of ODC from its own promoter lead to increased putrescine levels in the tissues with elevated ODC activity, but there was relatively little effect on spermidine and spermine levels (*52-54*) This is likely a reflection of limited AdoMetDC activity and the multiple mechanisms which regulate polyamine homeostasis. Although forced overexpression of ODC has been shown to transform cells in culture and form tumors in nude mice (*46, 55*), these mice were not more prone to spontaneous tumorigenesis than their syngenic littermates. The mice were more sensitive to a two-stage chemical carcinogenesis protocol than their wild-type littermates. Accumulation of high putrescine levels in the testes during late spermatogenesis was detrimental to germ cells and caused male sterility. This may help explain the importance of a testis-specific antizyme, antizyme-3 (*43*).

Overexpression of a C-terminally truncated ODC (which stabilizes ODC by increasing the $t_{1/2}$ of the protein) from promoters that target expression to specific skin populations significantly enhanced the animals' susceptibility to tumor development (*50*). The level of susceptibility is dependent on the genetic background. For example, ODC transgenic mice on a B6C3F2 background develop spontaneous tumors, but when crossed onto a more resistant C57BL/6J background the transgenic mice require an initiating dose of 7,12-dimethylbenz(*a*)anthracene (DMBA) but no tumor promoter. Nonetheless, the ODC transgenic mice are more susceptible to tumor development than their non-transgenic littermates. When these mice were crossed with transgenic animals expressing Ras, the resulting double transgenic pups developed tumors without initiation or

promotion (*56*). The tumors rapidly regressed in response to DFMO treatment. These and other mouse models in which ODC was perturbed in the skin are discussed in greater detail in Chapters 4 and 7.

ODC has also been demonstrated to be important in a forestomach carcinogenesis model (*50*). Mice treated with the carcinogen *N*-nitrosomethylbenzylamine (NMBA) develop tumors in the forestomach, and the tumor response is enhanced by maintaining the mice on a zinc-deficient diet. Expression of antizyme in the epithelial cells of the forestomach from a K5 promoter significantly reduces tumor formation in C57BL/6J mice fed zinc- deficient or sufficient diets. Immunohistochemistry revealed that a number of markers of proliferation were reduced and apoptosis increased. The reduction in carcinogenesis brought about by antizyme expression was likely due to the effect of antizyme on ODC because similar results were obtained in NMBA/zinc-deficient mice administered DFMO.

**ODC and the Cell Cycle**

A strong body of evidence suggests that the proliferative effect of ODC may mediated through an involvement with the cell cycle. As first reported by Heby, ODC is intimately involved with the cell cycle. Many early studies have shown that its activity fluctuates throughout the cell cycle in a pattern apparently specific to the cell line tested (*33, 57-59*) and inhibition of ODC results in cell cycle arrest (*33, 60-65*). Translation of ODC mRNA peaks twice during the cell cycle at the $G_1$/S transition and at $G_2$-M. There is an internal ribosome entry site in ODC mRNA allowing translation during mitosis,

when cap-dependent translation is impaired (*27*).

The ODC gene, which contains c-Myc transcription factor responsive elements, is regulated at the transcriptional level by the c-Myc protein (*66-68*). The increased ODC transcription contributes to the proliferative actions of c-Myc but the interrelationship between ODC and c-Myc is complex. Increased ODC content is also known to be a factor in c-Myc-induced apoptosis (*69*). In normal serum-starved or growth factor deprived cells, *c-myc* gene expression is down-regulated and the cells halt in the $G_0/G_1$ phase of the cell cycle. Enforced expression of *c-myc* under the same conditions drives the cell into S phase (*70*), presumably through the transcription of ODC. When F9 teratocarcinoma cells were treated with DFMO and blocked in the $G_1$ phase of the cell cycle, c-Myc was up-regulated suggesting that polyamines are required for c-Myc induced cell cycle progression and may act as negative regulators of *c-myc* expression (*71*).

Early studies in cultured cells revealed that DFMO treatment, and subsequent depletion of putrescine and spermidine, accompanied by a modest (if any) decrease in spermine levels, altered cell cycle progression. Inhibition of ODC pointed to polyamine-dependent restriction points in the $G_1$ (*64, 65, 72-74*) and S phases (*62, 63, 73*) of the cell cycle. Addition of exogenous putrescine negated the effect of DFMO, thereby demonstrating that the product of ODC activity, putrescine, is sufficient to restore cell cycle parameters to the levels of untreated control cells (*63, 65, 73, 74*).

DFMO treatment has been shown to increase the doubling time in several cells lines including the IEC-6 non-transformed line of intestinal epithelial cells derived from adult rat crypt cells (*65, 75*), Caco-2 human colon cancer cells (*75*), MKN45 human

gastric cancer cells (*76*), and MALME-3M human melanoma cells (treated with DFMO and the AdoMetDC inhibitor AbeAdo) (*77*). Co-treatment with DFMO and putrescine or spermidine restores a normal growth rate, indicating that the increased doubling time is the direct effect of depleting polyamine pools through inhibition of ODC. The pathway between ODC inhibition and cell cycle arrest is not well elucidated, but recent evidence suggests that decreases in polyamine levels, through the inhibition of ODC, induce $p21^{WAF1/CIP1}$, and that this up-regulation of $p21^{WAF1/CIP1}$ appears to be at least one of the mechanisms mediating the increased doubling time.

$p21^{WAF1/CIP1}$ blocks the formation of active cyclin/cdk complexes through its interaction with cdk2, cdk3, cdk4, and cdk6, thereby preventing $G_1$/S transition (*78*). $p21^{WAF1/CIP1}$ inhibition of cyclin/cdk complex formation can maintain Rb in its hypophosphorylated state, preventing the release of the E2F transcription factor and subsequent transcription of genes coding for proteins necessary for $G_1$/S progression. In the aforementioned studies, $p21^{WAF1/CIP1}$ protein levels were increased in response to DFMO treatment (*75, 77, 79*) and DFMO-treated IEC-6 (*65, 75*) and MKN45 (*80*) cells arrested in the $G_1$ phase of the cell cycle. Upregulation of $p21^{WAF1/CIP1}$ and $G_1$ arrest has also been observed in MALME-3M cells treated with the combination of DFMO and AbeAdo (*77*) or with the polyamine analogue BE-3-3-3 (*60*). Interestingly, c-Myc has been shown to promote cell cycle progression not only by increasing the transcription of ODC as mentioned above, but also by down-regulating $p21^{WAF1/CIP1}$ transcription (*81*). Some reports also suggest that DFMO-induced increases in $p21^{WAF1/CIP1}$ are dependent upon ERK-1/2 (*79, 82*) and JNK (*79*).

NO has been shown to inhibit ODC via *S*-nitrosylation of the critical active site

residue Cys-360 (*82, 83*). NO-mediated inhibition of ODC represents at least one of the cGMP-independent mechanisms by which NO inhibits cell proliferation (*82*). Two NO donors, *S*-nitroso-*N*-acetylpenicillamine (SNAP) and (Z)-1-[N-(2-aminoethyl)-N-(2-aminoethyl)-amino]-diazen-1-ium-1,2-diolate (DETA/NO), inhibited rat aortic smooth muscle cell (RASMC) proliferation via an ODC-dependent mechanism (*82*). Addition of putrescine, but not ornithine, released the cytostatic effect of the NO-donors providing evidence that the decrease in cell growth was dependent on the inhibition of ODC. Moreover, 1H-(1,2,4)oxadiazolo[4,3-α]quinoxalin-1-one (ODQ), a soluble guanylate cyclase inhibitor, and zaprinast, a cGMP phosphodiesterase inhibitor, had no effect on cell proliferation in untreated or DETA/NO or SNAP-treated RASMC, showing that the effect is not cGMP-dependent. Inhibition of ODC using either of the NO-donors or DFMO resulted in an increase in $p21^{WAF1/CIP1}$ protein levels.

Two p53-responsive elements are located in the promoter of $p21^{WAF1/CIP1}$, however its transcription can be mediated by a number of other factors in response to various signals, including; AP2, E2Fs, STATs, C/EBPα, C/EBPβ, and the homeobox transcription factor *gax* (*84*). Therefore, it is possible that inhibition of ODC can lead to both p53-dependent and independent induction of $p21^{WAF1/CIP1}$ in various types of cells, or even the same cell line. There is evidence to support both possibilities. An increase in both p53 and $p21^{WAF1/CIP1}$ protein expression has been observed in DFMO-treated IEC-6 cells, but unfortunately, the sequence of induction of p53 and $p21^{WAF1/CIP1}$ in relation to the onset of $G_1$ arrest and polyamine depletion was not investigated (*75, 79*). DFMO-mediated inhibition of ODC appears to mediate the increase in p53 at a post-transcriptional level (*85*). The DFMO treatment resulted in significantly increased half-

life of p53 mRNA (with no concomitant change in p53 gene transcription), increased p53 protein synthesis, and increased p53 protein stability (*85*). Each effect was reversible with DFMO/spermidine co-treatment, suggesting that the subsequent reduction in polyamines, due to ODC inhibition, led to enhanced stability of p53 mRNA and protein and increased translation. The increase in p53 could thereby upregulate the transcription of $p21^{WAF1/CIP1}$.

Evidence points to a p53-independent induction of $p21^{WAF1/CIP1}$ as well. DFMO treatment increased expression of $p21^{WAF1/CIP1}$ in MKN45 human gastric cancer cells, with little change in p53 levels (*76*), and DFMO-mediated induction of $p21^{WAF1/CIP1}$ leading to $G_1$ arrest occurred in KATO III gastric cancer cells that lack p53 expression (*76*). Polyamine depletion induced $p21^{WAF1/CIP1}$ leading to $G_1$ arrest in MALME-3M cells treated with the combination of DFMO and AbeAdo. The sequence of induction resulting from this treatment was studied and the increase in $p21^{WAF1/CIP1}$ preceded the increase in p53, suggesting that the increase in $p21^{WAF1/CIP1}$ was, at least in part, p53-independent (*86*). It should be noted that this combination of DFMO with an AdoMetDC inhibitor distinctly alters the balance among the individual polyamine levels compared to DFMO treatment alone.

The pathway whereby inhibition of ODC leads to induction of $p21^{WAF1/CIP1}$ likely represents only one of a multitude of mechanisms by which ODC and other polyamine related proteins affect the cell cycle. It is worth noting that there is a possibility that antizyme (which is induced by polyamines) may impact the cell cycle to hold cells in $G_1$ by a direct effect on cyclin D1 or cdk4 (*45*). Antizyme may also be important in the response to polyamine analogues since it has now been shown that in rat liver HCTR cells, antizyme is induced by treatment with many polyamine analogues including BE 3-

3-3 and BE 4-4-4-4 (*87*).

*In vivo* experiments utilizing transgenic mice that overexpress ODC under control of a keratin 6 promoter revealed increased cellular proliferation in the skin of these mice (*88*). Epidermal and dermal tissue contained elevated cyclin E/cdk2 and cyclin A/cdk2-associated kinase activity compared to nontransgenic controls, but there was no effect on cyclin D/cdk4-dependent phosphorylation of Rb. This suggests that cellular proliferation in the skin of these ODC transgenic mice is driven through late $G_1$/S and from S to $G_2$ by the increased kinase activity of the cyclin E/cdk2 and cyclin A/cdk2 complexes, respectively. Intriguingly, p53, $p21^{WAF1/CIP1}$, and $p27^{KIP1}$ protein levels were increased in the skin tissue from these ODC-overexpressing transgenic mice. These proteins are generally associated with cell cycle arrest and/or apoptosis, and as discussed previously, have been shown to be induced by an inhibitor of ODC in immortalized cells. However, it has been postulated that low stoichiometric levels of $p21^{WAF1/CIP1}$ or $p27^{KIP1}$, may prime cyclin/cdk complexes to promote their kinase activation (*88*). Because ODC activity is elevated and proliferation is increased, the increase in these proteins may represent a form of feedback inhibition, although the balance still remains largely in favor of proliferation.

Overall, although the effects are complex, it is clear that polyamines exert important effects on the cell cycle and in apoptosis. The balance between cell proliferation and cell death, which is of critical importance in tumor development and neoplastic growth, can be altered by changes in the content and relative proportions of polyamines. Interference with polyamine synthesis or application of polyamine analogues, which may induce polyamine catabolism or block interaction of natural

polyamines with critical sites, can perturb these processes. This provides a real opportunity for therapeutic intervention but major challenges to identify and optimize appropriate therapeutic regimes.

**Inhibition of ODC**

In light of research defining the importance of polyamines and ODC in cellular growth, keen interest arose in the development of ODC inhibitors to be used as effective treatment for neoplastic diseases. The history of polyamine drug development is extensive and continues to grow (reviewed in (*89, 90*)). α-difluoromethylornithine (DFMO, eflornithine), an inhibitor of ODC, is the most well-known and studied inhibitor of the enzymes involved in polyamine biosynthesis. Drugs targeting ODC can be categorized into three main classes: cofactor (PLP) antagonists, product analogs and substrate analogs (which includes DFMO). α-Hydrazino-δ-ornithine, α-hydrazino-δ-aminovaleric acid and 1,3-propanediamine derivatives with aminooxy groups are potent inhibitors of ODC (*89*). They react with PLP in the active site of ODC to inhibit ODC in the nM range, but their usefulness is limited by poor selectivity. The diamine analog 1,3-propanediamine is effective in diminishing polyamine pools and inhibiting cell proliferation, but extensive metabolism negates its usefulness.

Thirty years ago, α-methylornithine was developed as the first true competitive inhibitor of ODC. It displayed good activity ($K_i$ = 40 μM) and was useful to study ODC, but targeting ODC with a reversible inhibitor has limitations. Reversible inhibitors prevent ODC degradation and the initial depletion of spermidine results in transcriptional

upregulation of ODC. The Merrel Dow Research Institute (Strasbourg, France) synthesized a series of α-substituted ornithine derivatives with either an unsaturation (ethylene-, ethynyl- or allenyl-) or a methyl group with a suitable leaving group (chloromethyl, fluoromethyl, difluoromethyl, chlorofluoromethyl or cyanomethyl). DFMO emerged as a good candidate after initial biological and pharmacological evaluations. DFMO acts as a competitive enzyme-activated irreversible inhibitor of ODC. After reaction with ODC, DFMO was found to form adducts with lysine 69 and cysteine 360—important residues in the active site of ODC (*91*). About 90% of the reactive intermediate bound to cysteine 360. The major inactivating adduct is formed by a nucleophilic attack of cysteine 360 on the conjugated imine.

Great promise was held for DFMO as a chemotherapeutic and chemopreventative agent in humans (*92*). Although clinical trials with DFMO continue more than 25 years after its development and some therapeutic usages have been established, the anticipated impact of DFMO to this end has yet to be realized. However, this is most likely a reflection of the pharmacokinetic properties of DFMO and the need for more appropriate adjuvant agents, rather than the validity of ODC as a target. As discussed previously, polyamine homeostasis is highly regulated and targeting one enzyme alone may not be effective. Combination therapy, such as an ODC inhibitor and an inhibitor of polyamine transport to block the uptake of exogenously derived polyamines, is more likely to be effective.

DFMO has proven to be a clinically relevant drug target, but for uses not initially foreseen. DFMO is the only FDA approved drug for the treatment of unwanted facial hair (labeled as Vaniqa™, 13.9% eflornithine; Bristol-Myers Squibb). Little is known

about the mechanism by which DFMO slows hair growth in humans. DFMO is also approved by the FDA for use in the treatment of West African trypanosomiasis (sleeping sickness) transmitted by *Trypanosoma brucei gambiense*. DFMO has poor oral availability (54%) and 100 mg/kg must be intravenously administered every 6 hr for 14 days (*91*). It has trypanostatic rather than trypanocidal effects and it is believed that a functional immune system is needed to achieve a cure. It is remarkably effective against the parasite with an overall efficacy of 85-90%, a relapse rate of 5.3% and death rate of 7% (*93*). Several theories have been proposed to explain why the effectiveness of DFMO has not translated into humans (*93*). Trypanosome ODC has a much longer $t_{1/2}$ than mammalian ODC (>4 hr vs. 10-60 min). The parasites are limited in their ability to transport putrescine and spermine. They can not synthesize spermine and do not contain the SSAT/PAO retroconversion pathway. Inhibition of ODC by DFMO has little effect on spermine pools which has been implicated in the lack of success of DFMO as a chemotherapeutic in humans (*33*).

Hope for use of DFMO as a chemopreventative/therapeutic agent is not lost—even 26 years after its development. Eight clinical trials with DFMO are currently being conducted for chemopreventation/therapeutics (www.clinicaltrials.gov). One Phase III study is investigating the efficacy of DFMO in patients with newly diagnosed or recurrent bladder cancer. DFMO is being investigated as a chemopreventative for a number of different cancers including skin, colorectal, prostate, esophageal, bladder and cervical cancer. DFMO alone (i.e. without other agents that alter polyamine homeostasis) may be better suited to a chemopreventative role in which maintaining

polyamines levels below a certain threshold may have a greater impact than it would in a more advanced stage of progression.

Many in the pharmaceutical industry believe that a significant number of drugs that show disappointing efficacy in Phase II clinical studies may still be effective for a subset of the population. Companies are developing programs to identify "good responders" to their drugs; that is to identify genotypes that respond well. DFMO, in combination with procarbazine, CCNU and vincristine, increased survival of patients with anaplastic gliomas (AG) but not glioblastoma multiforme (GBM) (*94*). The authors of the study postulate that this is a function of the ODC levels in the different cancers; AG has been shown to have lower ODC levels than GBM and cancers (or patients) with lower levels of ODC will respond better to DFMO. There are two known alleles of the human ODC gene—the A allele (which is considered the minor allele, but the population tested was small, n<1000) and G allele—that may affect an individual's ODC activity (*95*). The difference between the two is a single nucleotide polymorphism located between the two Myc E boxes in intron 1 (*96*). It has been demonstrated that transcription from the promoter/regulatory region of the A allele is more efficient than transcription from the same region of the G allele (*96*). Therefore, *Odc* transcription and activity may be elevated in individuals carrying the A allele versus the G allele in response to stimuli that promote Myc induction of *Odc*. The A and G alleles are reportedly differentially regulated by Mad1, a negative regulator of Myc (*97*). If the levels of ODC do affect how an individual responds to DFMO and a known polymorphism in *Odc* affects ODC activity, then it would merit an attempt to identify subpopulations that may respond better to DFMO when conducting clinical trials.

We have pursued a different approach to regulate ODC activity. The drawbacks of inhibiting the ODC protein, with a reversible or irreversible inhibitor, were noted above. ODC may be a good candidate for mRNA knockdown because the ODC protein has a very short $t_{1/2}$, therefore continued ODC activity is dependent upon translation of new protein. We decided to investigate the potential of modulating ODC activity by targeting ODC mRNA with catalytic nucleic acids.

**Approaches to RNA Silencing**

The use of nucleic acid-based inhibitors to silence mRNA is a relatively new strategy to reduce active protein. The idea originated in 1978 with the first study with antisense oligodeoxynucleotides (AS-ODNs) shortly followed by the discovery of ribozymes in the early 1980s. The field expanded with the development of the DNAzyme in 1997 and the more recent discovery of small interfering RNA (siRNA) and micro RNA (miRNA). Aptamers represent a distinct class of nucleic acid-based inhibitors. Unlike the aforementioned nucleic acids, aptamers manipulate gene products or epitopes and almost never exert their effects on the genetic level (*98*).

The five different methods share similarities and have differences. They can be categorized based on their chemistries and mechanism of silencing. AS-ODNs and DNAzymes are DNA-based, while ribozymes, siRNA and miRNA are composed of RNA. DNA is much more stable than RNA and proteins. The absence of an enslaved nucleophile (the 2'-hydroxyl group) at each phosphodiester linkage makes DNA ~100,000-fold more stable than RNA under physiological conditions (*99*). On the other

hand, RNA-based ribozymes and siRNA can be expressed from a plasmid which can be useful for research purposes. The five methods of silencing can also be broadly categorized based upon their mechanism of action. Ribozymes and DNAzymes have catalytic activity—they catalyze the cleavage of RNA. AS-ODNs and siRNA do not have intrinsic enzymatic activity but both are capable of recruiting catalytic enzymes to degrade RNA.

AS-ODNs are single-stranded DNA molecules of various sizes that are complementary in sequence to the targeted mRNA. AS-ODNs can silence mRNA by two mechanisms, depending on the chemistry of the DNA (*100, 101*). AS-ODNs with a net negative charge (e.g. phosphodiester, phosphorothioate backbones) can elicit RNase H-mediated cleavage of the mRNA. RNase H cleaves only the RNA moiety of the DNA-RNA heteroduplex and the AS-ODN is then free to hybridize to another mRNA molecule and repeat the process. Strategies have been identified to recruit other RNases, including RNase III, L or P, to an AS-ODN-DNA complex (*102*). Modifications to the ODN backbone that do not support this RNase H mechanism include AS-ODNs that lack a negative charge or form a type of helix with the target RNA that prevents RNase H mediated degradation. These AS-ODNs work by steric hindrance and include morpholinos, 2'-O-methyls, 2'-O-allyls, locked nucleic acids and peptide nucleic acids. Steric hindrance can interfere with a number of processes necessary for the translation of mRNA into protein including: 5' capping, splicing and polyadenylation of the pre-mRNA, transport of the mRNA from the nucleus to cytoplasm and translation of the mRNA (*102*).

Vitravene™ (formiversen, Isis Pharmaceuticals, Carlsbad, CA), a member of the AS-ODN class is the only drug approved by the FDA that works by a RNA silencing mechanism of action. Vitravene™ is a 21-nt phosphorothioate (nonbridging oxygen is replaced with a sulfur atom) ODN. Vitravene™ is administered by intravitreal injection for the treatment of cytomegalovirus-associated retinitis by targeting the cytomegalovirus (CMV) *IE2* mRNA. IE2 has been reported to encode proteins that regulate viral gene expression and the encoded proteins are considered crucial for the production of infectious CMV. A number of other AS-ODN clinical trials are ongoing. To date all AS-ODNs that have entered clinical trials have been designed to use the RNase H mechanism of action.

siRNA and related miRNAs are the most recently identified forms of RNA silencing that occur in a wide range of eukaryotic organisms (reviewed in (*103*)). siRNA and miRNA are processed from varied length double-stranded (ds) RNA into shorter 21-28-nt dsRNA. miRNA is first processed by a dsRNA-specific RNase-III-type endonuclease Drosha in the nucleus and then exported to the cytoplasm. In the cytoplasm, both siRNA and miRNA are processed by another dsRNA-specific RNase-III-type endonuclease Dicer. Processed siRNA duplexes are rearranged into a RNA-induced silencing complex (RISC). Processed miRNA duplexes are rearranged into a similar complex called the miRNA-containing effector complex (referred to as miRNP). Both RISC and miRNP contain a member from the Arogonaute (Ago) family of proteins. Assembly of the RISC complex is ATP-dependent, presumably reflecting the need to unwind the duplex RNA although an associated helicase has not yet been identified. It has not been demonstrated whether assembly of the miRNP complex is energy

dependent, but it is believed to be. Nonetheless, both the siRNA and miRNA duplexes are unwound and, through a poorly understood mechanism, one strand is left in the complex tightly bound to Ago. The single-stranded siRNA in RISC targets the complex to a complementary or near-complementary mRNA. The mRNA is cleaved ten nucleotides upstream of the nucleotide paired with the 5' end of the complementary siRNA strand associated with RISC. This is an energy-independent process, but becomes more efficient with the addition of ATP. Cleavage of the mRNA yields a 5' phosphate and 3' hydroxyl termini. Like ribozymes and DNAzymes, the cleavage reaction is dependent on $Mg^{2+}$, but the reaction mechanism is different because cleavage by ribozymes and DNAzymes yield a 2', 3'-cyclic phosphate on the 5' product and 5'-hydroxyl on the 3' product.

The miRNP complex can cleave mRNA by a similar mechanism, but the major silencing mechanism exerted by the miRNP complex is through translational repression, not mRNA cleavage. Evidence suggests that miRNP interferes with translational elongation or termination. To further confound our knowledge of this field, siRNA can act as miRNA and miRNA can act as siRNA. It is tempting to speculate that siRNA will act through the "siRNA" mechanism when the degree of complementarity is high and through a "miRNA" mechanism when it is low (and vice-versa for miRNA). This is likely a naïve conclusion. Indeed, it has been demonstrated in animals that miRNA can cleave even significantly mismatched sequences. It is more likely that siRNA and miRNA have divergent functions that are regulated by different mechanisms.

Ribozyme are catalytic RNA molecules that also exist in nature. There are several different types of naturally occurring ribozymes including, the RNA component

of RNase P (which cleaves precursor tRNAs to generate mature tRNAs), self-splicing group I and group II introns, self-cleaving RNAs (including the hammerhead, hairpin hepatitis delta virus [HDV] and *Neurospora* Varkud satellite [VS] motifs) and the RNA component of the large ribosomal subunit which catalyzes the peptidyl transferase step of translation (*104*). Ribozymes that catalyze ligase reactions have also been developed using *in vitro* screens (*104*). These "artificial" ribozymes catalyze a reaction analogous to the reaction carried out by a RNA-dependent RNA polymerase. The hammerhead and hairpin ribozyme motifs have been widely adopted for use in RNA silencing because of their small size and simplicity. In Chapter 5, the use of hammerhead ribozymes to silence ODC is described.

The hammerhead ribozyme model is based on the satellite RNA strand (+) of the tobacco ringspot virus (*105*). It is comprised of a 22-nt conserved catalytic domain flanked by sequence specific hybridization arms. The hybridization arms are complementary to the targeted region of the RNA. The hammerhead ribozyme targets cleavage 3' to an NUH (where N = any nucleotide and H = C, U or A) site of the target RNA. The H of the target RNA is unpaired in the ribozyme; the catalytic domain is inserted at this position. Cleavage of the RNA substrate is dependent upon the presence of $Mg^{2+}$, which is believed to not only participate directly in the cleavage mechanism but also assist in RNA folding (*106*).

DNAzymes, RNA-cleaving DNA enzymes, are not known to exist in nature. Several models of DNAzymes have been developed that are able to catalyze more than seven distinct chemical transformations including the 10-23 DNAzyme, histidine-dependent DNAzyme, copper-dependent DNAzyme, copper-dependent DNA ligase and

calcium-dependent kinase (*107*). The 10-23 DNAzyme has generated great interest because it can achieve catalytic rates greater than all known DNAzymes and ribozymes (*107*). The 10-23 DNAzyme was developed from a novel *in vitro* screen (*108*). Briefly, a biotinylated single-stranded DNA-RNA hybrid was tethered to a steptavidin support. The DNA-RNA consisted of (5' to 3') a biotinylated DNA linker, RNA sequence (substrate) and a 50-nt random sequence flanked by defined ends (for PCR). The single stranded DNA was allowed to fold around the RNA substrate under selected reaction conditions. The solid support was washed and only the DNA species that were able to cleave the substrate and free itself from the solid support were present in the eluent. The eluted DNAzymes were then enriched by PCR using the defined ends as a template and the process was repeated. The name of the 10-23 DNAzyme was derived from its selection; it was the 23$^{rd}$ clone identified after 10 rounds of selection.

The 10-23 DNAzyme has a relatively small catalytic domain (15 nucleotides) flanked by hybridization arms (generally 6-12 nucleotides each) that target it to bind to a cognate RNA substrate via Watson-Crick base pairing and subsequently catalyze cleavage of a phosphodiester bond of the RNA (*109, 110*). The reaction mechanism for the 10-23 DNAzyme and hammerhead ribozyme are believed to be similar (see Figure 1.2) (*110*).

Ribozymes and DNAzymes have been successfully used to silence a number of genes *in vitro* and to a lesser extent *in vivo* for a number of applications (*104, 105, 111*). DNAzymes have also been creatively applied to various biotechnology applications, including the basis of an autonomous DNA motor and to detect amplification of nucleic acids (*112, 113*). An approach to develop an effective DNAzyme (Chapter 2) and

ribozyme (Chapter 5) to silence ODC is described in Chapter 2. The effectiveness of a catalytically optimized DNAzyme is demonstrated in both cell culture (Chapter 3) and *in vivo* (Chapter 4).

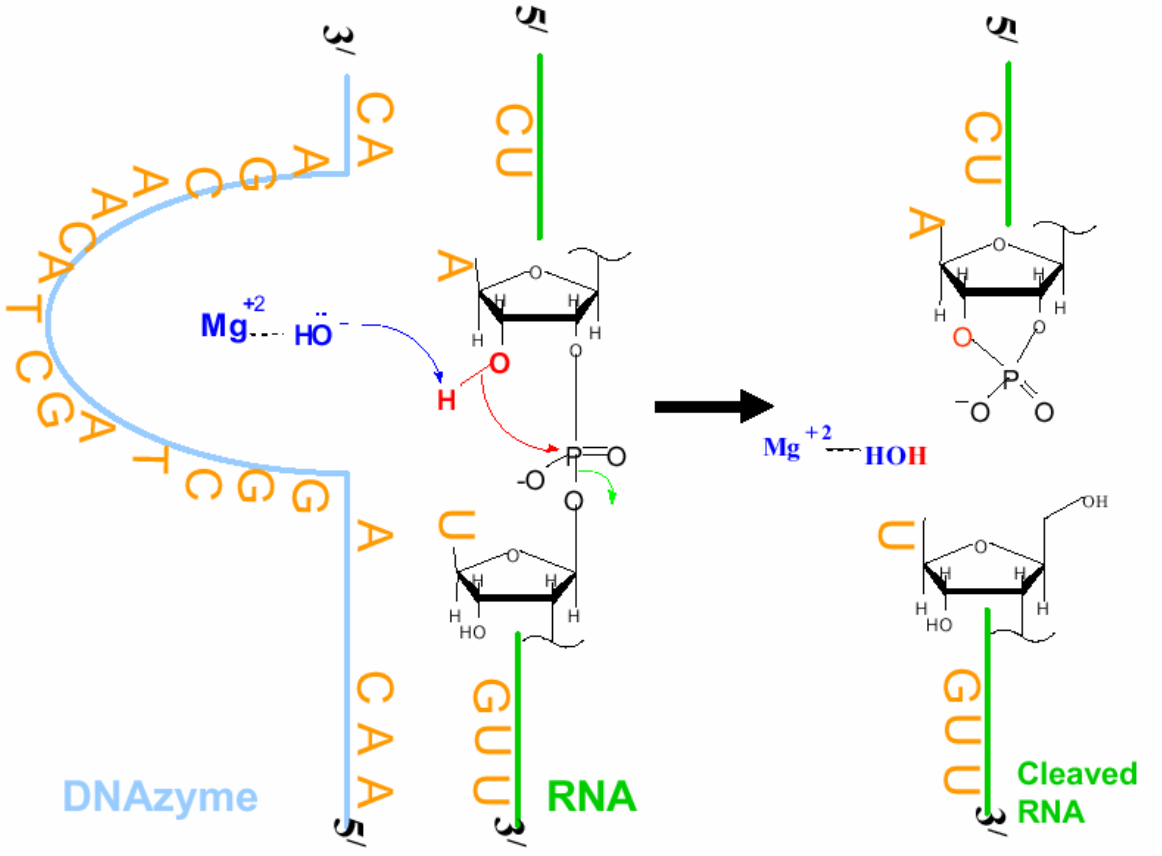


**Figure 1.2**: *Proposed Reaction Mechanism of the 10-23 DNAzyme*

$Mg^{2+}$ is positioned to assist in the deprotonation of the 2' hydroxyl (in red) that is adjacent to the cleavage site. The resulting 2'-oxyanion attacks the neighboring phosphate to form a 2',3'-cyclic phosphate at the 3' end of the 5' product and a 5'-hydroxyl at the 5' end of the 3' product.

## Hypotheses

This thesis was driven by three hypotheses. Two of the hypotheses dealt with developing novel approaches to modulate the activity of ODC. The third hypothesis was derived to further elucidate the role that ODC plays in cell transformation to understand if and why ODC is a good drug target.

### *I. Targeting ODC mRNA may be an effective strategy to reduce ODC activity due to its regulation at the translational and protein levels.*

### Specific Aims

- Design and evaluate a catalytically optimized DNAzyme targeted to the sequence of ODC mRNA that is effective at silencing ODC in *in vitro* studies. (Chapter 2)
- Determine whether the catalytically optimized DZ IV can silence ODC in a cell culture model that is more representative of a physiological environment than *in vitro* experiments. (Chapter 3)
- Demonstrate that DZ IV can silence endogenous ODC in a model relevant to the potential clinical uses of a DNAzyme targeted to ODC. (Chapter 4)
- Identify hammerhead ribozyme cleavage sites in ODC mRNA and evaluate the effectiveness of hammerhead ribozymes targeted to ODC at these sites. (Chapter 5)

***II. Small molecules that prevent ODC homodimerization would be effective inhibitors of ODC enzymatic activity.***

**Specific Aim**

- Develop an assay for use as a high-throughput screen to detect ODC inhibitors that mechanistically inhibit ODC by interfering with ODC homodimerization. (Appendix A)

***III. The established ability of a dominant-negative mutant of ODC to revert the transformed phenotype of Ras-transformed cells is mediated through differential gene expression of downstream effector proteins.***

**Specific Aim**

- Use a genomics approach to identify genes downstream of ODC that are essential for Ras transformation in NIH/3T3 cells. (Appendix B)

# Chapter 2

## Identification of DNAzymes That Effectively Target ODC *In Vitro*

### Specific Aim

To design and evaluate a catalytically optimized DNAzyme targeted to the sequence of ODC mRNA that is effective at silencing ODC in *in vitro* studies.

## Introduction

The biosynthesis of putrescine, spermidine and spermine, collectively referred to as polyamines, is well-studied. All known living organisms contain polyamines, with the exception of two orders of Archaea (*114*), and in fact, polyamines are essential for cell growth in humans and other mammals. ODC is the enzyme that decarboxylates ornithine to putrescine, a rate-limiting step in the biosynthesis of polyamines. Deletion of the ODC gene in mice results in lethality at early embryonic stages (*115*) and the importance of ODC in cellular physiology has been further demonstrated in numerous cell culture (*116, 117*) and animal models (reviewed in (*50, 51*)). These studies demonstrate that ODC plays a role in cell transformation and that ODC overexpression renders mouse models more susceptible to tumor development, which can be reversed by reducing ODC activity by either pharmacological intervention or overexpression of antizyme, a protein that targets ODC for degradation (*118*). Therefore, there is keen interest in the development of ODC inhibitors.

ODC is a proven drug target for diverse applications. DFMO is the drug of choice for the treatment of West African trypanosomiasis (sleeping sickness) transmitted by *Trypanosoma brucei gambiense*, but due to poor oral bioavailability, it must be administered intravenously every 6 hr for two weeks—a less than practical proposition in rural hospitals (*119*). DFMO is the only FDA approved drug (labeled as Vaniqa™, 13.9% eflornithine; Bristol-Myers Squibb) for the treatment of unwanted facial hair. It is likely that there are other unrealized uses for ODC inhibitors. The poor pharmacokinetic

profile of DFMO, the limitations of it as a chemotherapeutic/preventative in humans and the scope of "alternative uses" for an ODC inhibitor make the development of improved ODC inhibitors attractive.

ODC is a good candidate for gene silencing because the mammalian protein has a very short half-life (10-60 min, (*120, 121*)) and ODC is highly regulated at the translational level (for review see (*122*)). Due to the rapid turnover of ODC protein, cells are reliant on translation of new protein to maintain or elevate ODC activity. A number of reports have indicated that little to no change in ODC mRNA content is often detected upon substantial increases or decreases in ODC protein content and activity (*29, 32, 123-125*). Reversible inhibitors of ODC protein are at a disadvantage because they prevent ODC from antizyme-mediated degradation and the initial inhibition of ODC would lead to increased ODC transcription by depleting spermidine pools (*89*). Active ODC would accumulate in the cells. Conversely, the efficacy of irreversible inhibitors may be limited by the short $t_{1/2}$ of ODC. Therefore targeting ODC mRNA, rather than protein, may be a better strategy. Antisense-mediated silencing of ODC has been successful (*46, 126*). In one of the studies, an antisense oligodeoxynucleotide (AS-ODN) targeted against the initiation codon regions of ODC silenced the translation of ODC protein in an *in vitro* system (*126*).

Several methods of silencing mRNA have been identified (*100*), including AS-ODNs, ribozymes, siRNA (and miRNA) and DNA enzymes. Although each of the silencing strategies has merits, the 10-23 DNAzyme was chosen for these studies for several reasons. A DNAzyme is comprised of DNA, so it is inherently more stable than the RNA-based ribozyme and siRNA. DNAzymes possess catalytic activity, whereas

AS-ODNs and siRNA rely on cellular machinery to achieve silencing. Moreover, the 10-23 DNAzyme has a favorable catalytic efficiency compared to the hammerhead and hairpin ribozymes. The lower $K_m$ of DNAzymes (*109*), is advantageous because ODC mRNA is not abundant.

These experiments describe the development and evaluation of the 10-23 model DNAzyme directed against the sequence for ODC mRNA. All DNAzymes designed were active in cleaving synthetic ODC RNA *in vitro*. The length of the hybridization arms for one DNAzyme, DNAzyme IV, exhibited good activity and was further analyzed to determine the optimal catalytic efficiency based on the $k_m$ and $K_{cat}$. The catalytically optimized DNAzyme is a promising candidate for further evaluation in cell culture.

## Methods

### *Preparation of Oligonucleotides*

Seven 33-mer oligonucleotides (DZ I, II, III, IV, V ,VI, IV-mut, see Figure 1 for sequences) comprised of a 15 nucleotide domain flanked by equal 9 nucleotide length arms were purchased from Invitrogen Life Technologies (Carlsbad, CA, USA) for use in *in vitro* cleavage studies. A DNAzyme designed against a target unrelated to ODC (DZ-UR) which exhibited extensive *in vitro* cleavage activity against the intended target was purchased from Qiagen Inc. (Valencia, CA, USA, see Figure 2.1). Four additional derivatives of DZ IV (DZ IV- 8/8, 10/10, 11/11, 7/11, see Figure 2.1) with varying hybridization arm lengths were synthesized (Invitrogen Life Technologies) to examine the effect of altering the length of the arms for DZ IV.

### *Preparation of In Vitro Transcript*

To ensure that only full-length RNA substrate was used in the cleavage reaction, the sequence coding for a poly$(A)_{24}$ tail was added 3' to the stop codon of the cDNA encoding for a truncated mouse ODC (425 out of 461 amino acids) lacking the 5' and 3' UTR. Poly(A) purification of the *in vitro* transcribed RNA removed premature transcripts, thereby reducing background in DNAzyme cleavage experiments. To introduce the poly$(A)_{24}$ tail, PCR was performed on pGEM-ODC (425) (*127*)

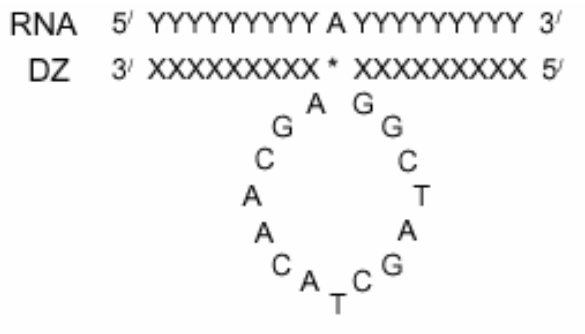


| DNAzyme | 5' Arm | Catalytic Domain | 3' Arm |
|---|---|---|---|
| I | AGCTGCTCA | GGCTAGCTACAACGA | GGTTCTCGA |
| II | CATCAAGGA | GGCTAGCTACAACGA | GTGGCAGTC |
| III | GGTCCAGAA | GGCTAGCTACAACGA | GTCCTTAGC |
| IV | TCCGCAACA | GGCTAGCTACAACGA | AGAACGCAT |
| IV-mut | TCCGCAACA | GGCTA*C*CTACAACGA | AGAACGCAT |
| 8/8 | CCGCAACA | GGCTAGCTACAACGA | AGAACGCA |
| 10/10 | GTCCGCAACA | GGCTAGCTACAACGA | AGAACGCATC |
| 11/11 | GGTCCGCAACA | GGCTAGCTACAACGA | AGAACGCATCC |
| 7/11 | CGCAACA | GGCTAGCTACAACGA | AGAACGCATCC |
| V | TGCTCACTA | GGCTAGCTACAACGA | GGCTCTGCT |
| VI | GCCTTTGGA | GGCTAGCTACAACGA | GTGCTCTGG |
| UR | CTCCACGGCA | GGCTAGCTACAACGA | CAGCTGCAG-T |

**Figure 2.1**: *Sequences and Schematic Representation of DNAzymes and Controls.*

The 10-23 DNAzyme (DZ) is comprised of a 15 nucleotide catalytic domain flanked by target-specific hybridization arms. Cleavage of the RNA occurs 3' to the unpaired purine (A, adenine). The catalytic domain of the DNAzyme is inserted in place of the unpaired A (denoted by asterisk). The sequences of all the DNAzymes used in this study are listed in the table. Six DNAzymes (I, II, III, IV, V and VI) were evaluated *in vitro* and DNAzyme IV, and derivatives of it (listed within the same box), were used in subsequent studies. The sequence for DNAzyme IV-mut, a negative control, is the same as DNAzyme IV, except for a G→C nucleotide change (underlined, italicized C) in the catalytic domain which abolishes cleavage activity. DNAzymes IV 8/8, 10/10, 11/11 and 7/11 are variations of DNAzyme IV in which the length of the 9/9 nucleotide hybridization arms has been altered. A DNAzyme, DNAzyme UR, which effectively cleaves a RNA sequence unrelated to ODC, but whose hybridization arms do not target it to ODC, serves as another negative control.

with the sense primer 5'-CATCTGCTTGATATTGGTGGTGGC-3' and antisense primer 5'-GAACTTGGATCC($T)_{24}$CTAGGCGCCATGGCTC-3' (*Bam*HI site underlined). The PCR product was precipitated, electrophoresed, extracted and gel-purified. pGEM-ODC (425) and the PCR product were digested with *Pfl*MI and *Bam*HI. The digests were precipitated and the PCR product was ligated into pGEM-ODC (425) to make pGEM-ODC (425)-poly$(A)_{24}$. The construct was verified by sequence analysis. The plasmid, pGEM-ODC (425)-poly$(A)_{24}$, linearized by *Bam*HI digestion, was transcribed from the T7 promoter using the AmpliScribe T7 High Yield Transcription kit (Epicentre, Madison, WI, USA) following the manufacturer's instructions. *In vitro* transcription was carried in the presence or absence of [$\alpha$-$^{32}$P]-UTP (3 μCi/pmol, PerkinElmer, Boston, MA, USA). The full-length transcript was purified from premature transcripts by poly(A) purification using Ambion's (Austin, TX, USA) Poly(A) Purist reagents and procedure. This synthetic ODC RNA contained 1381 nucleotides—1274 nucleotides coding for ODC with an additional 104 nucleotides resulting from cloning the gene into the vector and the addition of the poly$(A)_{24}$ tail. The $^{32}$P-labeled synthetic RNA substrate was used to evaluate DNAzyme-mediated cleavage of the RNA and for kinetic analysis, while the unlabeled synthetic RNA was used as the substrate for experiments in which the DNAzyme-incubated RNA was subsequently translated *in vitro* (ODC translation and ODC activity experiments).

***DNAzyme-Mediated Cleavage Reaction***

Poly$(A)_{24}$ purified, $^{32}$P-labeled ODC RNA substrate was heat denatured at 65°C for 5 minutes then immediately cooled in an ice water bath. 16 µl of the substrate mix containing $^{32}$P-labeled RNA substrate was added to 4 µl of the enzyme mix containing either respective DNAzyme or nuclease-free $H_2O$ (No DZ reaction) to initiate the reaction. The reactions were incubated at 37°C for 60 min at which time 20 µl of Stop Solution (71% formamide, 22 mM EDTA and loading dye) was added to terminate each reaction and the reactions were placed on ice. The incubated reactions contained 1 pmol of poly$(A)_{24}$ purified, $^{32}$P-labeled ODC RNA and 10 pmol of respective DNAzyme (or nuclease-free $H_2O$) in DNAzyme Buffer (final concentration: 5 mM Tris, pH 7.5, 30 mM NaCl, 10 mM $MgCl_2$). A 12 µl aliquot of each reaction was electrophoresed on a 5% denaturing polyacrylamide gel containing 7 M urea. Gels were dried and the radiolabeled RNA was detected using a PhosphorImager and quantified with ImageQuant software (Molecular Dynamics, Sunnyvale, CA, USA, Figure 2.2).

***Protein Translation and Activity Determination of Translated ODC RNA Preincubated with DNAzyme***

ODC RNA treated with DNAzyme was further analyzed by translating the RNA into protein. The percent translated full-length protein and the activity of the translated protein were measured (Figure 2.2). The DNAzyme-mediated cleavage reactions were carried out as described above, except unlabeled ODC RNA was substituted for the $^{32}$P-labeled RNA. Increased reaction volumes were used, however the concentrations and

ratios of all reactions components remained constant. Following the DNAzyme-mediated cleavage reaction, the RNA was precipitated, heated at 65°C for 3 min, cooled in an ice water bath and translated into protein using the Flexi Rabbit Reticulocyte Lysate System (Promega, Madison, WI, USA) according to the manufacturer's instructions. One 25 µl reaction contained the precipitated DNAzyme-treated RNA substrate, 70 mM KCl, 2 mM DTT, 0.2 mM amino acids minus methionine, 20 units RNasin Ribonuclease Inhibitor, 16 µl Flexi Rabbit Reticulocyte Lysate and either 1.5 µl of L-[$^{35}$S]-methionine (15 µCi, 12.5 µmol, PerkinElmer, for use in the protein translation experiments) or 40 µM of unlabeled methionine (for use in ODC activity experiments). The reactions were incubated at 30°C for 90 min. An aliquot of the reactions incubated with the L-[$^{35}$S]-methionine was electrophoresed on a 12.5% polyacrylamide gel to determine the relative amount of ODC protein translated from the DNAzyme-treated ODC RNA template. The gels were dried and the protein bands representing ODC were quantified with a PhosphorImager and ImageQuant software (Molecular Dynamics). The specific activity of ODC was determined on an aliquot of the translation reaction in which unlabeled methionine was used. ODC activity was determined by measuring the release of $^{14}CO_2$ from L-[1-$^{14}$C]ornithine as previously described (*128*). The data is reported as the average of two or more experiments.

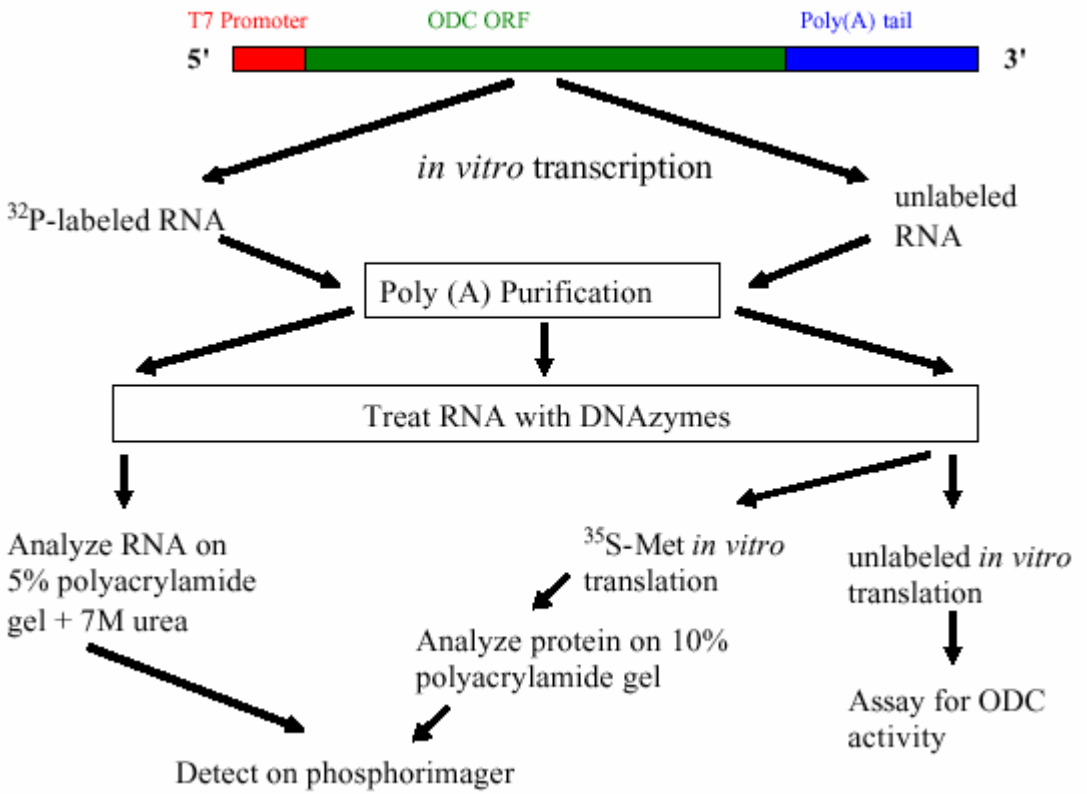


**Figure 2.2**: *Schematic Representation of the Experimental Design for the In Vitro Analysis of the DNAzymes.*

ODC was transcribed, in the presence or absence of [α-$^{32}$P]-UTP, from a linearized plasmid in vitro. Labeled and unlabeled full-length transcript was purified from premature transcripts via a poly(A)24 tail using oligo(dt) cellulose. After treating the transcribed RNA with DNAzymes, the paths for the labeled and unlabeled RNA diverged. The DNAzyme-cleaved $^{32}$P-labeled RNA products were separated from the full-length RNA substrate by electrophoresis and detected on a phosphorimager to determine whether the DNAzyme effectively cleaved the RNA. The unlabeled DNAzyme-treated RNA was translated in vitro in a reaction mix with or without $^{35}$S-methionine. The $^{35}$S-labeled protein/polypeptides was resolved by gel electrophoresis and detected and quantitated with a phosphorimager to determine the amount of translated full-length ODC. The unlabeled protein was assayed for ODC activity.

*Kinetic Assays*

The amount of substrate cleaved by DNAzyme IV was determined by comparison to a standard curve created using a fragment of RNA (referred to as DZ Standard). DZ Standard was constructed by PCR using pGEM-ODC (425) as the template. PCR was performed on the template linearized with *Bam*HI and/or *Sal*I using a sense primer (5'-CACGACGTTGTAAAACGACGGC-3') upstream of the promoter and start codon and a downstream antisense primer (5'-$(T)_{18}$TAGAACGCATCCTTATCGTCAG-3'). When transcribed, the resulting RNA was the same size and sequence as ODC RNA cleaved by DNAzyme IV, except for a poly$(A)_{18}$ nucleotide tail at the 3' end used to purify full-length DZ Standard. The PCR product was gel-purified and precipitated. Linearized pGEM-ODC (425)-poly$(A)_{24}$ and the PCR product coding for DZ Standard were transcribed in the presence of [$\alpha$-$^{32}$P]-UTP and poly(A) purified as described above. Both were transcribed side-by-side under the same conditions using the same lot of [$\alpha$-$^{32}$P]-UTP so that equimolar amounts of the 5' cleavage product from ODC RNA reacted with DZ IV and DZ Standard would give equal signal intensity. The kinetic assays were performed under multiple-turnover conditions. The reaction was initiated by adding equal volumes (10 µl) of enzyme mix and substrate mix. The enzyme mix contained 0.5 pmol of DZ IV- 8/8, 9/9, 10/10, 11/11 or 7/11 or no DNAzyme (nuclease-free $H_2O$). The substrate mix consisted of one of seven varied concentrations of labeled ODC RNA. In the final reaction mix, ODC RNA concentrations ranged from 0-5 µM and the final buffer concentration was the same as for the *in vitro* cleavage reactions. After incubation for 20 min at 37 °C, the reaction was terminated with the addition of 180 µl of DNAzyme Stop Solution and placed on ice. For any given substrate concentration, <10% of the substrate

was converted to product. Cleavage products were resolved from substrate by gel electrophoresis. Each gel contained the entire range of points for the kinetic analysis of one DNAzyme along with a standard curve. The standard curve consisted of six concentrations of DZ Standard ranging from 0-2 pmol, which bracketed the concentration of product formed. Bands representing product and standard were quantified as described before. Background directly above and below each band of interest was subtracted from that band to negate the difference in background due to the varying substrate concentrations. The amount of product formed was converted to pmol using the standard curve, and rectangular hyperbola plots were generated in SigmaPlot 2000 (ver. 6.00, SPSS Inc., Chicago, IL, USA) to fit the Michaelis-Menten equation, $k_{obs} = (k_{cat}\ [S]) / (K_m + [S])$.

## Results

### *DNAzyme Design and Cleavage of In Vitro Transcribed ODC RNA*

Six 10-23 DNAzymes targeted to cleave mouse ODC mRNA were designed and evaluated *in vitro*. The initial evaluation was performed with 33-mer oligonucleotide DNAzymes comprised of a central 15 nucleotide catalytic domain (5'-GGCTAGGTACAACGA-3') and flanked by two nine nucleotide arms (Figure 2.1). Nine nucleotide length arms were chosen based upon previously determined kinetics (*110*). The variable flanking arms confer the specificity of the DNAzymes to target the sequence for ODC mRNA through Watson-Crick base pairing. Two additional DNAzymes, DZ IV-mut and DZ-UR, served as negative controls. The hybridization arms of DZ IV-mut are complementary to ODC RNA, but DZ IV-mut contains a G→C mutation at position 6 of the catalytic domain, which has been demonstrated previously to abolish the cleavage activity of the 10-23 DNAzyme (*110*). DZ-UR is an unrelated DNAzyme that effectively cleaves RNA unrelated to ODC (data not shown). The substrate recognition arms of DZ-UR are not complementary to ODC, but it contains an intact catalytic domain. The 18 nucleotide substrate recognition arms span a 19 nucleotide stretch of the target RNA, with the asterisk representing a purine of the target RNA that is unpaired in the DNAzyme (Figure 2.1). The cleavage reaction occurs at the phosphodiester bond between this unpaired purine and the adjacent 3' pyrimidine; A-U and G-U are reportedly the preferred sites (*129*). Therefore the six ODC DNAzymes

were designed to target A-U sites toward the 5' end of a long RNA (1381 nucleotides), which encodes for the first 425 of 461 amino acids of mouse ODC. Truncations near the C-terminus of ODC stabilize the protein by decreasing the rate of degradation, while not affecting activity of the enzyme (*127, 130*). Although DNAzymes exhibit better activity against short RNA substrates (*131*), the long RNA was chosen over a short fragment of ODC RNA for *in vitro* experiments because it more closely represents the endogenous ODC mRNA.

The predicted secondary structure of full-length ODC mRNA (with 5' and 3' UTRs) is very complex, as expected for a protein that is highly regulated at the translational level (Figure 2.3). It is believed that DNAzymes cleave better at single stranded regions within folded mRNA than regions in which the mRNA base pairs with another region of the mRNA. All the DNAzymes, except DZ III, were targeted to these so called single-stranded "bulge" regions as predicted by the mRNA secondary structure. Initial *in vitro* characterization determined that all six DNAzymes were capable of cleaving *in vitro* transcribed ODC RNA. Figure 2.4 represents the cleavage sites in ODC RNA targeted by the DNAzymes and the expected cleavage products upon successful cleavage. All six DNAzymes cleaved the target RNA and the size of the cleavage products agreed with the targeted site of DNAzyme cleavage of the ODC RNA (Figure 2.4B). DZ I targets the start codon for ODC, a site that had been previously successfully targeted by an 18-mer AS-ODC (*126*). Cleavage occurs at this site, but it is less complete than some of the other DNAzymes (e.g. DZ III, IV). No cleavage of ODC RNA was detectable for the negative control reactions: No DZ, DZ IV-mut and DZ-UR. This suggests that; (1) the reaction components, minus a DNA oligo, are not sufficient for

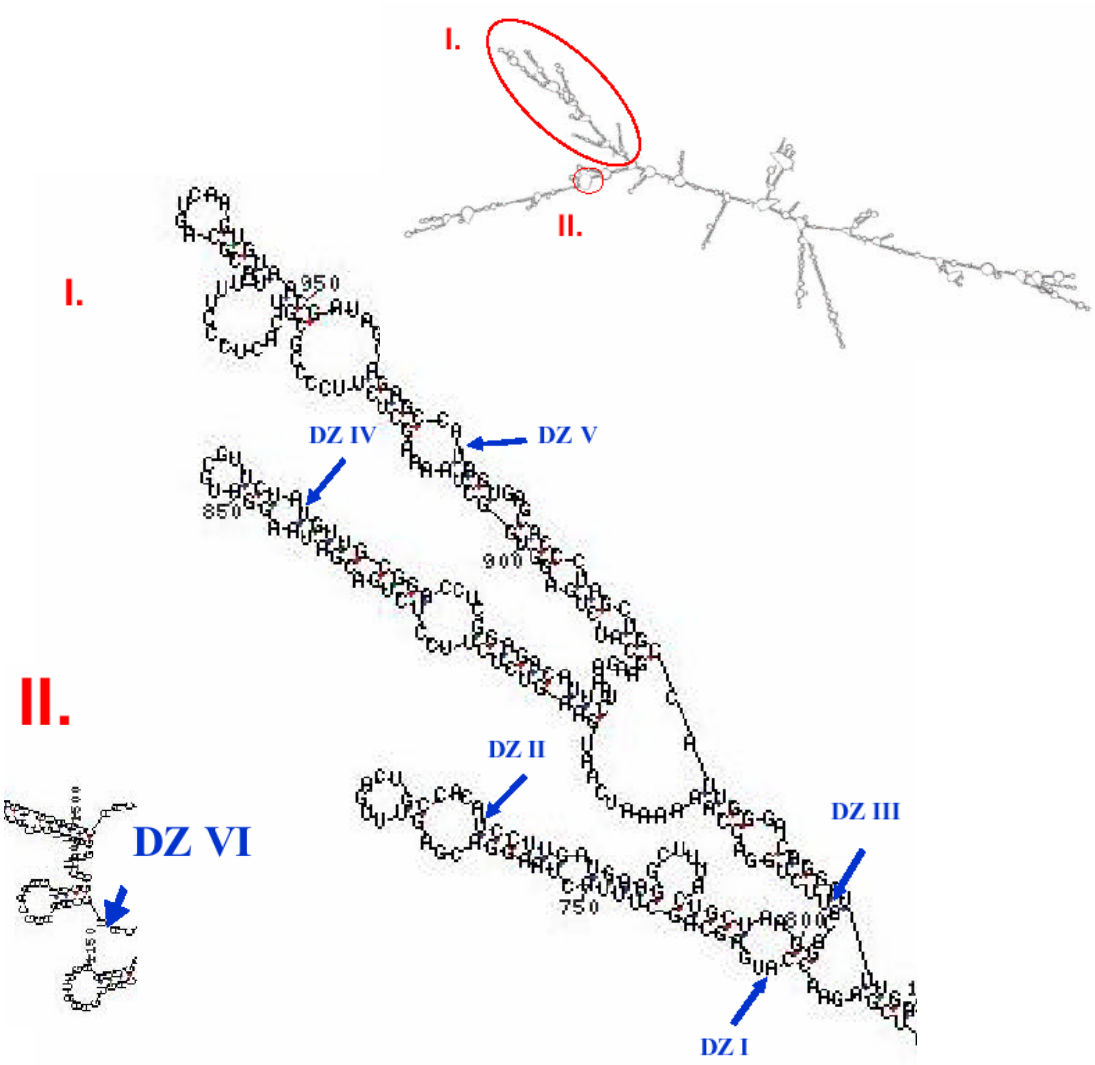


**Figure 2.3:** *Targeted DNAzyme Sites Within ODC mRNA.*

The structure of ODC mRNA (with 5' and 3' UTRs) was modeled using mFOLD modeling program (http://www.bioinfo.math.rpi.edu/~zukerm/rna/). This structure represents the form with the lowest free energy. Region I and II are enlarged to show the regions targeted by DNAzymes. DNAzymes I-V target sites within Region I; DZ VI targets a site in Region II. All DNAzymes target cleavage at A-U junctions.

A.

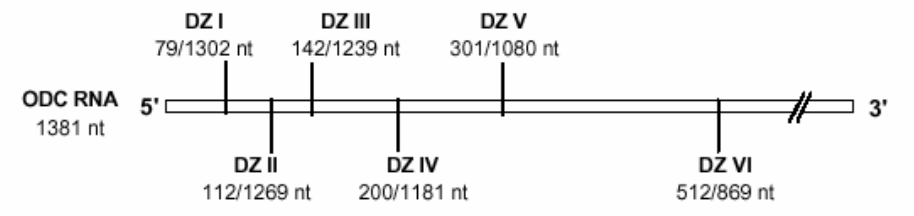


B.

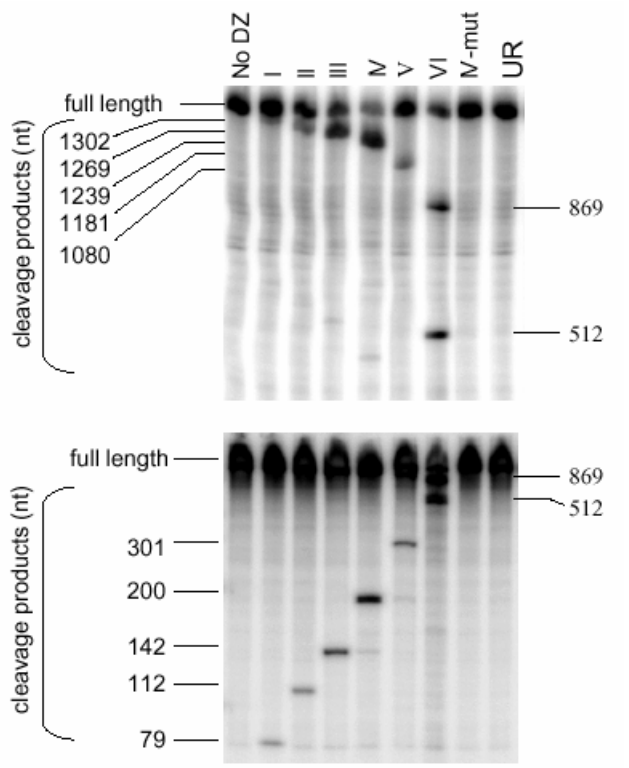


**Figure 2.4**: *In vitro Cleavage of ODC RNA by DNAzymes.*

A schematic representation of ODC RNA indicating the targeted cleavage sites for each DNAzyme. Labels indicate size of the expected RNA products (in nucleotides) after successful cleavage by the different DNAzymes (A). 10 pmol of DNAzyme I, II, III, IV, V and VI or controls were incubated with 1 pmol of $^{32}$P-labeled ODC RNA for 60 min at 37° C (B). The smaller cleavage product was resolved on a second gel (B, lower panel). Each DNAzyme cleaved the target at the intended site. No cleavage was detected in the absence of DNAzyme (No DZ) or with negative controls IV-mut (DNAzyme IV with mutation in catalytic domain) and UR (unrelated DNAzyme).

RNA degradation (Figure 2B, No DZ), (2) an intact catalytic domain is necessary for cleavage to occur—the mutation in the catalytic domain of DZ IV-mut abolishes cleavage activity (Figure 2.4 B, IV-mut) and (3) arms that target the DNAzyme to Watson-Crick basepair with a specific region of the substrate are necessary for the cleavage reaction, as no cleavage was observed with DZ-UR (Figure 2.4 B).

### *Evaluation of Translated DNAzyme-Treated ODC RNA*

Translation of ODC RNA cleaved by a DNAzyme is expected to result in lower protein yield and less ODC activity compared to translation of untreated ODC RNA. To test this, ODC RNA treated with DNAzymes or controls was translated *in vitro* either in the presence or absence of L-[$^{35}$S]-methionine. An aliquot of the L-[$^{35}$S]-methionine reaction was electrophoresed and the band representing the labeled protein translated from the uncleaved ODC RNA was quantified (Figure 2.5, black bars). The results are presented as percentage of expressed protein compared to the translation of ODC RNA that was not treated with a DNAzyme (No DZ), which was taken as 100% translation. All six of the DNAzymes (DZ I, II, III, IV, V, VI) reduced the percent protein translated by at least 40%. DNAzyme II, III and IV showed the greatest reduction (84%, 91%, and 94% respectively). The two negative controls, DZ IV-mut and DZ-UR, did not decrease the amount of protein translated compared to No DZ and actually increased it slightly (particularly DZ IV-mut). It is possible that these controls stabilize the RNA template and facilitate translation and/or reduce degradation. The sites of cleavage of the

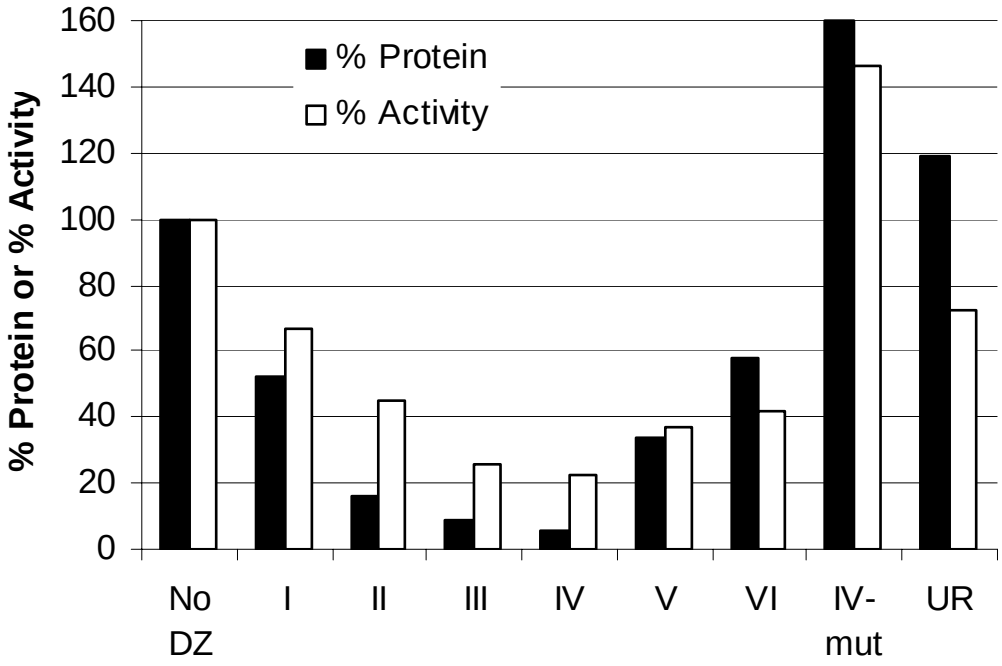


**Figure 2.5**: *In Vitro Translation of DNAzyme-Treated ODC RNA.*

Following DNAzyme treatment, ODC RNA was translated *in vitro* to determine the relative amount of ODC protein translated (black bars) and ODC activity (white bars). No DZ (no DNAzyme) was taken to be 100% for both measurements. Data represents the average of at least two experiments.

DNAzymes are such that, even if the cleaved 5' fragment of the RNA was translated, the truncated polypeptides would not have ODC activity. A decrease in translated protein would be expected to result in decreased ODC activity and to determine this, L-[$^{35}$S]-methionine was replaced with unlabeled methionine in the translation mix and ODC activity was determined for an aliquot of the translation reaction. The ODC activity profile for the DNAzymes and controls (Figure 2.5, white bars) closely follows the percentage of translated protein results. DNAzyme III (26%) and IV (22%) show the lowest ODC activity compared to no DNAzyme control (No DZ). These results establish that DNAzyme-mediated cleavage of ODC RNA, for all six DNAzymes, functionally results in reduced ODC protein, thereby silencing ODC activity. The degree of protein and activity reduction correlates well and reduction in both these measures is dependent upon the ability of each DNAzyme to cleave ODC RNA.

### *Kinetic Analysis of the Effect of Altering Hybridization Arm Length*

Previously, the activity of DNAzymes has been demonstrated to be dependent upon hybridization arm length (*110, 132*). It is apparent from looking at the catalytic cycle of the 10-23 DNAzyme why the length of the arms can affect the catalytic activity (Figure 2.6). Both the rate of formation of the enzyme-substrate complex (DNAzyme-RNA complex) and the rate of release of the products could be altered with changes in the length of the hybridization arms. The optimal length of the hybridization arms is dependent on the RNA substrate, specifically the composition and structure.

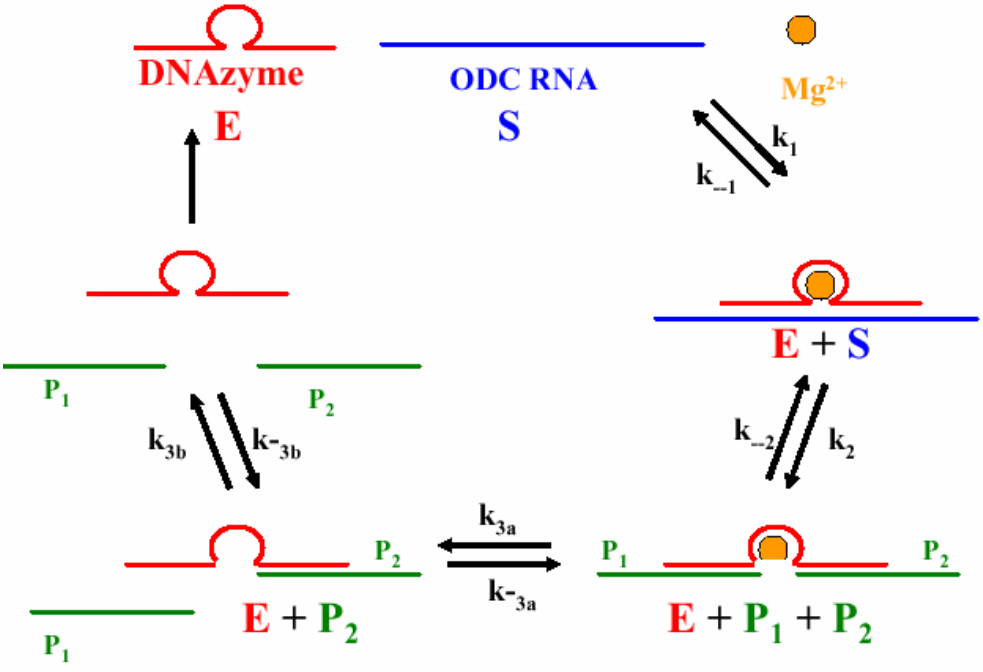


**Figure 2.6**: *Catalytic Cycle of the 10-23 DNAzyme.*

Free DNAzyme (the enzyme) hybridizes to the substrate RNA via the hybridization arms ($k_1$). Upon forming the enzyme-substrate complex, the DNAzyme, with the aid of a divalent cation (e.g. $Mg^{2+}$) catalyzes the cleavage of a phosphodiester bond between an unpaired purine and paired pyrimidine ($k_2$). The RNA substrate is converted into two products at this step, $P_1$ and $P_2$. The two products dissociate from the hybridization arms of the DNAzyme. Although often this is considered one step for simplicity, the rate of release of $P_1$ and $P_2$ are two separate rates ($k_{3a}$ and $k_{3b}$). These rates are dependent upon the base composition and structure of each product and likely affected by the rate of release of each other. Once both products dissociate from the DNAzyme, the enzyme is free to catalyze another cycle.

We sought to determine the optimal length arms for DNAzyme IV—a promising candidate based upon the previous experiments. A new method to determine enzyme kinetics was developed to avoid potential issues with the dynamic range of the densitometer when quantitating bands at higher substrate concentrations. This approach utilized a standard curve to quantitate the cleavage product. A linear DNA template coding for the first 79 nucleotides of ODC RNA plus a poly$(A)_{18}$ tail at the 3' end was constructed. Transcription of this template produced RNA, referred to as DZ Standard, the same size and sequence as that produced by the cleavage of ODC RNA by DNAzyme IV, plus the addition of a poly$(A)_{18}$ tail at the 3' end. Kinetic experiments were carried out under steady-state, multiple-turnover conditions for DNAzyme IV with varying length hybridization arms: 8/8, 9/9, 10/10, 11/11 and 7/11 (where the first number represents the 5' hybridization arm and the second number the 3' arm). Figure 2.7A is a representative gel of a kinetic experiment for DNAzyme IV 9/9. Aliquots of reactions with increasing concentrations of ODC RNA and DZ Standard were resolved by electrophoresis. The bands representing the 79-nucleotide product and DZ Standard were quantitated by densitometry. The DZ Standard runs higher than the cleavage product because of the additional 18 nucleotides of the poly$(A)_{18}$ tail of the DZ Standard. A standard curve, generated from the DZ Standard data, was used to convert the product band into pmol and this data was plotted using the Michaelis-Menten equation to determine the apparent $K_m$ and $k_{cat}$ (Figure 2.7B).

Lengthening the hybridization arms can affect the kinetics of the DNAzyme, in theory, by lowering the $K_m$ (assuming this does not alter the DNAzyme's accessibility to the RNA). However, this may also stabilize the interaction of the DNAzyme and RNA

A.

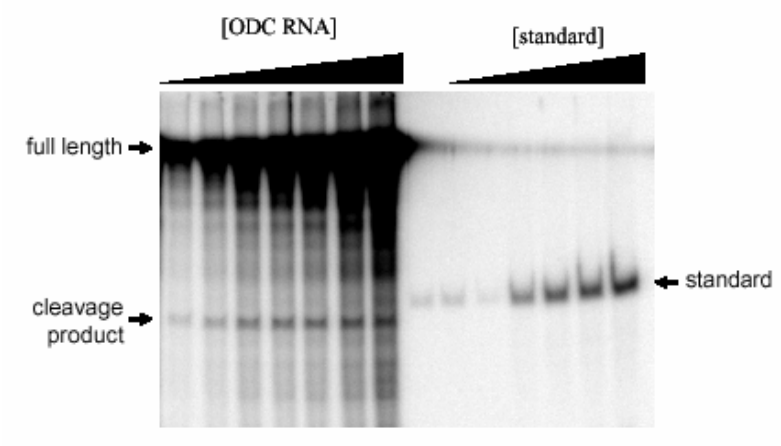


B.

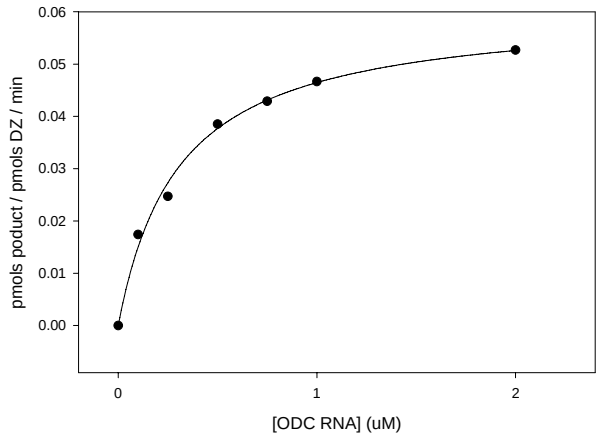


**Figure 2.7**: *Determination of Kinetic Parameters.*

$K_m$ and $k_{cat}$ values were determined under multiple turnover conditions in the presence of 10 mM $MgCl_2$. The 5' cleavage product was separated on a gel from the uncleaved $^{32}$P-labeled ODC RNA and the signal of the cleavage product was converted into pmol by comparison to a standard curve (representative gel in A). The standard used to create the curve was the same sequence and size as the 5' cleavage product, but had the addition of a poly$(A)_{18}$ tail used to purify it, which caused the standard to run slightly higher. $K_m$ and $k_{cat}$ were determined from a rectangular hyperbola plot fitted to the Michaelis-Menten equation (B).

substrate, hence slowing the rate of product release and reducing the $K_{cat}$. DNAzyme IV with arm lengths that result in the optimal balance between the $K_m$ and $k_{cat}$ will be the most catalytically efficient. It was found that the $K_m$ for DNAzyme IV decreases by ~50% when the arm lengths are increased from 8/8 (0.65μM) to 9/9 (0.30 μM) nucelotides, with a further decrease to 0.16 μM at 11/11 nucleotides (Figure 2.8A). No change in the $k_{cat}$ is detected between DNAzyme IV 8/8 (0.062 $min^{-1}$) and 9/9 (0.061 $min^{-1}$) nucleotide length arms, but it does decrease step-wise when the length is increased to 10/10 (0.046 $min^{-1}$) and 11/11 (0.026 $min^{-1}$) nucleotides. The offset 7/11 length arms displayed the highest $K_m$ and lowest $k_{cat}$. By virtue of combining the highest $k_{cat}$ and moderate $K_m$, DZ IV with 9/9 nucleotide length arms attains the greatest catalytic efficiency (measured by $k_{cat}/K_m$, Figure 2.8B). Despite having a $k_{cat}$ equal to that of DNAzyme IV- 9/9, the catalytic efficiency of DNAzyme 8/8 is less favorable due to the high $K_m$. The differences in the $K_m$ and $k_{cat}$ for 10/10 and 11/11 offset each other resulting in similar catalytic efficiencies.

A.

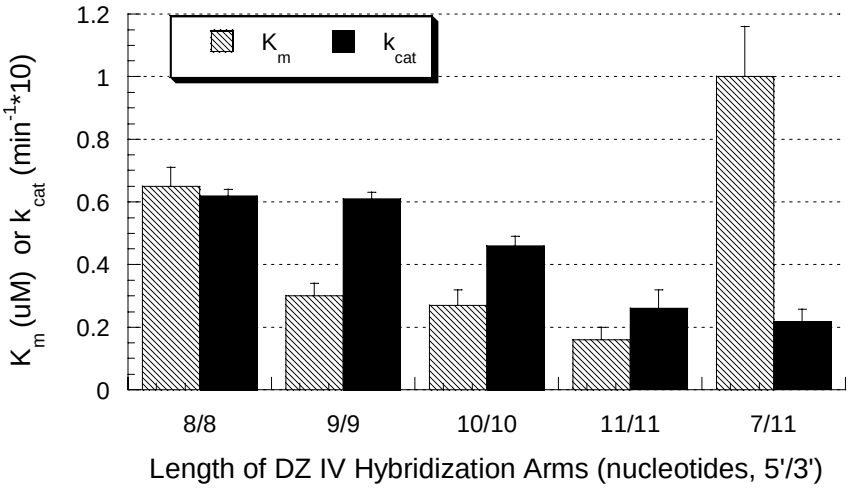


B.

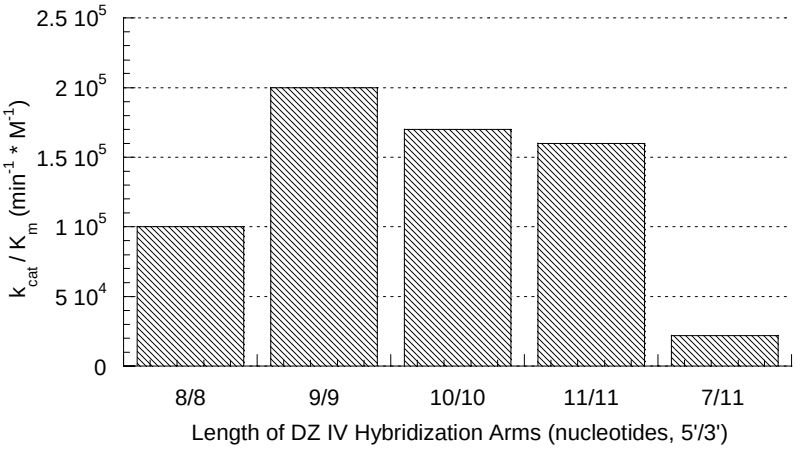


**Figure 2.8**: *Effect of Altering Hybridization Arm Length on DNAzyme IV Kinetics.*

$K_m$ and $k_{cat}$ values for each arm configuration are plotted in A. Error bars represent standard deviation derived from the curve fit for a representative experiment. Catalytic efficiency ($k_{cat}/K_m$) was calculated for the DNAzymes (B).

**Discussion**

ODC is a validated drug target and the ability to modulate its activity is proven (i.e. African sleeping sickness and unwanted facial hair) and potential applications (e.g. chemopreventative/therapeutic uses). ODC is tightly regulated at the translational level and the protein has a very short half-life, thereby making it an attractive target for gene silencing via mRNA cleavage. The 10-23 model DNAzyme was chosen as the method to silence ODC based on the stability, catalytic activity and the diverse applications of this method.

Six DNAzymes were designed and all exhibited the ability to cleave an *in vitro* transcribed ODC transcript at the targeted site (Figure 2.3), but the extent to which each cleaved ODC RNA differed. This is illustrated in Figure 2.4, in which the DZ-reacted ODC RNA was translated *in vitro*. The extent of cleavage is reflected by the amount of protein translated and the resulting ODC activity. Even though successful DNAzyme cleavage sites are much more readily identified in short RNA substrates versus long RNA, a long RNA substrate (1381 nucleotides) was chosen for these studies to better recapitulate the mRNA that the DNAzyme would encounter in the cell. Previous studies have reported as few as 10% of DNAzymes designed to putative target sites were very effective at cleaving long (>700 nucleotides) RNA substrates (*133, 134*).

Next, the catalytic efficiency of the DNAzyme was optimized by altering the length of the hybridization arms. Limitations of the method most widely used to determine DNAzyme kinetics lead us to develop a new method. Most of the reports describing DNAzyme kinetics use a method in which the concentration of product

formed is determined by quantitating the fraction of cleaved and uncleaved RNA resolved by gel electrophoresis and comparing this percentage to the known amount of substrate RNA used in the reaction. This method is not ideal for determining kinetics under multiple turnover (saturating substrate concentrations) conditions in which only a small percentage of the substrate is being converted to product at the lowest substrate concentration. The difference in the intensity of the bands representing the product formed at the lowest substrate concentration and the uncleaved substrate at the highest substrate concentration makes it difficult to measure both bands accurately. For example, if the range of substrate concentration used is 10-fold below and above the $K_m$ and the reaction is not allowed to surpass 10%, then the densitometer would need to have a dynamic range capable of linear quantitation of signals differing 1000-fold for end-labeled RNA. The range could be even greater for internally labeled RNA. The difference in band intensities may exceed the linear dynamic range of the instrument software used to quantitate the bands.

This problem is circumvented in the method described here because only the bands representing the product formed are quantitated. The intensity of these bands is converted into amount of product formed by comparison to a standard curve of known concentration (Figure 2.7). Internally labeled RNA was used for these studies, but end-labeled RNA would work well with this method also.

It has been demonstrated that the length of the hybridization arms affects the catalytic efficiency of DNAzymes (*110, 132, 135*). The optimal length is likely to be target specific, depending on the GC content and structure of the RNA. DZ IV was chosen for optimization because it showed favorable results in the *in vitro* experiments

(Figure 2.3, 2.5). Also, the same region of ODC targeted by DZ IV was identified by a ribozyme SELEX screen (*136*) to be an optimal site for ribozyme targeting, which suggests that this is an accessible site of the RNA molecule (see Chapter 5). It was expected that the $k_{cat}$ and $K_m$ would both decrease as the length of the hybridization arms increased from 8 to 11 nucleotides. In general, this was the case, however no change in the $k_{cat}$ was observed between 8 and 9 nucleotide length arms. In the kinetic analysis performed by Santoro and Joyce (*110*), similar results were observed with a 27 nucleotide synthetic RNA substrate and DNAzyme unrelated to ODC. They observed that the $k_{cat}$ remained relatively constant for hybridization arms 7-9 nucleotides in length and then decreased step-wise when lengthened beyond 9 nucleotides because the rate-limiting step shifts from the rate of cleavage (for arm lengths ≤ 9 nucleotides) to the rate of product release (for arm lengths ≥ 10 nucleotides). Nine nucleotides was the most catalytically efficient length for the hybridization arms for DZ IV. The DNAzyme with the offset arms (7/11) exhibited the least favorable kinetics—the highest $K_m$ and lowest $k_{cat}$. A previous study that investigated the effect of asymmetric length arms of a DNAzyme on the $k_{obs}$ found no distinct pattern to help predict the effect of arm asymmetry (*137*).

Others have concluded that it is difficult, or even impossible, to determine kinetics for DNAzymes and ribozymes using long RNA substrates because the cleavage rates are so low (*131, 138*). The $K_m$ (0.3 μM) and $k_{cat}$ (0.06 $min^{-1}$) for DZ IV 9/9 are similar to those previously reported for DNAzymes designed to different targets (*132, 135, 139, 140*) despite differing conditions which can have a profound negative impact on the activity of DNAzymes. Catalytic nucleic acids targeted against long RNA substrates versus short RNA substrates reportedly exhibit activities several orders of

magnitude lower (*131, 138, 141, 142*). The 1381 nucleotide RNA target used for this study was much longer than the short RNA substrates employed in other DNAzyme kinetic studies (≤27 nucleotides (*132, 140*), 92 and 121 nucleotides (*135*)). Elevated concentrations of $Mg^{2+}$ have been shown to increase the catalytic rate of the 10-23 DNAzyme (*109*). The 10 mM $MgCl_2$ concentration used in this study was significantly less than the 25 mM concentration used in other studies in which kinetics were determined and is more physiologically relevant (*135, 139*). In spite of these differences, the kinetics for DZ IV-9/9 were comparable to DNAzymes targeting short RNA targets and some of which used higher concentrations of $MgCl_2$.

We have identified DNAzymes that cleave a long transcript of ODC and subsequently reduce the amount of translated ODC protein resulting in a concomitant decrease in activity *in vitro*. A new method to determine kinetics for DNAzymes was developed and using this method, it was found that the optimum hybridization arm length for DZ IV was 9/9 nucleotide length arms. The $K_m$ and $k_{cat}$ for DZ IV 9/9 compared favorably to the kinetics reported for other DNAzymes even when the other studies were performed under conditions favoring the enhancement of kinetics (i.e. short RNA substrates, higher $Mg^{2+}$ concentrations).

In conclusion, DZ IV with 9 nucleotide length arms displays good *in vitro* activity. However for a surprisingly high percentage of DNAzymes, *in vitro* activity does not translate into effective DNAzymes in cell culture or *in vivo*. The next stage of development is to test the activity of DZ IV in cell culture.

# Chapter 3

## Evaluation and Application of ODC DNAzymes in Cell Culture

### Specific Aim

To determine whether the catalytically optimized DZ IV can silence ODC in a cell culture model that is more representative of a physiological environment than *in vitro* experiments.

## Introduction

In Chapter 2, DNAzymes were identified that demonstrated good cleavage activity *in vitro*. The catalytic activity of one DNAzyme, DZ IV, was optimized. *In vitro* characterization is a first and necessary step in DNAzyme development, but *in vitro* activity has proven to be a poor predictor of DNAzymes that are active in cell culture and *in vivo*. DNAzymes encounter several additional obstacles in cell culture and *in vivo*, where they must silence endogenously folded mRNA with complex secondary and tertiary structure. The mRNA may also be bound to proteins that can protect the mRNA from the DNAzyme. The DNAzyme is subjected to nucleases which can potentially degrade it. Temporal and spatial considerations also determine whether the DNAzyme is active.

This chapter describes experiments designed to determine if one of the DNAzymes that exhibited good *in vitro* activity is active in cell culture when exposed to the aforementioned obstacles. A co-transfection method was used in which the DNAzyme and target ODC are together transfected into cells and the DNAzymes are evaluated by measuring ODC activity. Because basal ODC activity is near the limit of detection in most unmodified cell lines, including the HEK 293 cells used in these experiments, measuring ODC activity also selects for the cells that were transfected with DNAzyme (assuming that the cells that take up the plasmid coding for ODC also take up the DNAzyme). This allows an accurate assessment of DNAzyme activity. Using this model, it was determined that the catalytically optimized DZ IV is effective at silencing

ODC mRNA in cell culture—a model representative of a physiological environment in which the DNAzyme is exposed to nucleases and compartmentalization and accessibility of ODC mRNA is limited by its folded structure and interactions with cellular transcription and translation machinery.

## Methods

### *Preparation of Oligonucleotides*

The following oligonucleotides were purchased from Qiagen Inc. (Valencia, CA, USA) with an inverted 3' T (3'-3' phosphodiester linkage, denoted by "-T") to protect the DNA from degradation (*132*): DZ IV-T, DZ IV-mut-T, DZ IV-SCR-T, IV-tamra-T, NS-T, DZ III-T, DZ V-T and AS IV-T (Table 3.1).

### *Fluorescence Microscopy*

NIH/3T3 + pMV7eIF4E cells (P2 cells, (*143, 144*)) were cultured in complete growth medium (Dulbecco's modified Eagle's medium supplemented with 10% (v/v) fetal calf serum and 100 μg/ml penicillin and streptomycin and 333 μg/ml G418) at 37°C with 5% $CO_2$. NIH/3T3 + pMV7eIF4E cells were plated (2.5 x $10^5$ cells) in 6 well plates containing coverslips in each well. Two days later, DZ IV-tamra (Qiagen) was transfected into the cells using siPORT Lipid (Ambion, Austin, TX) transfection reagent, according to the manufacturer's recommendation, with or without transfection reagent. The final concentrations of DZ IV-tamra were either 0.1 or 0.5 μM (1.1 or 5.5 μg per well respectively). Two days post-transfection, the cells were incubated with 80 μg

| DNAzyme | 5' Arm | Catalytic Domain | 3' Arm |
|---|---|---|---|
| IV-T | TCCGCAACA | GGCTAGCTACAACGA | AGAACGCAT-T |
| IV-mut-T | TCCGCAACA | GGCTACCTACAACGA | AGAACGCAT-T |
| IV-SCR-T | ACAACGCCT | GGCTAGCTACAACGA | TACGCAAGA-T |
| IV-tamra-T | tamra-TCCGCAACA | GGCTAGCTACAACGA | AGAACGCAT-T |
| NS-T | NNNNNNNNN | NNNNNNNNNNNNNNN | NNNNNNNNN-T |
| III-T | GGTCCAGAA | GGCTAGCTACAACGA | GTCCTTAGC-T |
| V-T | TGCTCACTA | GGCTAGCTACAACGA | GGCTCTGCT-T |

AS IV-T TCCGCAACATAGAACGCAT-T

**Table 3.1**: *Sequences and Schematic Representation of DNAzymes and Controls*.

All the DNAzymes are comprised of a 15 nucleotide catalytic domain flanked by 9 nucleotide target-specific hybridization arms. The DNAzymes and controls used for cell culture studies contained an inverted 3' T (denoted in sequence by "-T") to enhance stability. The sequences for DNAzyme IV-T, IV-mut-T, III-T and V-T are the same as the sequences for DNAzyme IV, IV-mut, III, and V (Figure 2.1) except that each contains an inverted 3' T. The hybridization arms of DNAzyme IV-SCR-T are comprised of the same nucleotide composition as DNAzyme IV, except that the sequence is scrambled so the arms do not target the DNAzyme to basepair with the sequence for ODC mRNA. NS-T is a degenerate 33mer (plus the inverted 3' T) oligo which does not contain a catalytic domain or ODC-specific hybridization arms. DZ IV-tamra-T is an oligo with the same sequence as DZ IV-T except with a fluorescent tamra dye attached to the 5'-end of the oligo. An antisense ODN targeting the same sequence of ODC mRNA as DZ IV was also designed (AS IV-T). AS IV-T does not contain the sequence for the catalytic domain.
(N = A, C, G or T)

Hoechst 33342 for 10 min at 37ºC. Cells were washed with 1 ml of cold PBS and fixed in methanol. The coverslips were removed from the bottom of the wells, fixed on slides and viewed with a fluorescent microscope under 32x magnification.

***Confocal Fluorescence Microscopy***

P2 cells were plated (3 x $10^5$ cells) in 3.5 cm glass bottom petri dishes (Matek Corp., Ashland, MA). These plastic petri dishes have a 0.16-0.19 mm glass coverslip affixed underneath the dish over a 10 mm hole cut in the bottom of the dish. Live cells can be viewed on these dishes with the same optical quality of a glass coverslip. Two days later, 2 µg of DZ IV-tamra was transfected into the cells using a transfection reagent or no transfection reagent. Six transfection reagents were tested: DOTAP (Roche, Indianapolis, IN), Lipofectamine with Plus Reagent (Invitrogen, Carlsbad, CA), Lipofectamine 2000 (Invitrogen), Oligofectamine (Invitrogen), Metafectene (Biontex, Dunedin, New Zealand) or siPORT Lipid (Ambion, Austin, TX). Transfection protocols were followed per manufacturers' recommended procedure. Twelve hours post-transfection, the cells were incubated with 1 µg Hoechst 33342 for 10 min at 37ºC. Cells were washed with 2 ml of warm Opti-MEM I reduced serum media (Invitrogen). One ml of Opti-MEM I was added back to the cells and the cells where viewed by laser scanning confocal microscopy using a Leica TCS SP2 AOBS confocal microscope with an inverted stage (Leica Microsystems, Mannheim, Germany). Fluorescence was excited using 405 nm (Hoechst 33342) and 535 nm (tamra) laser lines and emission was recorded at 483 nm (Hoechst 33342) and 580 nm (tamra). Cells were viewed under a 63x

objective lens. Once focused on a field, images were captured in 0.35 μm increments along the z-axis, so that the cell(s) was viewed from top to bottom.

***Transfection Efficiency of P2 Cells.***

The day before transfection, 4 x $10^5$ P2 cells were plated in 3.5 cm plates. The cells were transfected with either 0, 0.5, 2 or 5 μg of pSV-ß-Galactosidase vector (Promega, Madison, WI) using Metafectene transfection reagent. Transfection procedure followed the manufacturer's recommended instructions. Twenty-four or 48 hr after transfection, cells were washed with 2 ml of prewarmed PBS and fixed in 1.5 ml Fixative Solution (20% formaldehyde, 2% glutaraldehyde in PBS) at room temperature for 10 min. The Fixative Solution was washed off the cells with two rinses with 2 ml PBS. Cells were stained with Staining Solution (4 mM potassium ferricyanide, 4 mM potassium ferrocyanide, 2 mM magnesium chloride and 0.1 mg X-Gal in *N*-*N*-dimethylformamide). Cells were incubated at 37ºC and visualized with light microscopy 2-24 hr post staining.

***Transfection Efficiency of HEK 293 Cells.***

Human embryonic kidney (HEK 293) cells were cultured in complete growth medium (Dulbecco's modified Eagle's medium supplemented with 10% (v/v) fetal calf serum and 100 μg/ml penicillin and streptomycin) at 37°C with 5% $CO_2$. One day prior to transfection, 600,000 cells were plated in 6 cm plates. Cells were transfected with 0 or

4 µg of pSV-ß-Galactosidase with Lipofectamine and Plus Reagent according to the manufacturer's instructions. Cells expressing ß-Gal were detected as described above.

### *Evaluation of DNAzymes in Cell Culture*

General Procedure

HEK 293 cells were cultured as previously described. One to two days prior to transfection, 0.8 - 1.2 x $10^6$ cells were plated in 60 mm plates. Before transfection, the cells were washed twice with PBS and each plate was incubated with a transfection mix containing specified DNA, 12 µl of Lipofectamine Reagent (Invitrogen, Carlsbad, CA, USA) and 8 µl Plus Reagent (Invitrogen) in Opti-MEM I Reduced Serum Medium (Invitrogen) for 1.5 hours. After the incubation period, the transfection mix was aspirated, the cells were washed once with PBS and incubated in complete growth medium for 24 hr (unless otherwise noted), after which the cells were harvested in ODC Buffer (25 mM Tris-HCl pH 7.5, 2.5 mM DTT, 0.1 mM EDTA). Harvested cells were lysed by freeze-thawing three times in liquid nitrogen and centrifuged at 4°C at 12,000 x g to isolate ODC in the cytosolic fraction. An aliquot of the supernatant was assayed for protein concentration and ODC activity as described in Chapter 3. ODC specific activity was calculated in pmol $^{14}CO_2$/30 min/mg protein. The activity of the different treatment groups was expressed in specific activity of ODC and/or as a percentage of ODC activity compared to that of NS-T, a nonsense oligo containing the same number of nucleotides.

***Activity of Full-length Vs. Truncated ODC***

HEK 293 cells ($8 \times 10^5$) were plated in 6 cm plates in triplicate for each condition. Forty-eight hours later, the cells were transfected with 600 pmols (6.2 μg) of NS-T or DZ IV-T and either 0.1 ug of pCMV-Zeo-ODC or pCMV-Zeo-ODCtr (mammalian expression vectors coding for full-length [461 amino acids] or truncated mouse ODC [425 amino acids] respectively, lacking the 5' and 3' UTR; a generous gift from Dr. L. M. Shantz, Pennsylvania State College of Medicine, Hershey, PA). Cells were harvested 24 hr after transfection.

***ODC Activity Time Course***

HEK 293 cells ($8 \times 10^5$) were plated in 6 cm plates in triplicate (except for 12 hr time point, duplicate) for each condition. Forty-eight hours later, the cells were transfected with 300 pmols (3.1 μg) of NS-T or DZ IV-T, 1 μg pSV-CAT and 0.1 ug of pCMV-Zeo-ODCtr. Cells were harvested 6, 12 or 24 hr after transfection.

***Effect of Varying Amount of Transfected ODC Plasmid***

HEK 293 cells ($1.5 \times 10^6$) were plated in 6 cm plates in triplicate (except for DZ IV-T at 0.1 ug ODC plasmid, duplicate) for each condition. Twenty-four hours after plating, the cells were transfected with 300 pmols (3.1 μg) of NS-T or DZ IV-T, 1 μg pSV-CAT and 0.05, 0.1 or 0.2 ug of pCMV-Zeo-ODCtr. Cells were harvested 24 hr after transfection.

***DZ IV-T Dose-Response Experiment***

HEK 293 cells ($1.5 \times 10^6$) were plated in 6 cm plates in triplicate for each condition. Twenty-four hours after transfection, the cells were transfected with 100 (1.0 μg), 300 (3.1 μg) or 600 pmols (6.2 μg) of NS-T or DZ IV-T, 1 μg pSV-CAT and 0.1 μg of pCMV-Zeo-ODCtr. Cells were harvested 24 hr after transfection.

***Active DNAzyme Vs. Control DNAzymes***

One day prior to transfection, $1.2 \times 10^6$ cells were plated in 60 mm plates. Cells were transfected with no DNAzyme or 600 pmol (6.2 μg) of DZ IV-T, DZ IV-mut-T or DZ IV-SCR-T, 0.1 ug pCMV-Zeo-ODCtr. Each data point was derived from two independent experiments performed in triplicate. Error bars represent standard deviation and *p*-values were calculated using Student's *t*-Test.

Western blotting was also performed on the cell lysate. An equal protein amount (75 μg) of cell lysate was resolved by SDS-PAGE for each treatment and transferred to a PVDF membrane (Pall Corporation, Pensacola, FL, USA). The membrane was probed with an affinity-purified ODC polyclonal antibody (0.5 μg/ml) (*116*) and detected using a chemiluminescent detection system (Cell Signaling Technology, Beverly, MA, U.S.A.). To control for protein loading, the membrane was stripped in Stripping Buffer (100 mM 2-mercaptoethanol, 2% (w/v) SDS, 62.4 mM Tris-HCl, pH 6.7) for 30 min at 60°C, reprobed with a monoclonal antibody to GAPDH (Biodesign, Saco, ME, U.S.A.) and detected using a chemiluminescent detection system (Cell Signaling Technology). Bands representing ODC and GAPDH were quantified by densitometry using a GeneGenius

BioImaging System (Syngene, Federick, MD, USA). The signal obtained for ODC was normalized to the signal of GAPDH and the normalized ODC protein for each treatment group was expressed as a percentage of ODC protein for NS-T treatment.

### *Cleavage Activity of Modified DNAzymes*

The activity of DZ IV-T and DZ IV-tamra-T were compared to DZ IV by measuring percent cleavage of in vitro transcribed ODC RNA. The procedure followed was described previously in Chapter 2. The incubated reactions contained 3 pmol of poly$(A)_{24}$ purified, $^{32}$P-labeled ODC RNA and 1 pmol of respective DNAzyme (or nuclease-free $H_2O$) in DNAzyme Buffer. The reactions were terminated at time 0 and 60 min after adding the enzyme mix to the substrate mix. No RNA cleavage was detected at t = 0 for all reactions. Cleavage activity for each DNAzyme was assayed in triplicate reactions.

### *ODC Activity of DZ IV-T Derivatives and Related DNAzymes*

HEK 293 cells ($1.2 \times 10^6$) were plated in 6 cm plates in triplicate for each condition. Twenty-four hours after transfection, the cells were transfected with 600 pmols (6.2 μg) of NS-T or DZ IV-T, DZ IV-mut-T, DZ IV-SCR-T, DZ IV, DZ III-T, DZ V-T or AS IV-T and 0.1 μg of pCMV-Zeo-ODCtr. Cells were harvested 24 hr after transfection.

## Results

### *Fluorescence and Confocal Fluorescence Microscopy to Evaluate Cell Lines for DNAzyme Transfection*

Transfection efficiency was evaluated to determine if uptake of the DNAzyme was sufficient to proceed with studies to determine DNAzyme efficacy. In many cell lines, basal ODC activity is at the limit of detection. NIH/3T3 cells that overexpress eIF4E (P2 cells), the limiting component of the eIF4F complex needed for cap-dependent translation, exhibit elevated ODC activity (*124*). Therefore, these cells were chosen as a model to determine if DZ IV could silence endogenous ODC. DZ IV was synthesized with a fluorescent tamra dye on the 5' end of the oligo and a 3' inverted T. The fluorescent DNAzyme was transfected into P2 cells without (Figure 3.1.A) or with (Figure 3.1.B) a transfection reagent, however the fluorescence appeared the same for both treatments. The fluorescence of DZ IV-tamra, depicted in red, emanates continuously and fully throughout almost all cells. In Figure 3.1, the nucleus stained with Hoechst 33342, is depicted in blue and then overlaid on the red tamra fluorescence. DZ IV-tamra fluorescence does overlap with the nuclear staining; but it is not possible from these experiments to determine whether DZ IV-tamra is only coating the cell membrane or has actually penetrated into the cell.

Laser scanning confocal microscopy (LSCM) was used to determine if the DNAzyme penetrated into the cell. LSCM enables the user to focus in different planes of the cell, therefore allowing one to scan z-axis sections throughout the entire cell. P2 cells were transfected with DZ IV-tamra, using various transfection reagents. Fluorescent

A.

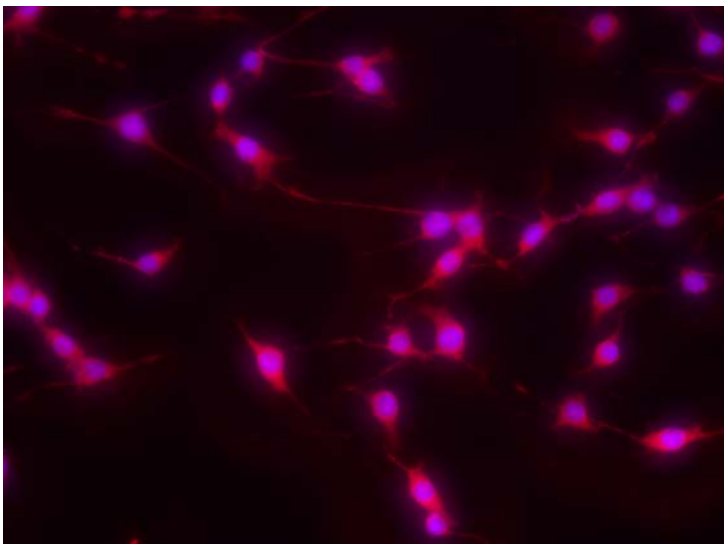

B.

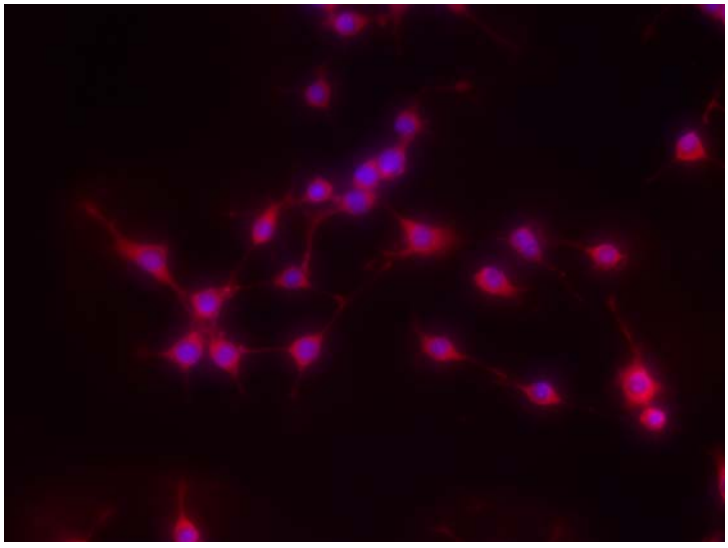

**Figure 3.1**: *Fluorescence microscopy of NIH/3T3 + eiF4E cells transfected with DZ IV-tamra.*

DZ IV-tamra (5.5 μg) was transfected into the cells without a transfection reagent (A) or with a transfection reagent, siPORT Lipid (B). Pictures shown are representative fields of overlaid total fluorescence. DZ IV-tamra is shown in red and the HO33342 nuclear stain is represented in blue.

cells throughout the slide were analyzed. A z-axis section within a representative cell transfected with DZ IV-tamra using siPORT Lipid transfection reagent revealed that DZ IV-tamra (red) was excluded from the nucleus (blue) of the cell (Figure 3.2). The elliptical absence of red fluorescence (Figure 3.2, upper left panel) clearly coincides with the nucleus (Figure 3.2, upper right panel), as depicted in the overlaid micrographs (Figure 3.2, lower left panel). Z-axis sectioning throughout entire cells showed that disappearance of red DNAzyme fluorescence coincided with the appearance and location of blue nuclear fluorescence, indicating that DZ IV-tamra fluorescence is limited to regions outside the nucleus. The majority of cells did not show significant intracellular fluorescence from DZ IV-tamra. All six transfection reagents, DOTAP, Lipofectamine with Plus Reagent, Lipofectamine 2000, Oligofectamine, Metafectene and siPORT Lipid showed similar results (data not shown). Cells transfected with DZ IV-tamra, but without using a transfection reagent, did show DZ IV-tamra fluorescence but fluorescence was generally fainter than when a transfection reagent was used (data not shown). Intracellular DZ IV-tamra was found in only a small percentage of the analyzed cells. These experiments demonstrate that for the majority of cells, DZ IV-tamra did not penetrate the cell membrane, but for the few cells that did take up the DNAzyme, the DNAzyme was localized in the cytoplasm.

The confocal microscopy experiments suggest that the DNAzyme was only penetrating the cell membrane in a relatively small percentage of cells. Confocal

A, B

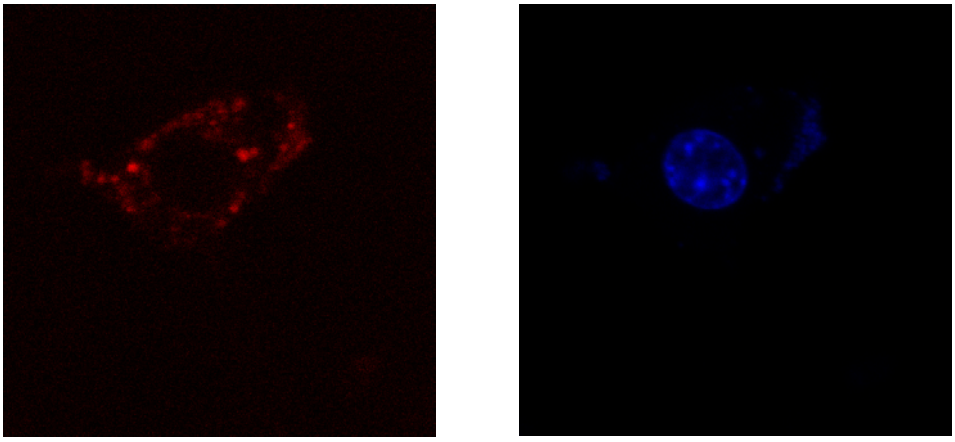

C, D

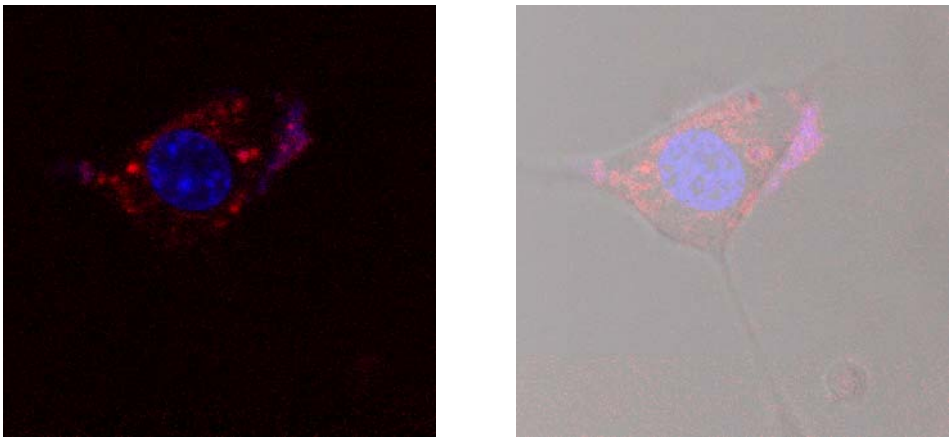

**Figure 3.2**: *Confocal microscopy of P2 cells transfected with DZ IV-tamra using siPORT Lipid.*

Fluorescence of a z-axis section focused within a single cell revealed that DZ IV-tamra (red, upper left panel) penetrates the cell membrane and is within the cell. The DNAzyme is excluded from the cell nucleus (blue, upper right panel). The lower panels show an overlay of the fluorescence from DZ IV-tamra and nuclear staining without (lower left panel) and with (lower right panel) the light micrograph of the cell.

microscopy is not an ideal technique to determine transfection efficiency of the DNAzyme. Most of the cells transfected with DZ IV-tamra are fluorescent, but each cell field must be analyzed individually to determine whether the fluorescence is intracellular. This would be very time consuming and impractical. Therefore, transfection efficiency was determined by transfecting a plasmid encoding for ß-galactosidase (ß-gal) reporter gene. Cells successfully transfected with pSV-ß-galactosidase will express ß-gal and the activity of this enzyme converts the X-gal substrate into a blue product that can be visualized by light microscopy.

Transfection of the vector into P2 cells yielded a very low (<5%) transfection efficiency (Figure 3.3A). The number of blue stained cells did not significantly differ 24 or 48 hr post-staining. No blue stained cells were visible for cells transfected without the vector (data not shown). All three concentrations of vector (0.2, 2, 4 μg) showed a similar number of stained cells (data not shown). NIH/3T3 + HRas(61L) cells, another cell line with high ODC activity, also exhibited a low transfection efficiency (<5%) as measured by ß-gal activity (data not shown). Therefore, the only cell lines at our disposal that express measurable ODC activity, are not efficiently transfectable. If the DNAzyme was effective at silencing 100% of ODC activity once it entered the cell, transfection into either of these cell lines would lead to <5% overall silencing—a reflection of the poor transfection efficiency of the DNAzyme into these cells.

A.

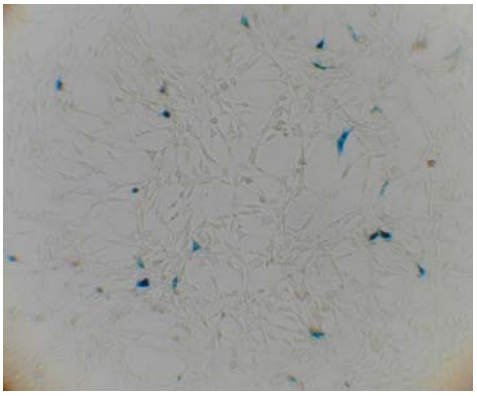

B.

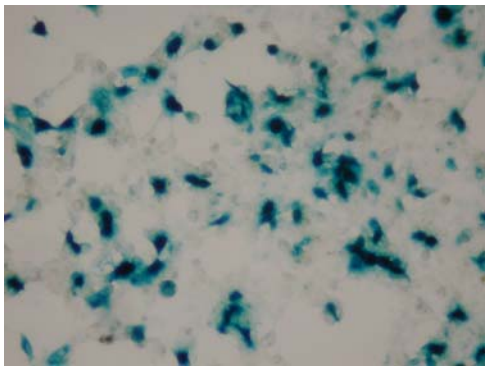

C.

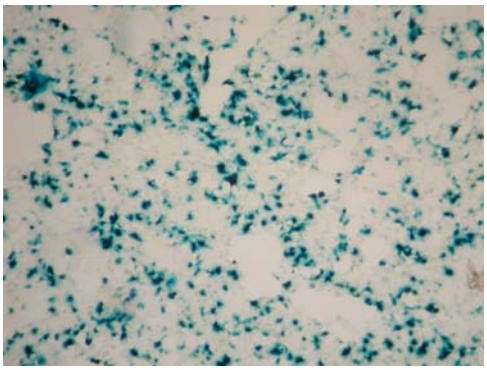

**Figure 3.3:** *Transfection efficiency of ß-gal into cells.*

P2 (A) or HEK 293 (B, C) cells were transfected with 5 or 4 µg, respectively, of pSV-ß-Galactosidase. ß-gal activity was determined by the conversion of X-gal substrate into a blue staining product. P2 (A) and HEK 293 cells (B) were viewed under 200X magnification. Panel C is a representative field of the HEK 293 cells at lower 100X magnification.

***Development of a DNAzyme-ODC Co-Transfection Model***

Another cell culture model was developed to assess the efficacy of the DNAzymes. HEK 293 cells are generally considered highly amenable to transfection but basal ODC activity of these cells is near the limit of detection (data not shown). Transfection efficiency of these cells was evaluated for use in a co-transfection method in which the DNAzyme and a plasmid coding for the target, ODC, are co-transfected. This method is advantageous to accomplishing the objective of these experiments because in essence, the cells transfected with DNAzyme are selected for analysis. The effectiveness of the DNAzyme will be evaluated by measuring ODC activity of the cells. Only the cells that have taken up the ODC plasmid will exhibit ODC activity and these cells are also capable of taking up the transfected DNAzyme.

Transfection efficiency of HEK 293 cells was first evaluated using the ß-gal reporter plasmid. Preliminary studies in HEK 293 cells with various transfection reagents (Metafectene, Lipofectamine 2000 and Lipofectamine with Plus Reagent) demonstrated that transfection with Lipofectamine with Plus Reagent resulted in the highest transfection efficiency in these cells (data not shown).Transfection efficiency for HEK 293 cells using Lipofectamine with Plus Reagent approached 40%—much higher than for the P2 or NIH/3T3 + HRas(61L) cells (Figure 3.3B, C). Cells transfected with 0 µg of the vector coding for ß-gal did not show any detectable blue cells (data not shown). The relatively high transfection efficiency of HEK 293 cells permits the study of DNAzymes co-transfected with target.

The full-length coding region of ODC codes for a 461 amino acid protein that is rapidly turned over with a half-life measured between 10-60 min (*34, 120*). Truncations to the C-terminus are known to stabilize the protein by altering the rate of degradation (*145, 146*). A plasmid encoding a truncated ODC or full-length ODC was transfected into HEK 293 cells to determine (1) if there is a difference in activity between the two plasmids and (2) if DZ IV-T has similar effects on both plasmids. The plasmid pCMV-Zeo-ODCtr is a mammalian expression vector that codes for a truncated mouse ODC (425 of 461 amino acids). Plasmid pCMV-Zeo-ODC codes for full-length ODC protein (461 amino acids) from the same promoter. Both plasmids code for ODC transcripts which lack the 5' and 3' UTR because the UTRs play important roles in repressing the translation of ODC mRNA (*22*). ODC activity of cells transfected with NS-T and the truncated ODC is almost three times greater than cells transfected with full-length ODC (35 vs. 13 pmol $^{14}C$/30 min/μg protein, Figure 3.4A). NS-T is a nonsense oligo the same length as DZ IV-T that should have no effect on the activity of the transfected plasmid. Transfecting different amounts of DNA can alter transfection efficiency; therefore NS-T provides a matched control for DZ IV-T. The second question addressed by the experiment is whether the percent change in ODC activity would differ for ODC protein with a short half-life (full-length ODC) versus a longer half-life (truncated ODC). DZ IV-T treatment leads to reduced ODC activity for both length ODC proteins (Figure 3.4A). Thirty-six percent of ODC activity remained for DZ IV-T transfected cells expressing either the truncated or full-length ODC 24 hr after transfection (Figure 3.4B). At this time frame, the DNAzyme appeared equally effective on full-length and truncated ODC. The plasmid coding for truncated ODC was chosen for subsequent experiments

A.

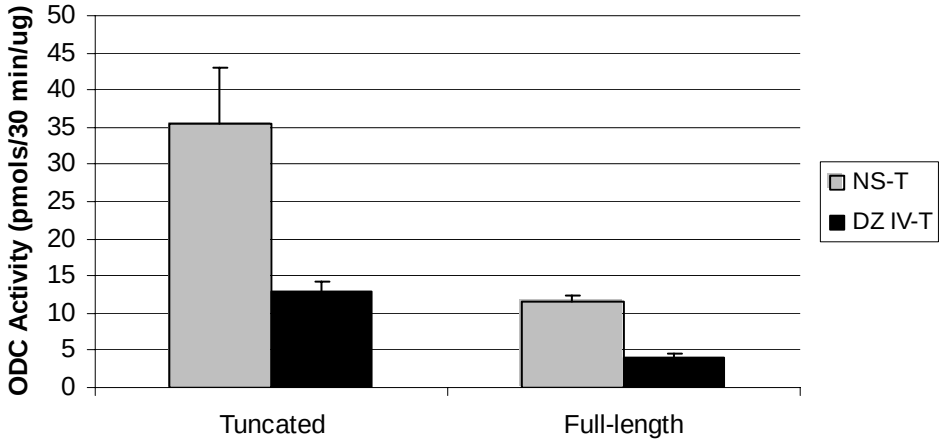


B.

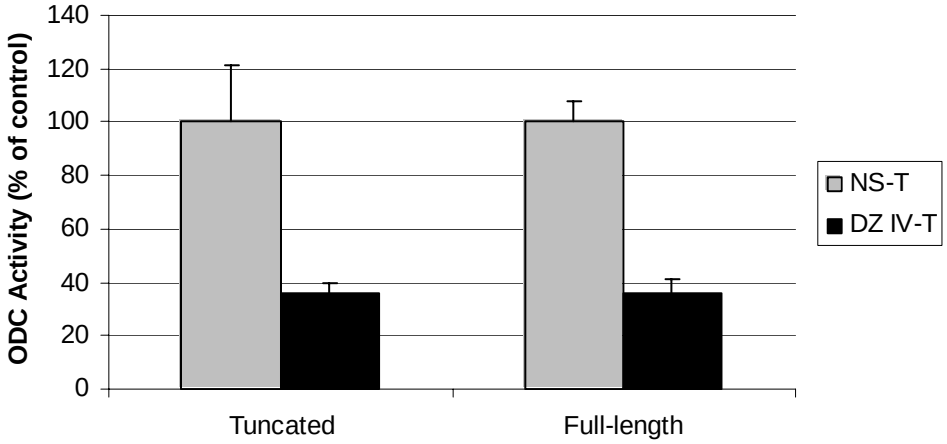


**Figure 3.4**: *ODC Activity of truncated and full-length ODC in HEK 293 cells treated with DZ IV-T.*

HEK 293 were co-transfected with 0.1 μg of either a plasmid coding for a truncated or full-length ODC protein and 600 pmols of either NS-T or DZ IV-T. ODC activity, normalized to the protein concentration, is expressed in specific ODC activity (A) or as a percentage of ODC activity relative to the control, NS-T (B).

because absolute ODC activity for cells transfected with this plasmid was higher.

A time-course of ODC activity was designed to address the kinetics of ODC expression and the effect of the DNAzyme over time. HEK 293 cells were transfected with the plasmid coding for truncated ODC and either NS-T or DZ IV-T. ODC activity was measured at various time points post-transfection. ODC activity is detectable 6 hr post-transfection (22 pmol $CO_2$/30 min/μg protein, NS-T, Figure 3.5A) and activity continually increases at 12 and 24 hr (115, 310 pmol $^{14}C$/30 min/μg protein respectively, NS-T, Figure 3.5A). DZ IV-T silences ODC up to at least 24 hr post-transfection (Figure 3.5A) and therefore must be stable up to this time. Despite the increase in ODC activity over time, DZ IV-T is able to maintain a relatively constant silencing of ODC (~55-70% silencing).

The amount of transfected plasmid coding for truncated ODC is expected to affect ODC activity. Three concentrations of the plasmid were transfected into HEK 293 cells. Increasing the amount of transfected plasmid from 0.05 to 0.1 to 0.2 μg lead to additive increases in ODC activity (244, 477, 754 pmol $^{14}C$/30 min/μg protein respectively, NS-T Figure 3.6A). Similar to the time course experiment (Figure 3.5), DZ IV-T silenced ODC activity to a similar degree irrespective of the amount of plasmid and the resulting change in ODC activity (Figure 3.6B).

Increasing the amount of DNAzyme transfected into the cells is expected to have two independent effects. First, increasing amounts of DNAzyme may be inversely associated with ODC activity—the more DNAzyme in the cells will lead to greater silencing. The amount of DNAzyme is also likely to alter the transfection efficiency. A

A.

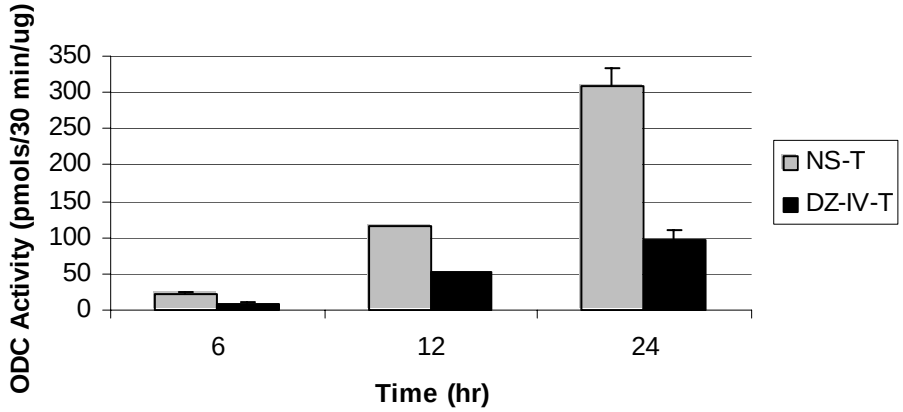


B.

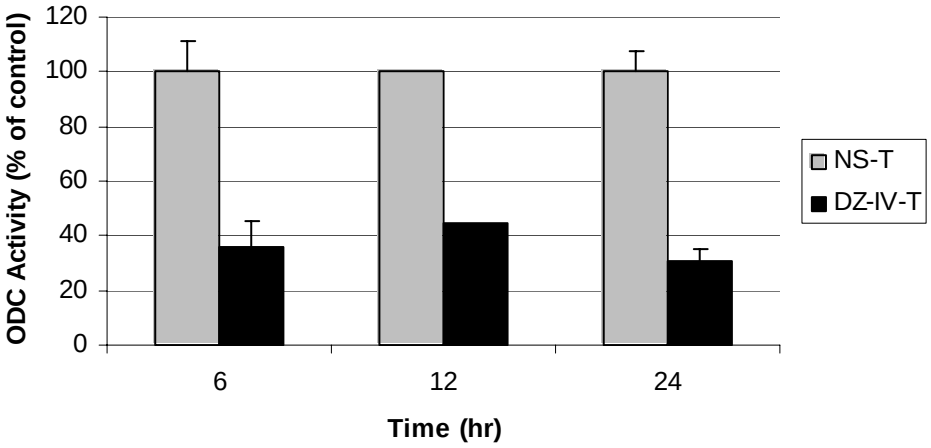


**Figure 3.5**: *Time Course of ODC Activity.*

HEK 293 cells were co-transfected with 0.1 μg of a plasmid coding for a truncated ODC and 300 pmols of either NS-T or DZ IV-T. Cells were harvested 6, 12 or 24 hr post-transfection and ODC activity was determined. ODC activity is expressed in specific ODC activity normalized to protein (A) or as a percentage of ODC activity relative to the control, NS-T, at each time point (B).

A.

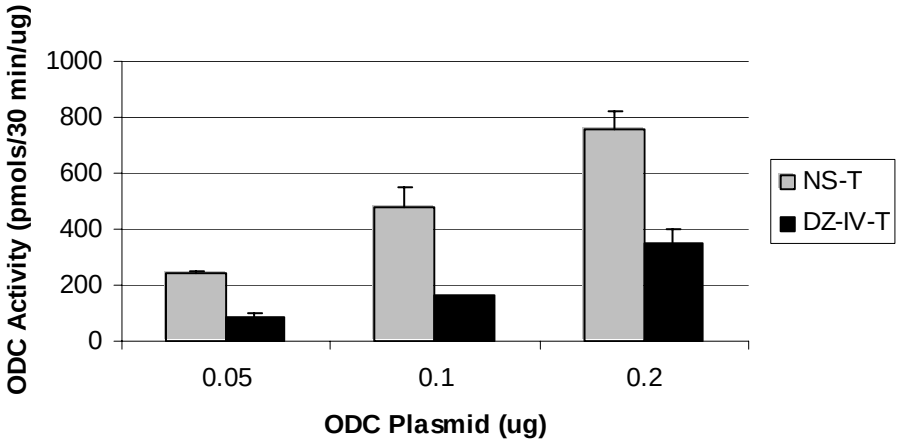


B.

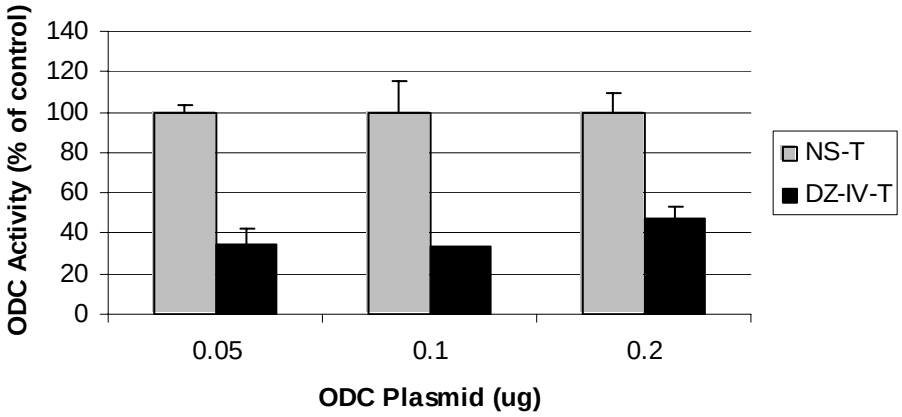


**Figure 3.6**: *Effect of Varying Amount of Transfected ODC Plasmid.*

HEK 293 cells were co-transfected with 0.05, 0.1 or 0.2 μg of a plasmid coding for a truncated ODC and 300 pmols of either NS-T or DZ IV-T. Cells were harvested 24 hr post-transfection and ODC activity was determined. ODC activity is expressed in specific ODC activity normalized to protein (A) or as a percentage of ODC activity relative to the control, NS-T, at each time point (B).

minimum amount of DNA is needed for efficient transfection efficiency, yet too much DNA will also decrease transfection efficiency. Dose-response of various amounts of DZ IV-T into HEK 293 cells shows that absolute ODC activity decreases as the amount of DNAzyme is increased from 100 to 300 to 600 pmol (295, 112, 37 pmols $^{14}C$/30 min/μg protein respectively, NS-T, Figure 3.7A). As the amount of DNAzyme is increased, the percent of ODC silenced also increases (Figure 3.7B). Treatment with 100, 300 and 600 pmol DZ IV-T silences ODC activity by 15%, 36% and 73% respectively compared to the same amount of NS-T control (Figure 3.7B).

***Evaluation of a DNAzyme Targeted to ODC In Cell Culture: DZ IV Vs. Controls***

Ultimately, the goal is to develop useful DNAzymes to silence ODC in cell culture and animal models. This end was pursued by transiently co-transfecting the catalytically optimized DZ IV 9/9, along with a plasmid coding for ODC, into HEK 293 cells under the optimal conditions determined from the previous experiments. After 24 hr treatment, ODC activity and ODC protein was determined for the treated cells. Cells were treated with one of four oligos, all 34-mers (33-mers + 3' inverted T). DZ IV-mut-T and DZ IV-SCR-T served as negative controls. DZ IV-mut-T is identical in sequence to DZ IV-T, except for a G→C mutation in the catalytic domain that renders it catalytically inactive (see Figure 3.1). DZ IV-SCR-T has an intact catalytic domain, but scrambled hybridization arms that do not target it to ODC (see Table 3.1). After DZ IV-T treatment, ODC activity was reduced by 79% compared to NS-T—a statistically significant decrease in activity (Figure 3.8A). No change in ODC activity was detected in DZ IV-

A.

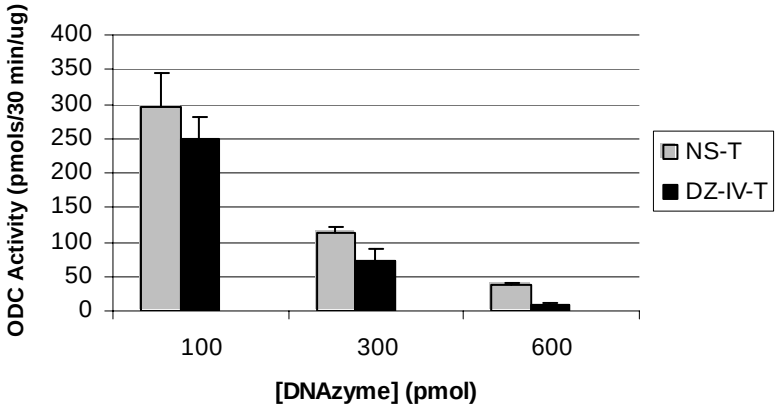


B.

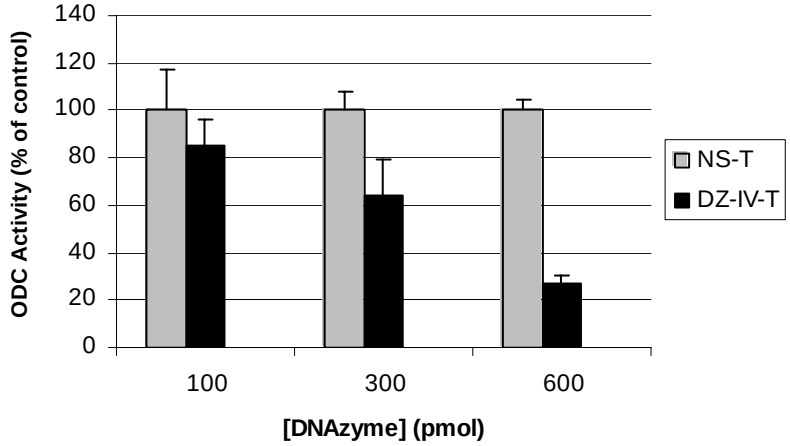


**Figure 3.7***: DZ IV-T Dose-Response Experiment.*

HEK 293 cells were co-transfected with 100, 300 or 600 pmol of either NS-T or DZ IV-T and 0.1 µg of a plasmid coding for a truncated ODC. Cells were harvested 24 hr post-transfection and ODC activity was determined. ODC activity is expressed in specific ODC activity normalized to protein (A) or as a percentage of ODC activity relative to the control, NS-T, at each time point (B).

A.

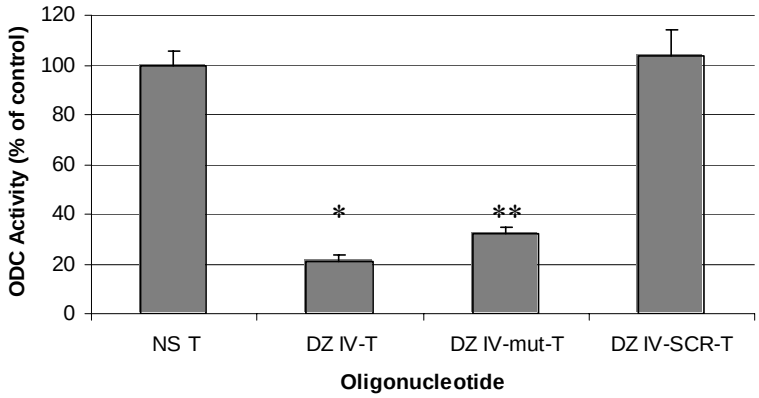


B.

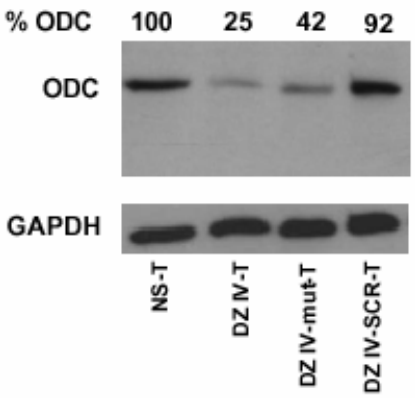


**Figure 3.8:** *Effect of DNAzyme IV-T in Cell Culture.*

HEK 293 cells were transiently co-transfected with 6 µg of DNAzyme or control and 0.1 ug of a plasmid coding for ODC (pCMV-Zeo-ODCtr) for 24 hours. Cells were harvested and ODC activity (A) or protein (B) was assayed. ODC Activity. The activity of each treatment group is expressed as a percentage of NS-T (a degenerate oligo) activity. Error bars represent standard deviation of two independent experiments performed in triplicate (n = 6). The decrease in ODC activity for DZ IV-T was statistically significant compared with both NS-T and DZ IV-mut-T (A). ODC Protein. Equivalent protein concentrations were analyzed by Western blotting for ODC and GAPDH. A representative blot is shown (B). Bands were quantitated by densitometry and percent ODC protein relative to NS-T was determined for each treatment group. ODC was normalized to GAPDH. NS-T, degenerate oligo; DZ IV-T, catalytically active DZ IV; DZ IV-mut-T, catalytically inactive mutant; DZ IV-SCR-T, intact catalytic domain with scrambled hybridization arms. All oligos are 33-mers plus an inverted 3' T (represented by "-T").

[(A) *DZ IV-T vs. NS-T and DZ IV-T vs. DZ IV-mut-T, $p < 0.0001$; ** DZ IV-mut-T vs. NS T, $p < 0.0001$; two-tailed Student's t-Test]

SCR-T treated cells, thereby showing that complementary target arms are necessary for target inhibition by DNAzymes and an intact catalytic domain alone is not sufficient. DZ IV-mut-T treatment reduced ODC activity by 68%, due to an antisense effect of the hybridization arms. Although this is a substantial decrease in ODC activity, the intact catalytic domain of DZ IV-T leads to further, and highly statistically significant, reduction ($p < 0.0001$) compared to the catalytically inactive mutant, DZ IV-mut-T.

Treatment with an effective DNAzyme reduces the amount of ODC mRNA available for translation, so the ODC protein profile should reflect the activity measurements. Indeed, Western blots of the cytosolic fraction for ODC protein levels revealed a trend similar to the activity results. DZ IV-T decreased the amount of translated ODC protein (normalized to GAPDH expression) by 75% compared with NS-T control, again representing a more complete reduction in ODC expression than DZ IV-mut-T treatment (58% reduction, Figure 3.8B). DZ IV-SCR-T had little effect on translated ODC protein (8% reduction, Figure 3.8B). Together, the activity data and Western blot results provide evidence that the DNAzyme IV-T effectively silences ODC and that catalytic activity enables it to be more effective in cell culture than an inactive DNAzyme (DZ IV-mut-T) that is complementary to the same region of ODC.

The 3' inverted-T stabilizes the DNAzyme from degradation, but it may possibly alter the catalytic activity of DZ IV also. This was examined by incubating unmodified DZ IV and DZ IV-T with *in vitro* transcribed ODC RNA for 60 min and then determining what percentage of the RNA was cleaved (Figure 3.9A). Unmodified DZ IV was more effective in cleaving ODC RNA than DZ IV-T—which converted almost one-third (32%)

A.

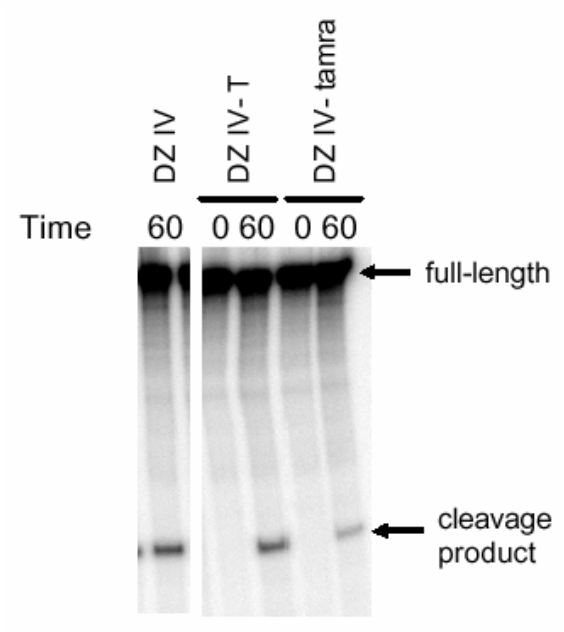


B.

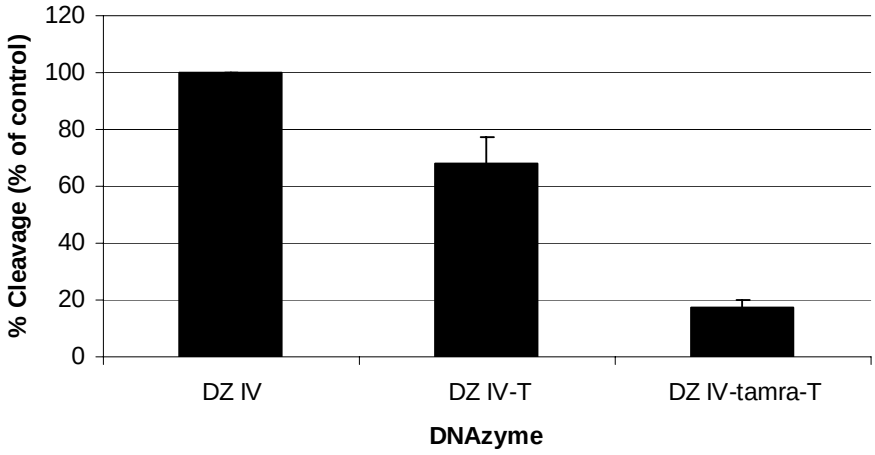


**Figure 3.9**: *Cleavage Activity of DZ IV Derivatives.*

*In vitro* transcribed ODC RNA (3 pmol) was incubated with 1 pmol of DZ IV, DZ IV-T or DZ IV-tamra-T. The reactions were terminated at 0 or 60 min after activation. The full-length RNA was separated from the cleavage products by electrophoresis (A) and quantified by densitometry to determine percent cleavage (B). Unmodified DZ IV is designated as the control. DZ IV-T and DZ IV-tamra-T are modified derivatives of DZ IV containing a 3' inverted-T. DZ IV-tamra-T contains an additional modification—a tamra dye labeled at the 5' of the DNAzyme.

less product into substrate (Figure 3.9B). This suggests that, although the 3' inverted T protects the DNAzyme from degradation, it impairs the ability of DZ IV to associate and/or cleave ODC RNA.

Several other DNAzymes and an AS-ODN were co-transfected into HEK 293 cells for comparison to DZ IV-T (Figure 3.10). Unmodified DZ IV (DZ IV-unmodified, also referred to as simple DZ IV) has the same sequence as DZ IV-T, except that it lacks the 3' inverted-T. Data from Figure 3.9 suggests that the unmodified DNAzyme may be more catalytically efficient at silencing ODC. However, DZ IV-T treatment silences ODC activity more completely than DZ IV-unmodified (79% vs. 39% silencing respectively, Figure 3.10). This suggests that the stability that this modification confers on the DNAzyme outweighs any decrease in catalytic activity brought about by this modification under the experimental conditions. However, it is possible that the enhanced effect of the DNAzyme containing the 3' inverted T is not due to stability, but for another reason (e.g. it penetrates the cell better than the unmodified DNAzyme).

The point mutation in the catalytic domain of DZ IV-mut has been shown to abolish the catalytic activity of this DNAzyme (Table 3.1), however this DNAzyme does lead to a reduction in ODC activity in the cell culture model (albeit to a lesser degree than DZ IV-T, Figure 3.8). The hybridization arms of DZ IV-mut-T still target it to ODC mRNA, and therefore it likely exerts an antisense effect. As depicted in Figure 2.1, DZ IV-mut-T hybridized to ODC mRNA spans a stretch of 19 nucleotides of the mRNA (although it basepairs with only 18 nucleotides due to the unpaired catalytic domain). An antisense ODN (AS IV-T) was designed to hybridize to the same 19

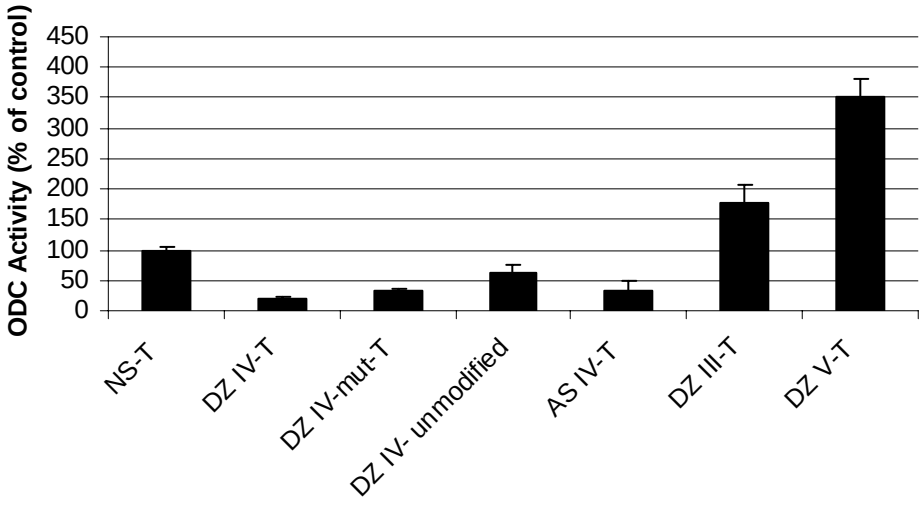


**Figure 3.10**: *Comparison of DZ IV-T and Related Oligos.*

HEK 293 cells were co-transfected with 600 pmol of the denoted oligo and 0.1 μg of a plasmid coding for a truncated ODC. Cells were harvested 24 hr post-transfection and ODC activity was determined. ODC activity normalized to protein is expressed as a percentage of ODC activity relative to the control, NS-T. DZ III-T and DZ V-T are DNAzymes that are effective at cleaving in vitro transcribed ODC RNA (see Figure 2.4, 2.5). AS IV-T is an antisense ODN with the same 3' inverted-T modification as the DNAzymes. This antisense oligo targets the same sequence of ODC as the hybridization arms of DZ IV-T, but it does not contain the catalytic domain. NS-T, DZ IV-T and DZ IV-mut-T were previously described in Figure 3.8. All the samples were transfected and assayed as one experiment.

nucleotides. AS IV-T does not have a DNAzyme catalytic domain; in lieu it contains the complementary base to ODC mRNA. AS IV-T has a similar effect on ODC activity as DZ IV-mut-T (33% and. 32% reduction respectively, Figure 3.10). This provides evidence that the hybridization arms of DZ IV-mut-T can lead to a reduction in ODC activity through an antisense mechanism.

Experiments were described in Chapter 2 (Figure 2.4, 2.5) that showed that several of the other DNAzymes effectively cleaved ODC RNA *in vitro*. Two of these DNAzymes, DZ III and DZ V, were tested in the cell culture model against DZ IV-T. Treatment with both DZ III-T and DZ V-T actually lead to a 179% and 351% increase in ODC activity (Figure 3.10). It is possible that these DNAzymes stabilize the mRNA and facilitate translation or reduce the rate of degradation of the mRNA. These results demonstrate the difficulty of targeting DNAzymes to endogenously folded mRNA and predicting the efficiency from *in vitro* results.

**Discussion**

DNAzymes targeted to the sequence for ODC mRNA were designed, evaluated and optimized *in vitro*, as described in Chapter 2. This is an essential and important step in the development of DNAzymes, however progression to a more relevant model is necessary for a more complete evaluation. We sought to analyze the DNAzymes in a cell culture model to assess the efficacy of the DNAzymes against endogenously folded ODC mRNA in which the DNAzyme must now interact/compete with cellular machinery and localization becomes an important factor. DZ IV-T effectively silences ODC activity in the cell culture model and shows promise for future applications.

The cell culture model used to evaluate the DNAzymes must have detectable ODC activity. P2 cells overexpress eIF4E which results in up to a 30-fold increase in ODC (*30*) and therefore provides a good model. Fluorescence and confocal fluorescence microscopy studies of P2 cells transfected with a fluorescent-tagged DNAzyme (DZ IV-tamra) showed that the DNAzyme did not penetrate the cell membrane in a high percentage of cells (Figures 3.1, 3.2). When the DNAzyme did get past the membrane, it was visualized as punctate structures localized in the cytoplasm and excluded from the nucleus (Figure 3.2). Others have also reported that DOTAP transfected DNAzymes localized to the cytoplasm and substantial delivery to the nucleus was not observed up to 24 hr post-transfection (*147*). Other studies with oligonucleotides suggest that over time transfected oligo do dissociate from punctuate cytoplasmic structures into the nucleus but this is dependent upon a number of factors including presence of serum and transfection

reagent (*148, 149*). DNAzyme treatment resulted in similar reductions in ODC activity at 6, 12 and 24 hr post-transfection (Figure 3.5B), therefore to achieve this level of silencing ODC does not need to be localized to the nucleus. The DNAzyme acts on mature mRNA in the cytoplasm. This is consistent with a previous report in which cytoplasmic ribozymes were considerably more active than their nuclear-localized counterparts (*150*). The authors also showed that an external guide sequence, which is an RNA that binds to its target RNA, is more effective in the nucleus because its silencing activity is dependent on nuclear RNase P. Therefore other forms of gene silencing, such as AS-ODNs and siRNA, may be more effective in the nucleus because of dependency on nuclear proteins.

The confocal fluorescence experiments suggested that the transfection efficiency for P2 cells was very poor and this was confirmed with transfection of a β-gal reporter gene (Figure 3.3A). Another NIH/3T3 cell line that constitutively expresses an activated form of HRas [NIH/3T3 + HRas(61L)] and has elevated ODC activity was equally resistant to transfection (data not shown). HEK 293 cells are more readily transfected (Figure 3.3B), however basal ODC activity is near the limit of detection. Three options were considered. ODC mRNA could be measured by quantitative RT-PCR and the effect of the DNAzyme could be reported as a change in mRNA levels. However, it can not be assumed that ODC activity will change proportionately to mRNA levels especially considering that the translation of ODC mRNA is highly regulated and multiple feedback mechanisms exist to control ODC activity. Indeed, the elevated ODC activity in the P2 cells is not accompanied by a significant concomitant increase in ODC mRNA (*30*). The biological endpoint is ODC activity, not ODC mRNA levels, therefore ODC activity must be able to be accurately determined.

The other two strategies involved elevating ODC activity by chemical-mediated induction or transient transfection. ODC activity can be induced in cultured cells by chemical treatment (e.g. 12-*O*-tetradecanoylphorbol-13-acetate [TPA]) or other means (e.g. addition of serum-containing media) (*151*). This would elevate ODC activity in all cells and the DNAzyme is only transfected into ~40% of HEK 293 cells (Figure 3.3). If the DNAzyme was 100% effective at silencing ODC once it entered the cell, it would only lead to a 40% reduction of ODC activity in this situation. Transient co-transfection of a DNAzyme and its target into cells is an accepted method to evaluate DNAzymes in cell culture (*152-154*). It overcomes the problems associated with the other strategies; ODC activity is elevated to a measurable level and in theory, the same cells transfected with ODC will be co-transfected with the DNAzyme.

Several experiments were designed to optimize the DNAzyme/target co-transfection method to evaluate the DNAzyme. The effect of the DNAzyme on ODC activity derived from plasmids coding for a truncated ODC or the full-length coding region was examined. The C-terminus of ODC is important for antizyme stimulated degradation (*145, 146*). Full-length ODC protein is rapidly turned over with a half-life measured as short as 10 min (*120*) and truncation of the C-terminus stabilizes the protein. As expected, the ODC activity was higher in cells transfected with the plasmid coding for the truncated, more stable ODC than full-length (Figure 3.4A). It was expected that the DNAzyme would cleave the full-length and truncated ODC mRNAs equally well, but it was not known whether the longer-lived truncated protein would accumulate, thereby masking the activity of the DNAzyme. DZ IV-T treatment resulted in a similar reduction in ODC activity for both truncated and full-length ODC (Figure 3.4B).

Other variables which affect ODC activity include the time and the amount of transfected plasmid and DNAzyme. ODC activity increases with time (up to at least 24 hr post-transfection, Figure 3.5A) and with the amount of transfected plasmid coding for ODC (Figure 3.6A). However, DZ IV-T silences ODC to the same degree even when absolute ODC activity increases (Figures 3.5B, 3.6B). This provides evidence that DZ IV-T with the 3' modification is stable up to 24 hr post-transfection, which agrees with other reports (*132, 147*). Increasing the amount of DZ IV-T decreased absolute ODC activity even though the other reaction conditions remained constant because the increase in total DNA transfected decreases transfection efficiency (Figure 3.7A). Increasing amounts of transfected DNAzyme results in increased silencing of ODC (Figure 3.7B). The observed dose response curve is likely due to the increase in DNAzyme, not decreased absolute ODC activity because 300 pmols of DZ IV-T silenced ODC activity to the same degree regardless of ODC activity (Figures 3.5, 3.6).

Since ODC translation is tightly controlled, it could be argued that it would be more difficult to silence the transcript in cell culture or *in vivo* due to complex folding, overall structure and proteins that may be associated with it. The previously described experiments were designed to develop a cell culture model to evaluate ODC DNAzymes. Based upon these conditions, DZ IV was then evaluated with the proper controls. Catalytically optimized ODC DZ IV (9/9 nucleotide length arms) with the 3'-3' inverted T effectively reduced ODC activity (Figure 3.8A), which correlated well with the reduction in ODC protein (Figure 3.8B), in HEK 293 cells. A similar reduction of ODC has been shown to revert the transformed phenotype of Ras-transformed NIH/3T3 cells back to normal (*116*). Therefore DZ IV sufficiently silences ODC to use it as a tool to study the

functional effects of ODC. The catalytically active DNAzyme was also able to silence ODC more completely than the antisense effect of DZ IV-mut-T and the difference might be even more pronounced if the inverted 3'-T did not reduce the catalytic activity of the DZ IV (Figure 3.9B). It is also possible that the residual activity of ODC in the DZ IV-T cells represents a population of mRNA that is folded differently or occupied by the translational machinery. It could also represent a subset of cells that are transfected with the ODC plasmid, but not DNAzyme. This data provides the first report that ODC can be silenced by a DNAzyme and provides support that a catalytically active DNAzyme has the potential to be more effective than oligos that work through an antisense mechanism.

The development and identification of a DNAzyme that is able to suppress endogenous ODC mRNA, as well as *in vitro* transcribed ODC RNA, opens many exciting possibilities, especially in light of recent developments in the DNAzyme field. An approach to express a 10-23 DNAzyme *in vivo* from a vector has been described and demonstrated to be effective against the intended target in cell culture (*155-157*). Expression of DZ IV-T in cells would allow for more flexibility to study the functional effects of silencing ODC than transfecting DNAzyme oligos. This would enable the selection of cells that constitutively express DZ IV-T, thereby permitting the study of the DNAzyme in cells with low transfection efficiency. A tetracycline-regulated DNAzyme expression system has also been developed, which further increases the power of this system (*157*). For example, the transformed phenotype of cells transfected with activated HRas(61L) or RhoA(63L) mutants or cells that overexpress eIF4E can be reverted by reducing ODC activity (*116, 158*). By controlling expression of DZ IV-T, the direct effect of silencing ODC on the transformed phenotype of these cells could be examined.

Future studies could also evaluate the effect of modified nucleic acids on the stability and activity of DNAzymes targeted against ODC. Antisense research has produced three generations of nucleic acids. The third generation not only protects the nucleic acid from nucleolytic degradation but also enhances the affinity toward target RNA over unmodified forms (*101*). A member of this third generation, locked nucleic acids (LNA) or 2'-O-methyl RNA, has been incorporated into the hybridization arms of DNAzymes. LNA-modified DNAzymes have been targeted to sites of RNA that were inaccessible to unmodified DNAzymes and degraded the RNA at a high catalytic rate, even to completion (*159*). Incorporating this modification into DZ IV may improve its activity. It would also be interesting to see what effect LNA-modification would have on DZ III and DZ V in cell culture. These DNAzymes cleaved denatured, *in vitro* transcribed ODC RNA well (Figure 2.4, 2.5), but did not lead to any reduction of ODC activity in cell culture (Figure 3.10). It would be useful to have more than one DNAzyme effective against ODC mRNA, so that a multi-DNAzyme approach could be pursued.

In progression from the *in vitro* studies described in Chapter 2, these studies in cell culture recapitulate a more physiologically relevant environment. The DNAzyme is exposed to potential degradation and compartmentalization and the ODC mRNA target is folded and may be protected through its interaction with the cellular transcription and translation machinery. In conclusion, we have identified a DNAzyme that reduces the amount of translated ODC protein resulting in a concomitant decrease in activity in a cell culture model. This is also one of the few reports that demonstrates that an active DNAzyme can more completely suppress the activity of the target mRNA in a cell culture model compared to a catalytically inactive counterpart, as measured by a direct

effect on the target. The development of a DNAzyme that is effective against ODC in cell culture opens many opportunities to better study ODC and to explore its role in various biological processes.

# Chapter 4

## *In Vivo* Studies: Evaluation of ODC DNAzyme on TPA-Induced ODC Activity In Mouse Skin

### Specific Aim

To demonstrate that DZ IV can silence endogenous ODC in a model relevant to the potential clinical uses of a DNAzyme targeted to ODC.

## Introduction

In Chapter 3, it was demonstrated that DZ IV could effectively suppress ODC activity in a cell culture model in which temporal and spatial considerations, as well as other potential obstacles (i.e. DNAzyme stability and localization, accessibility of folded ODC mRNA with interacting proteins) were addressed. DZ IV was active in this model and the next step in the development of a DNAzyme directed against ODC is to determine if it can silence endogenous ODC *in vivo* when topically applied to skin of mice. This model was chosen for two reasons. ODC activity can be induced to detectable levels in the mouse skin with TPA treatment, and therefore the effect of the DNAzyme on endogenous full-length ODC containing both the 5' and 3' UTR could be studied. Secondly, topically applied agents that reduce or inhibit ODC activity in the skin have proven or potential uses in chemoprevention/therapeutics and hair growth, and possibly psoriasis.

A number of studies have previously reported that topically applied AS-ODNs can be effective against their given target mRNAs (*160-163*). Recently, topical application of a 10-23 DNAzyme has been shown to be effective against its target when applied to the skin of C57Bl/6J mice providing proof of principle that a DNAzyme can be effective when applied topically to the skin (*164*). This DNAzyme targeted the mouse hairless gene which is essential for hair growth. Topically applied DNAzyme (in either 85% ethanol/15% ethylene glycol or Superfect liposomes [Qiagen]) was successfully delivered to a significant number of hair follicles. Hair growth was sparse and uneven

when the DNAzyme was applied twice daily (2 x 2 μg/cm$^2$) from the first day after delivery to 4 weeks. Short (4 weeks) and long (8 weeks)-term DNAzyme treatment recapitulated the hairless mouse phenotype as determined by histology (e.g. underdeveloped hair follicles, large cysts filled with keratinous material and degraded hair shafts).

Established and potential uses exist for a topical agent that reduces ODC activity in the skin. ODC has been shown to be involved in skin carcinogenesis (*165-168*) and to be important in the maintenance of hair follicles (*167, 169-171*). Indeed, difluoromethylornithine (DFMO), an inhibitor of ODC, is currently used or under investigation as a topical agent in both skin cancer chemoprevention and unwanted hair growth. DFMO is undergoing phase II clinical trials for the prevention of nonmelanoma skin cancer in patients with actinic keratosis and is the only FDA approved drug for the treatment of unwanted facial hair (labeled as Vaniqa™, Bristol-Meyers Squibb).

The catalytically optimized DZ IV was evaluated *in vivo* to determine its effect on silencing TPA-induced ODC activity in mouse skin. TPA-mediated induction of ODC activity in mouse skin is well-established. ODC activity increases rapidly, peaking at 6 hours post-TPA application followed by a rapid decline back to the low basal level (*172*). Importantly for this study, in which a DNAzyme targets ODC mRNA, the increase in ODC activity is the result of an increase in mRNA (*172*). Maximum induction of ODC mRNA occurs 2-3 hr post-TPA treatment (*173*).

This application provides an ideal model to study DZ IV for several reasons. As previously mentioned, there are established therapeutic benefits for silencing ODC activity in skin. ODC mRNA induction precedes, and is necessary, for TPA-induced

ODC activity. If the increase in ODC activity was due to a change in the half-life of the protein, this would not a desirable model to study a DNAzyme. DNAzymes are better suited for topical application than other gene silencing methods because, unlike AS-ODNs, DNAzymes possess catalytic activity and the nucleic acid composition of DNAzymes is more stable than RNA-based methods (e.g. ribozymes and siRNA). Using this model, it is demonstrated that DZ IV can silence endogenous ODC *in vivo* and is a viable strategy to modulate ODC activity in the skin.

Numerous studies show that modulating ODC activity in skin may be a useful strategy for the prevention or treatment of skin cancer and other disorders associated with skin including unwanted facial hair. The following sections will discuss these topics.

### *ODC Involvement in Chemically Induced and Spontaneous Skin Carcinogenesis*

Many mouse models have been described that link ODC with tumor development. Targeted overexpression of ODC from a keratin K6 promoter/regulatory region (*K6-ODC*) to the outer root sheath keratinocytes of the hair follicle in B6C3F2 mice results in an increased frequency of spontaneous tumors, the development of follicular cysts in the dermis and excessive wrinkling (*167*). The effect of ODC overexpression varies depending on the genetic background of the mouse (*174*). Breeding the *K6-ODC* transgene onto a C57BL/6J background prevents mice from developing spontaneous tumors, however these mice are much more sensitive to tumor development compared to nontransgenic littermates when exposed to the classical two-stage initiation-tumor promotion model of 7,12-dimethylbenz(*a*)anthracene (DMBA) – 12-*O*-

tetradecanoylphorbol-13-acetate (TPA) (*166*). In fact, the transgenic mice develop squamous papillomas independent of a tumor promoter and treatment with DFMO leads to rapid, and reversible, tumor regression (*165, 166*).

The mice in the aforementioned studies developed benign papillomas, however ODC has also been shown to be involved in more aggressive metastatic carcinomas. Two models that implicate ODC as having a role in squamous cell carcinomas (SCC) are both on a FVB/N background. Mice expressing the *K6-ODC* transgene on a FVB/N background rapidly develop malignant SCC after DMBA treatment (*175*). Treatment with 1% DFMO in the drinking water led to rapid tumor regression, due to reduction in tumor growth, which was maintained while the mice remained on DFMO. Polyamine levels, particularly putrescine, were also suppressed with DFMO treatment. Transgenic mice that overexpress protein kinase Cε (PKCε) targeted to the basal cells of the epidermis and hair follicles using the human cytokeratin 14 (K14) promoter develop metastatic SCC when subjected to DMBA-TPA (*169*). The development of SCC is completely prevented by the addition of 0.5% DFMO in the drinking water. Administration of DFMO also led to marked hair loss and a decrease in the number of intact hair follicles.

Reduction of ODC activity through antizyme has a similar effect to pharmacological inhibition of ODC with DFMO. Transgenic mice that express antizyme in specific skin cell populations exhibit decreased sensitivity to DMBA/TPA induced carcinogenesis as measured by a significant delay in tumor onset and a reduction in tumor incidence and the number of papillomas (*176*).

***ODC and UV-Induced Carcinogenesis***

The incidences of skin cancer is becoming increasingly more prevalent in the United States, with over 1 million cases diagnosed yearly accounting for ~40% of all new cancer diagnoses (*177, 178*). Nonmelanoma skin cancers (NMSC) make up the majority of skin cancers. Basal cell carcinomas (BCC) and squamous cell carcinomas (SCC) are the major classes of NMSCs (approximately 80% and 20% of NMSCs respectively) (*177*). Unlike BCCs which rarely metastasize, SCCs are more likely to metastasize and accounted for ~1200 deaths in 1998 (*178*). The majority of SCCs arise from pre-existing actinic keratoses (AK), although only 6-10% of AK progress to SCCs (*178*). AK represents SCC *in situ* at its earliest stages and therefore preventing AK or its progression to SCC is of keen interest.

Presently, AK is commonly treated with a topical application of 5% fluoruracil cream or liquid nitrogen (*179*). Due to untoward side effects, including severe inflammation, erythema and superficial ulcerations, of both these methods, better drugs are needed. A Phase II clinical trial is ongoing to study DFMO as chemoprevention of NMSC in patients with moderate to heavy AK. The initial findings look promising. Topical 10 % DFMO treatment to one arm of each patient reduced the number of AKs (23.5% reduction) and the skin level of spermidine (21% reduction) compared to the placebo-treated contralateral arm (*179*). Protein expression of p53 was also found to be significantly reduced (26%), although cell proliferation and apoptosis were not affected.

UV radiation is a complete carcinogen—it is sufficient for tumor initiation and promotion (*180*). Evidence suggests that ODC plays a role in UV-induced skin

carcinogenesis, notably in tumor promotion. SKH hairless mice are highly sensitive to photocarcinogenesis and therefore are the prototypical mice used in UV-induced carcinogenesis studies. SKH hairless mice receiving 0.4% DFMO in their drinking water exhibited a significant reduction in tumor multiplicity and tumor incidence (*181*). Transgenic SKH mice that overexpress ODC, driven by a K5 promoter, in the hair follicle keratinocytes were subjected to a UVB-exposure protocol that recapitulates a tumor-initiating dose (*180*). Under these conditions control nontransgenic mice did not develop tumors or pigmented cysts for up to 50 weeks. Forty percent of the ODC overexpressing transgenic mice developed benign papillomas and SCC. All the transgenic mice developed >10 pigmented cysts per mouse. DFMO (1% w/v) in the drinking water completely prevented tumorigenesis and significantly reduced the number of cysts in the transgenic mice.

ODC has also been shown to be an important target for BCC (*182*). The majority of BCCs have mutations in a tumor suppressor gene patch (*PTCH*). *K6-ODC* mice crossed with *Ptch1*+/- mice are more sensitive to BCC induction when exposed to UVB light than *Ptch1*+/- mice that don't overexpress ODC in the skin. Furthermore, overexpression of antizyme or treatment with DFMO significantly reduced UVB-induced BCCs in $Ptch1^{+/-}$ mice.

Xeroderma pigmentosum (XP) is a genetic disorder in which the patients are deficient in nucleotide excision repair (NER) and are highly sensitive (estimated thousand-fold increase susceptibility) to UV light (*183*). A mouse model was developed to represent the most severe phenotype in humans, knockout of complementation group A (*183*). When treated with 1% DFMO in the drinking water, UV-induced

carcinogenesis was significantly reduced in the *Xpa* knockout mice. Discontinuation of DFMO lead to a rapid appearance of skin tumors.

### *ODC and Hair Growth*

ODC has been shown to be important in the normal function of the hair follicle. Both overexpression of ODC and inhibition or reduction in ODC activity have been reported to alter hair growth in mice. The hair follicle in mice is characterized by three stages: anagen- growth phase, catagen- regression phase and telogen- resting phase (*184*). K6-ODC mice that overexpress a stable form of ODC in follicular keratinocytes completely lose their hair 2-3 weeks after birth (*185*), which coincides with the onset of ODC overexpression. Along with losing hair, these mice also exhibit excessive skin folds and wrinkling due to the increase and size of the number of dermal cysts. Administration of 1% DFMO in the drinking water of 6.5 week old transgenic mice with no hair and no normal hair follicles was able to substantially restore hair by 9 weeks of treatment. This was accompanied by the reappearance of normal hair follicles and fewer and smaller follicular cysts.

Overexpression of a stable ODC leads to alopecia in the aforementioned transgenic mice and reducing ODC with DFMO reverses the alterations in hair follicle and hair growth to a phenotype resembling wild-type mice. However, another mouse model reports the opposite. The transgenic mice previously described that overexpress protein kinase Cε (PKCε) from the K14-promoter exhibit marked hair loss and a decrease in the number of intact hair follicles when ODC is inhibited with 0.5% DFMO in the

drinking water (*169*). It is apparent that ODC plays a role in maintaining the follicle although the specific role is not understood. But it is likely that an equilibrium of ODC activity is required for a normal hair follicle. Too much or too little ODC activity can alter the normal hair follicle. It should be noted that other studies in different mouse models in which ODC is elevated or decreased have not reported changes in the phenotype of the hair (*50*). Therefore these effects are strain dependent or dependent on the level of ODC expression.

Vaniqa™ (13.9% eflornithine hydrochloride, DFMO) is the only FDA-approved drug for the treatment of unwanted facial hair. It is supplied in a cream formulation by prescription only for use in women to reduce unwanted facial hair. Users are prescribed to apply a thin layer to the affected facial areas twice a day, or ~ 1 g per day—the equivalent of 139 mg of eflornithine hydrochloride. Clinical trials reported in the Vaniqa™ FDA application, July 2000 (www.fda.gov), report a marked improvement in hair growth retardation, as determined by Physician's Global Assessment (PGA), after 8 weeks of treatment. The percent of subjects rated a success by PGA increased from 8 – 24 weeks at which time treatment was terminated. Hair growth eventually returned to pretreatment growth rates after Vaniqa™ treatment was terminated. There are studies in the literature that report that oral DFMO administration does decrease ODC activity in the skin. However, no studies exist in humans showing that the decrease in hair growth is due to inhibition of ODC. Nor are there any studies that ODC activity is decreased by Vaniqa™ treatment in human subjects.

***ODC and Psoriasis***

In addition to potential use in skin carcinogenesis and hair growth, ODC may be a valid target for the treatment of psoriasis, a chronic immune-mediated inflammatory skin disease, although more research is needed. Topical application of 10% DFMO to adult subjects with psoriasis led to a decrease in spermine levels and a marginal improvement in psoriatic lesions (*179, 186*).

Topical agents that could reduce ODC activity have potential applications in carcinogenesis, hair growth and psoriasis. Proof of principle that a topically applied DNAzyme can be effective has been established. Therefore, topical application is an ideal progression for evaluating the effectiveness of a DNAzyme directed against ODC. ODC is one of the early response genes to be induced by TPA application to the skin of mice (*172, 187*). The effect of topical application of DZ IV-T to the skin of mice following TPA-induction of ODC was evaluated. DZ IV-T treatment resulted in a statistically significant reduction in ODC activity compared to the control.

## Methods

### *Treatment of Mice*

One day prior to treatment, an approximately 2x2 cm area was shaved with surgical clippers 1 cm from the base of the tail on the dorsal area of 7-8 week old C57BL/6 mice. This age represents the onset of the second telogen phase in mice when the hair follicle is in the resting phase. At t=0 hr on the day of treatment, 17 nmol of TPA (Calbiochem-Novabiochem Corp., La Jolla, CA) in acetone (in 200 µl) was added to the shaved area on the back of each mouse followed by 200 µl of vehicle (85% ethanol/15% ethylene glycol), 200 µl DZ IV-T (10µg) in vehicle, 200 µl DZ IV-SCR-T (10 µg) in vehicle or approximately 100 mg Vaniqa™ (eflornithine hydrochloride, 13.9%, Bristol-Myers Squibb, Buffalo, NY). Vehicle, DZ-IV-T, DZ IV-SCR-T and Vaniqa™ treatments were repeated 2 hr post TPA application. Mice were sacrificed by asphyxiation 4 hr post TPA application (2x Rx Protocol, A, Figure 4.1). A second treatment protocol (4x Rx Protocol, B, Figure 4.1) was also used in which TPA was applied at t=0 followed by DZ IV-T treatment at t=0, 1, 2 and 3 hr. All other experimental parameters remained unchanged including the concentration and volume of TPA and DZ IV-T. The number of mice in each group is denoted in the Figure legend. Each group consisted of an equal number of male and female mice, except for the vehicle treated group (n=9; 4 male, 5 female).

A.

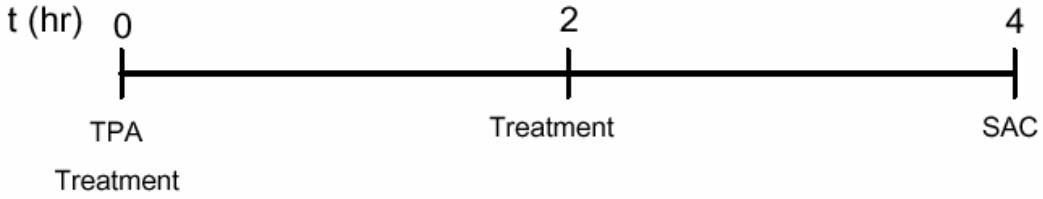


B.

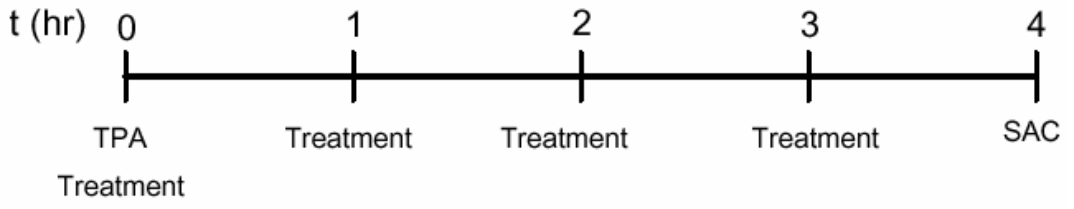


**Figure 4.1**: *Mouse Treatment Protocols.*

Mice were treated with TPA (17 nmol) at time 0 hr followed by treatment (vehicle [85% ethanol/15% ethylene glycol], 10 µg DZ IV-T, 10 µg DZ IV-SCR-T or 100 mg Vaniqa™). Treatment was repeated 2 hr after TPA application and the mice were sacrificed at time 4 hr (2x Rx Protocol, A). The 4x treatment protocol was similar, except the treatment (10 µg DZ IV-T) was applied 4 times (time 0, 1, 2, 3 hr; 4x Rx Protocol, B).

***Processing Skin Samples***

The treated dorsal skin was excised from each mouse, washed in ice-cold water for 5 min and incubated in water at 55°C for 20 s to facilitate the separation of the epidermis from the dermis (*176*). After scrapping the epidermis from the dermis, the tissues were separately processed. Epidermal tissue was resuspended in 500 µl of ice-cold Harvest Buffer [25 mM Tris-HCl (pH 7.5), 2.5 mM DTT, 0.1 mM EDTA and 1x Protease Inhibitor Cocktail Set I (Calbiochem-Novabiochem Corp.)] and lysed by sonication. The supernatant was collected by centrifuging the samples for 30 min at 30,000xg at 4°C. This step was repeated to further purify the supernatant fraction. The dermal tissue was minced into small pieces, resuspended in 1 ml of ice-cold Harvest Buffer and homogenized using a polytron. The supernatant was collected by centrifugation as described for the epidermis.

***ODC Activity and Protein Determination***

ODC activity was assayed and protein concentration determined for each epidermal and dermal sample as previously described (refer to Chapter 2).

**Results**

The effectiveness of topically applied DNAzyme targeted against ODC was evaluated in the skin of mice. A topical agent that can reduce ODC activity has potential clinical applications and therefore was a suitable model to test the DNAzyme. Application of DNAzyme to the shaved skin showed no visible signs of irritation or toxicity. The skin appeared indistinguishable among the different treatment groups. Topically applied DZ IV-T resulted in a 47% reduction in TPA-induced ODC activity in the dermis of mice compared to vehicle (A, Figure 4.2). This reduction is statistically significant, whereas treatment with the scrambled DZ IV-T, DZ IV-SCR-T, did not lead to a statistically significant reduction in ODC activity (A, Figure 4.2).

In the epidermis, no statistically significant reduction in ODC activity was found in the epidermis with DZ IV-T or DZ IV-SCR-T treatment (B, Figure 4.2). In the dermis, the hair shaft is the source of induced ODC activity and the DNAzyme likely penetrates better into the hair follicle than the epidermis. DZ IV-T treatment administered under the 4x RX protocol lead to a greater silencing than DZ IV-T treatment under the 2x RX protocol (dermis: 47% vs. 57% reduction; epidermis: 22% vs. 1% reduction in ODC activity). These differences are not statistically significant, but the addition of more mice to the DZ IV-T (4x) group may increase the statistical power.

Vaniqa™ virtually inhibits all DNAzyme activity in both the dermis and epidermis (95% and >99% reduction in ODC activity respectively, Figure 4.2). The

A.

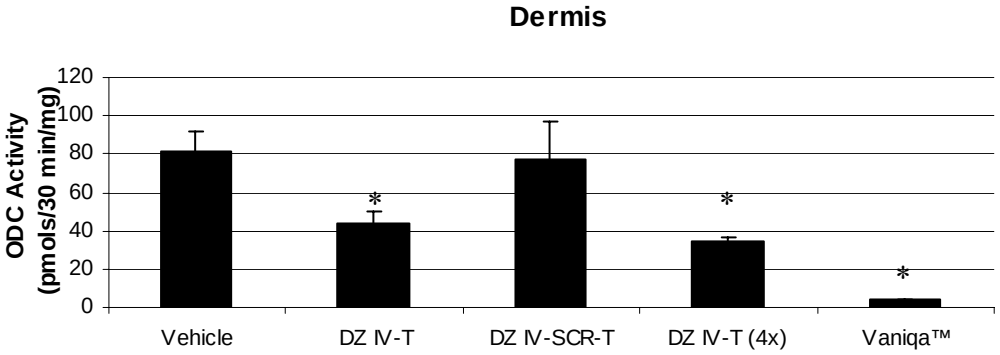


B.

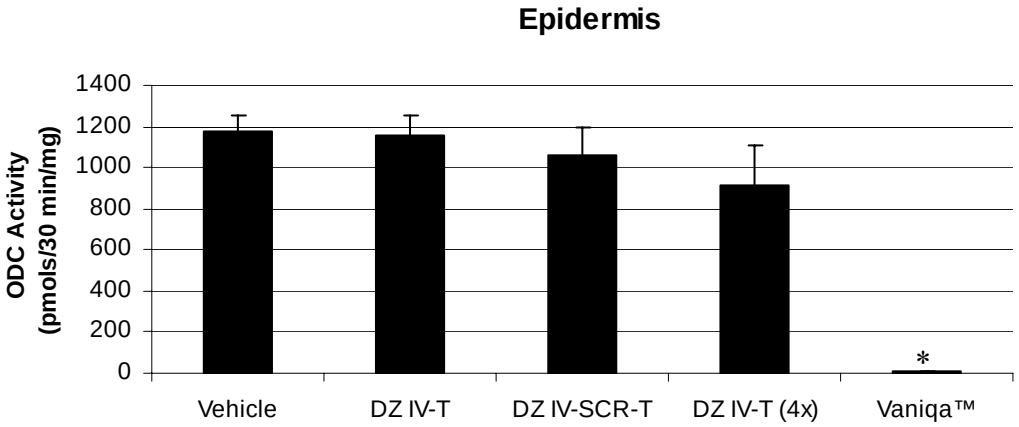


**Figure 4.2**: *Effect of Topically Applied DZ IV-T, DZ IV-SCR-T and Vaniqa™ In Mouse Skin.*

ODC activity was determined in the dermis (A) and epidermis (B) of the mouse skin after being treated with vehicle (85% ethanol/15% ethylene glycol), DZ IV-T (2x Rx Protocol), DZ IV-SCR-T, DZ IV-T (4x Rx Protocol) or Vaniqa™ (2 x 100 mg).

Dermis: vehicle, n=15; DZ IV-T 2x, n=9; DZ IV-SCR-T, n=6; DZ IV-T 4x, n=4, Vaniqa™, n=4

Epidermis: vehicle, n=15; DZ IV-T 2x, n=10; DZ IV-SCR-T, n=5; DZ IV-T 4x, n=4, Vaniqa™, n=4

Error bars represent mean standard error for each group

* $p < 0.05$ (compared to vehicle), two-tailed Student's t-Test

applied amount of DFMO in the Vaniqa™ solution was >60,000-fold greater than the applied amount of DZ IV-T (63,500 μmol DFMO hydrochloride vs. 1 μmol DZ IV-T). This is a modest approximation of the actual difference because the uptake of DFMO into the cells is likely to be more efficient than the uptake of the DNAzyme. These factors are likely to contribute to the difference in ODC activity between these two groups.

**Discussion**

Topically applied DZ IV-T successfully silenced TPA-induced ODC activity by ~50% *in vivo* in the dermis of mice and a scrambled form of DZ IV-T had no effect (A, Figure 4.2). A statistically significant reduction in ODC activity was not observed in the epidermis. The DNAzyme is most likely to taken up in the hair follicles of the skin, which contain keratinocytes located in the dermal fraction using this separation protocol. Therefore, the difference in silencing observed in the dermis and epidermis is likely to reflect the difference in penetration of the DNAzyme at these two areas of the skin.

It may outwardly appear that Vaniqa™ inhibits ODC activity more effectively than DZ IV-T silences it, but the two groups were not designed to be compared and a direct comparison can not be made from this data (Figure 4.2). The applied amount of DFMO in the Vaniqa™ cream exceeded a 60,000-fold molar increase over the applied DNAzyme. The differences in absorption would favor an even greater disparity between intracellular DFMO and DNAzyme. It is conceivable that Vaniqa™ does not inhibit ODC activity in the mouse skin *in vivo*, but that ODC activity is decreased because residual Vaniqa™ inhibits ODC activity in the *in vitro* assay. However, this is unlikely because the skin is extensively washed. To determine this, TPA could be administered to the mice at t = 0 hr and Vaniqa™ applied only once—at t = 4 hr just before the mice are sacrificed. The skin is washed as normal immediately after the mice are sacrificed. No decrease in ODC activity should be detected unless residual Vaniqa™ is present in the *in vitro* ODC activity assay.

The aim of these experiments was to determine if the catalytically optimized DNAzyme could silence ODC activity. The foremost purpose of the Vaniqa™ group was to provide a positive control for the experiment. DFMO is a known inhibitor of ODC and it was expected that Vaniqa™ could inhibit TPA-induced ODC when applied topically.

Doubling the number of DZ IV-T treatments from 2 to 4 leads to a further reduction in ODC activity (Figure 4.2). A control group (vehicle applied 4x) and more mice will need to be added to this group before it can be deemed statistically significant from the 2x treatment protocol. Large numbers of mice per group are needed because of the variability associated with experiments of this nature. Variability is confounded by the TPA-induction of ODC activity. ODC mRNA and activity rapidly increase within the first 5 hr after treatment and then rapidly falls again. The mice are sacrificed while ODC activity is still linearly rising as it approaches peak activity.

The most significant drawback of ODNs as a drug is poor delivery. ODNs have numerous properties, including large size and highly negative charge, which make them very difficult to deliver to cells. As a consequence, ODN drugs are usually administered by intravenous injection. Vitravene, an AS-ODN, is the only FDA approved drug that works by silencing mRNA. It is administered by intravitreal injection and requires that the affected eye be prepared with a standard local anesthetic and antimicrobial.

Numerous strategies exist to facilitate the uptake of ODNs into cells. It is believed that a receptor-mediated or adsorptive endocytosis mechanism is responsible for significant uptake of ODNs (*188*). Several ODN binding proteins have been described in different cell lines that bind ODNs and as a result, the ODN is internalized (*189*). ODN

uptake can be enhanced by conjugating the ODN to a molecule which is readily taken up by the cell. Cationic peptides, such as poly-L-lysine, are often conjugated to ODNs to facilitate internalization through nonspecific endocytosis (*190*). Cholesterol has also been used because it is internalized, at least in part, through the LDL receptor. Liposome formulations, electroporation and iontophoresis are also popular means to deliver ODNs.

An advantage of transdermal delivery of ODNs is that keratinocytes have been shown to be remarkably less resistant to ODN internalization than other cell types. Two high-affinity ODN-binding proteins that may be involved in the recognition and internalization of ODNs have been identified (*191*). Relatively efficient uptake of ODNs in keratinocytes occurs without the need of a cationic lipid and ODNs are found free in the cytoplasm, not confined to lysosomes (*163*). Chimeric ODNs containing a phosphodiester core and phosphorothioate 5' and 3' ends easily penetrated the keratinocytes in human skin explants (*162*). Phosphorothioate AS-ODNs targeting intercellular adhesion molecule-1 reduced the mRNA in a concentration-dependent manner when applied in a cream formulation to the skin of SCID mice (*192*). Compared to intravenous administration, a $\geq$ 150-fold increase in intact ODN was found in the dermis and epidermis when topically applied in the cream formulation. DNAzyme uptake would also be likely enhanced in the psoriatic skin because the lesions break down the barrier of entry. These reports suggest that topical DNAzymes application is feasible.

In our model, the DNAzyme is most effective in the dermis. The dermal layer contains the hair follicles, which is the source of the induced ODC activity in this layer. We propose that the DNAzyme has the greatest effect in the dermis because uptake is most efficient. The cornified layer in the epidermis is much more protective of the

underlying keratinocytes than the less developed cornified layer in the hair follicle. The DNAzyme passes through the cornified layer in the hair follicle more easily than in the dermis and then is taken up by the keratinocytes. This could be determined by treating mice with a fluorescent-labeled DNAzyme and then examining the uptake of the DNAzyme into the epidermis and dermis by fluorescence microscopy.

In conclusion, the results presented in this chapter provide evidence that DZ IV-T can silence endogenous ODC *in vivo*, even though ODC is induced to levels that far exceed basal levels. This DNAzyme is capable of being a useful tool to study ODC and the role it may play in skin related disorders, as well as a valuable tool to assess the viability of topically applied DNAzymes.

# Chapter 5

# Development of a Hammerhead Ribozyme Targeting ODC

## Specific Aim

To identify hammerhead ribozyme cleavage sites in ODC mRNA and evaluate the effectiveness of hammerhead ribozymes targeted to ODC at these sites.

## Introduction

In collaboration with Dr. Wei-Hua Pan in Dr. Gary Clawson's lab (Penn State College of Medicine, Hershey, PA), we have explored a second approach to silence ODC—using hammerhead ribozyme technology. Ribozymes and DNAzymes both act to cleave RNA in a catalytic manner. The development of effective ribozymes to ODC would permit us to design experiments to compare ribozymes and DNAzymes from a mechanistic standpoint as well as provide another means to modulate ODC activity.

The Clawson lab has developed several novel tools for ribozyme targeting. Many ribozyme site selection methods have been developed (*193*). A fair number of these methods scan RNA for site accessibility only and therefore do not assess the cleavage activity of the ribozymes. Other methods that do select for catalytically active ribozymes are typically labor intensive and not truly high-throughput. The SELEX (Systematic Evolution of Ligands by EXponential enrichment) screen developed by Pan *et al.* identifies accessible sites within the RNA and also selects for catalytically active ribozymes in a high-throughput fashion (*136*). Using this SELEX screen ribozymes highly active *in vitro* and in cell culture have been identified to target human papillomavirus type 16 E6/E7 mRNA.

One potential advantage of ribozymes over DNAzymes in cell culture is that ribozymes can be transcribed from a transfected plasmid by conventional means and therefore high expression levels can be obtained. Pan *et a*l. have also developed a novel ribozyme expression cassette (*194*). Each cassette is cloned into an expression vector

and, from that one cassette, two double internal, *trans*-acting hammerhead ribozymes (dITRZ) are released from the vector by flanking *cis*-acting ribozymes. This allows for multiple (up to four) ribozymes to be encoded by one vector. A multiple ribozymes approach against different sites within the target mRNA can be an effective strategy to more completely silence the target than one ribozyme alone. Release of the dITRZ by the cis-acting ribozyme frees the dITRZ with minimal unwanted vector sequence attached to the ribozymes that may interfere with activity. The 3' end of the dITRZ also contains several modifications to enhance ribozyme stability and activity.

Ribozyme targeting of mRNA is a proven method of gene silencing. Hammerhead ribozymes are currently being developed as therapeutic agents for a number of different therapeutic areas. In cancer therapeutics, a hammerhead ribozyme targeted to *MDR-1* (multidrug resistance) has been shown to revert the multi-drug resistant phenotype and consequently sensitize cancer cells to chemotherapeutic agents (*195*). Two clinical trials with ribozymes in cancer therapeutics are ongoing (*106*). In one trial, human epidermal growth factor receptor type 2, which is overexpressed in a high percentage of breast cancers, is targeted. In the other clinical trial *flt-1* mRNA, which codes for the high affinity VEGF receptor, is targeted by a hammerhead ribozyme to reduce angiogenesis. Ribozymes are well-suited to target viral diseases, such as hepatitis C, in which the viral genome is exclusively represented by RNA and ribozymes have been utilized in diverse areas such as diabetes, Alzheimer's and rheumatoid arthritis (*106*).

The development of ribozymes against ODC would provide another tool to study ODC and allow for studies comparing ribozymes and DNAzymes against the same target

and possibly similar sites. Through the SELEX screen, accessible sites will be identified in ODC mRNA that are potentially good areas to target DNAzymes, AS-ODN and siRNA, as well as ribozymes.

## Methods

### *Ribozyme Site Selection Screen*

The SELEX ribozyme selection screen was carried out in collaboration with Dr. Wei-Hua Pan in the laboratory of Dr. Gary Clawson (Penn State College of Medicine, Hershey, PA) as previously described (*136*). The concept of the screen is depicted in Figure 5.1 and 5.2. A single-stranded template oligonucleotide was synthesized (red sequence, Figure 5.1). The template consists of the hammerhead ribozyme core catalytic domain (23 nucleotides), flanked by two 9-nucleotide length arms of random sequence and fixed regions at both the 5' and 3' ends. The library contains $6.87 \times 10^{10}$ different sequences due to the diversity generated from the two randomized 9-nucleotide ribozyme hybridization arms. A primer to introduce a SP6 polymerase promoter (blue sequence, Figure 5.1) and two other primers ($Primer_A$, $Primer_B$) were used for PCR amplification. The resulting products were transcribed *in vitro* by SP6 polymerase to generate a diverse library of multiple RNAs with almost 70 billion different random hybridization arm sequences. The 5' and 3' fixed ends serve as primer templates for PCR to enrich the sequences that bind to the target RNA. The fixed ends also decrease the catalytic efficiency of the ribozyme, therefore the bound species selects for the most active ribozyme sequences.

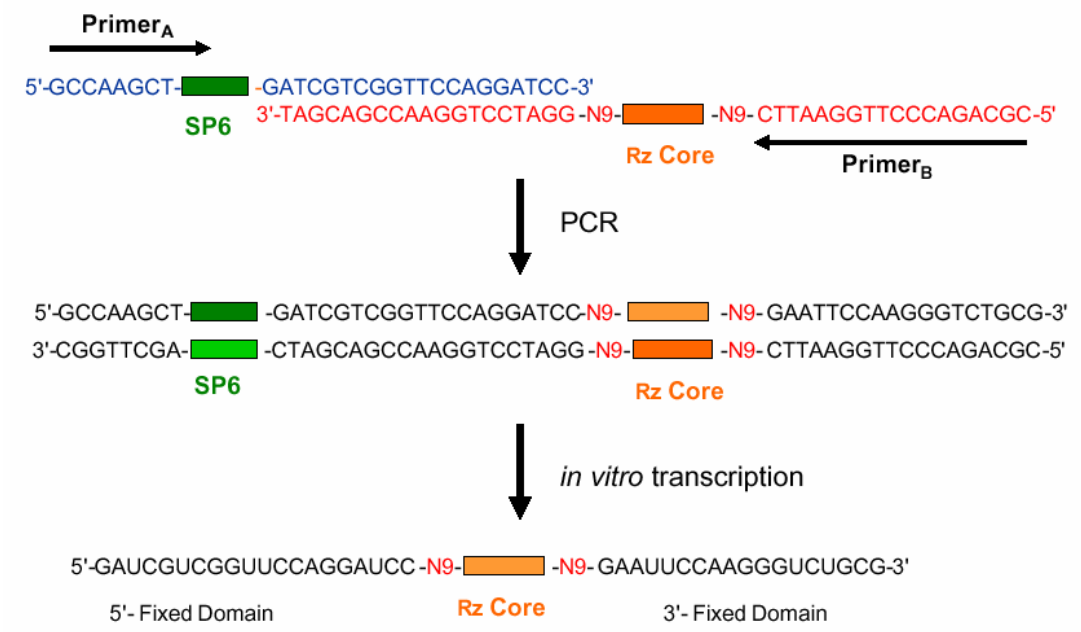


**Figure 5.1***: Generation of Ribozyme Selection Library*.

An oligonucleotide (in red) was synthesized containing a hammerhead ribozyme catalytic domain flanked by random 9-nt sequences with fixed sequences at the 5' and 3' ends. The randomization of the arms produced 6.87 x $10^{10}$ different sequences. An SP6 promoter was introduced by PCR and the PCR products were transcribed from the promoter to generate the ribozyme selection library.

Adapted from Pan *et al*. (*136*).

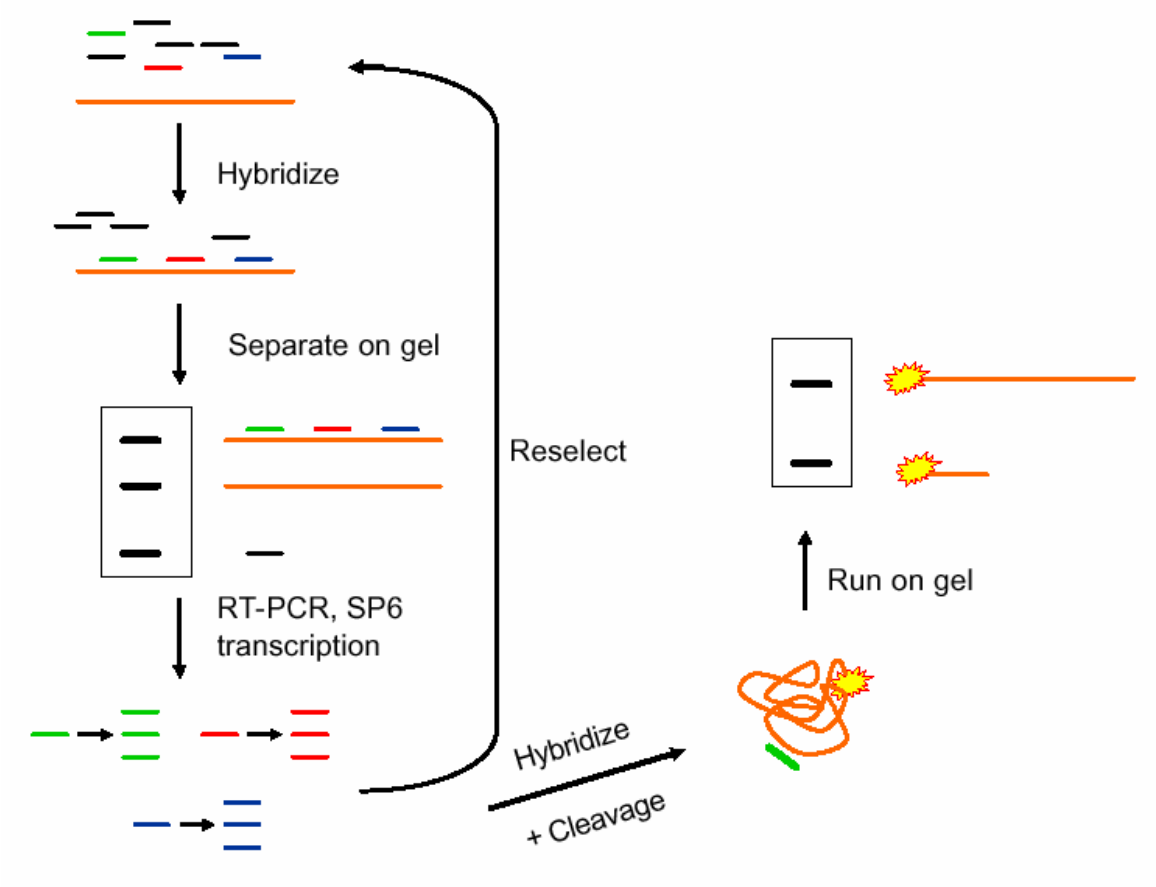


**Figure 5.2***: SELEX Screen.*

The SELEX screen involves hybridizing a randomized ribozyme library to the target RNA and enriching the ribozymes that bind to the target through RT-PCR followed by transcription of the PCR product back into RNA. The enriched ribozyme population undergoes another round of this screening and then is incubated with non-denatured target RNA in the presence of $Mg^{2+}$. The reaction products are separated by electrophoresis and the sites of ribozyme targeting are determined (see text for detail).

Adapted from Pan *et al.* (*136*).

The randomized ribozyme library was incubated with ODC RNA transcribed *in vitro* from pGEM-ODC. The ODC RNA was heat denatured in the presence of the ribozyme to allow it to hybridize without $Mg^{2+}$ (so no cleavage would occur). The ribozyme library RNAs that bound to ODC RNA were separated from the unbound ribozyme library RNAs by nondenaturing polyacrylamide electrophoresis. The RNA-RNA complexes were purified from the gel and the ribozyme library RNAs were reverse transcribed with $Primer_B$. The cDNA was amplified by PCR using $Primer_A$, $Primer_B$ and the SP6 primer. The PCR product was transcribed into RNA from the SP6 promoter and the resulting enriched ribozyme library RNA was subjected to a second round of selection. This round was performed as the first round except the stringency was increased in the second round by reducing the ODC RNA concentration by half. The selected ribozyme library RNA was then incubated with $^{32}$P-end-labeled ODC RNA in the presence of 25 mM $Mg^{2+}$. The resulting cleavage products were analyzed by gel electrophoresis and the sites of cleavage were identified by comparison to G-, A- and/or base-hydrolysis products of ODC RNA (Figure 5.2).

### *In Vitro Cleavage of Selected Ribozymes*

Ribozymes identified in the selection screen were evaluated *in vitro* against labeled ODC RNA as previously described (*136*). Briefly, nine selected ribozyme RNAs (40 nM) were incubated in vitro with trace amounts of 5'-$^{32}$P-labeled ODC RNA in 20 mM Tris-HCl, pH 7.4 and 25 mM $MgCl_2$ for 30 min. The cleavage products were

resolved from full-length ODC RNA on a polyacrylamide gel containing 6% urea. The bands were analyzed using a PhosphorImager.

### *Cloning Ribozymes Into Expression Vector*

Ribozymes that cleave at sites 857, 923, 941 and 1310 of ODC mRNA were cloned into the SNIP cassette (a ribozyme expression vector) as described previously (*194*). Each SNIP cassette expresses four ribozymes total from two internal, contiguous, double *trans*-acting hammerhead ribozymes (dITRz). The combinations of ribozymes cloned into each SNIP cassette is described in the text.

### *ODC Activity of HEK 293 Cells Transfected with Selected Ribozymes*

Human embryonic kidney (HEK 293) cells were cultured in complete growth medium (Dulbecco's modified Eagle's medium supplemented with 10% (v/v) fetal calf serum and 100 μg/ml penicillin and streptomycin) at 37°C with 5% $CO_2$. HEK 293 cells were cultured as previously described. One day prior to transfection, 1.0 - 1.5 x $10^6$ cells were plated in 60 mm plates or 0.85 x $10^6$ cells in 3.5 cm plates. Before transfection, the cells were washed twice with PBS and each plate was incubated with a transfection mix containing 0.1 μg pCMV-Zeo-ODCtr , specified ribozyme or a control vector, 12 μl of Lipofectamine Reagent (Invitrogen, Carlsbad, CA, USA) and 8 μl Plus Reagent (Invitrogen) in Opti-MEM I Reduced Serum Medium (Invitrogen) for 1.5 hours. After the incubation period, the transfection mix was aspirated, the cells were washed once

with PBS and incubated in complete growth medium for a specified time after which the cells were harvested in ODC Buffer (25 mM Tris-HCl pH 7.5, 2.5 mM DTT, 0.1 mM EDTA). Harvested cells were lysed by freeze-thawing three times in liquid nitrogen and centrifuged at 4°C at 12,000 x g to isolate ODC in the cytosolic fraction. An aliquot of the supernatant was assayed for protein concentration and ODC activity as described in Chapter 2. ODC specific activity was calculated in pmol $^{14}CO_2$/30 min/mg protein. The activity of the different treatment groups was expressed in ODC specific activity.

***ODC Activity Time Course***

HEK 293 cells (1.0 x $10^6$) were plated in 6 cm plates in triplicate for each condition. Twenty-four hours later, the cells were transfected with 0.1 ug of pCMV-Zeo-ODCtr and 3 μg of SnipA/pVAX (empty cassette) or RZ AA, AB, BB or CC. Cells were harvested 24 or 48 hr after transfection.

***Ribozyme Dose-Response***

HEK 293 cells (1.5 x $10^6$) were plated in 6 cm plates in triplicate for each condition. Twenty-four hours later, the cells were transfected with 0.1 ug of pCMV-Zeo-ODCtr and 1, 2, 4 or 6 μg of SnipA/pVAX (empty cassette) or RZ AB. Cells were harvested 36 hr after transfection.

***Determining the Effect of Empty Cassette on ODC Activity***

HEK 293 cells ($1.0 \times 10^6$) were plated in 6 cm plates in triplicate for each condition. Twenty-four hours later, the cells were transfected with 0.1 ug of pCMV-Zeo-ODCtr and 2 μg of SnipA/pVAX (empty cassette), RZ AB, pSV-βgal (Promega) or pIVEX- GFP (Roche). Cells were harvested 48 hr after transfection. This experiment was repeated, under slightly different conditions, to add another group in which ODC plasmid only was transfected into the cells. HEK 293 cells ($0.85 \times 10^6$) were plated in 3.5 cm plates in triplicate for each condition. Twenty-four hours later, the cells were transfected with 0.1 ug of pCMV-Zeo-ODCtr and 2 μg of SnipA/pVAX (empty cassette), RZ AB or pSV-βgal. Another group of cells was transfected with 0.1 μg of pCMV-Zeo-ODCtr only. Cells were harvested 24 hr after transfection.

## Results

### *SELEX Screen and In Vitro Evaluation of Ribozymes*

Seven of the nine ribozymes target sites localized to the same region of the very expansive mRNA (Region I, Figure 5.3). This suggests that this is the most accessible region of the mRNA. This was also the region that five of the six DNAzymes were targeted to. The other two sites selected were in the Region II arm of the mRNA. Five of the nine ribozyme sites identified (872, 923, 941, 1277, 1310) are in single-stranded, so-called bulge regions.

Nine ribozymes that were identified by the SELEX screen were tested for activity against *in vitro* transcribed ODC RNA. Five ribozymes, RZ 856, 857, 923, 941 and 1310, cleaved ≥ 74% of the substrate ODC RNA (A, Figure 5.4). Interestingly, the cleavage sites for RZ 856 and 857 are 4 and 5 nucleotides, respectively, away from the cleavage site of DZ IV, suggesting that this is a very good region to target. The expected size of the cleavage products for each ribozyme is listed in the schematic (B, Figure 5.4). The nomenclature used for the ribozyme's name (e.g. Rz 856) represents the site that the ribozyme cleaves full-length ODC mRNA containing the 5' and 3' UTRs. The ODC transcript used for the SELEX screen was a truncated form lacking both the 5' and 3' UTRs. Therefore, the expected size of the 5' cleavage product does not correlate with the ribozyme name.

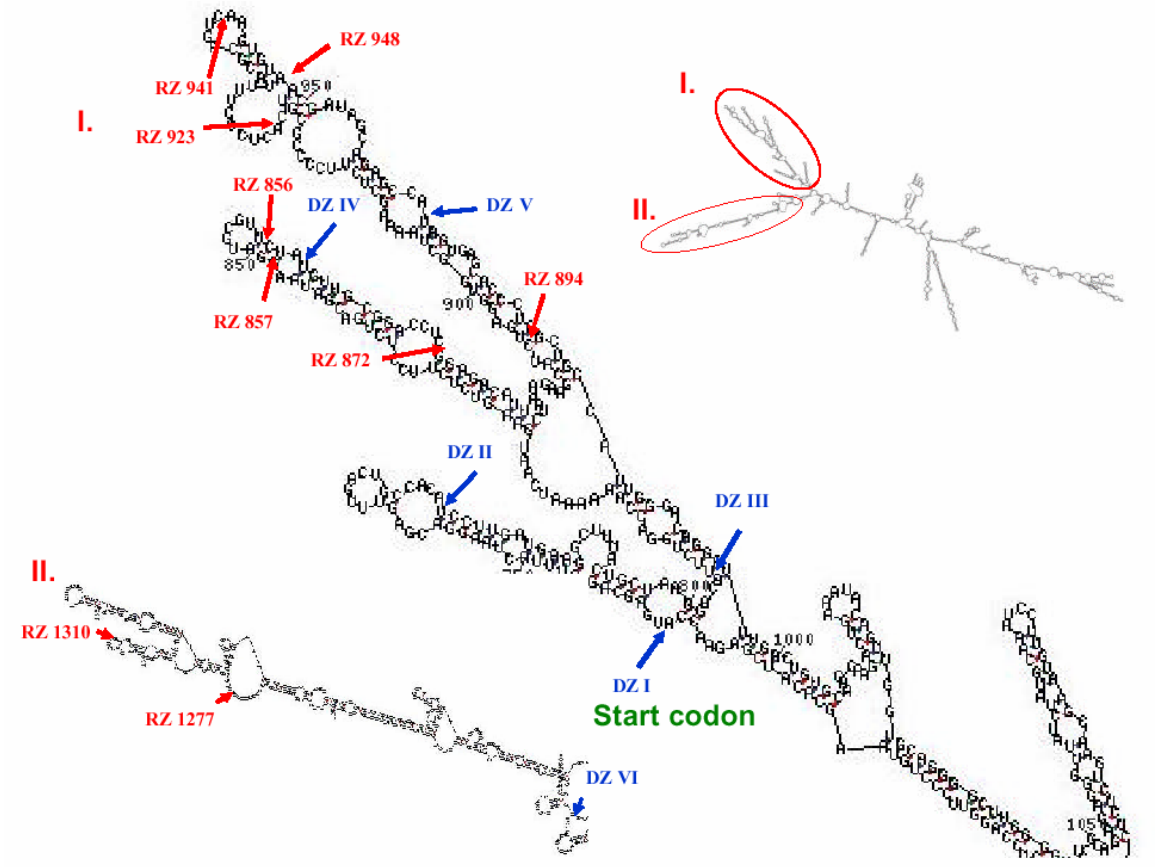


**Figure 5.3**: *Targeted Ribozyme and DNAzyme Sites Within ODC mRNA.*

The structure of ODC mRNA (with 5' and 3' UTRs) was modeled using mFOLD modeling program (www.bioinfo.math.rpi.edu/~zukerm/rna/). This structure represents the form with the lowest free energy. Region I and II are zoomed in to show the regions targeted by the ribozymes (listed in red). For reference, the DNAzyme target sites (from Figure 2.3) are noted in blue.

A.

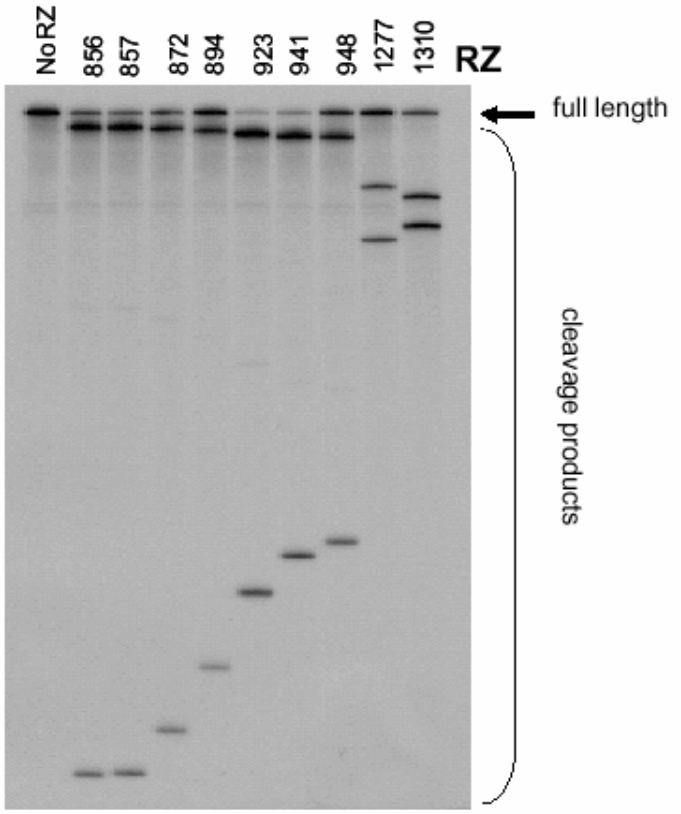


B.

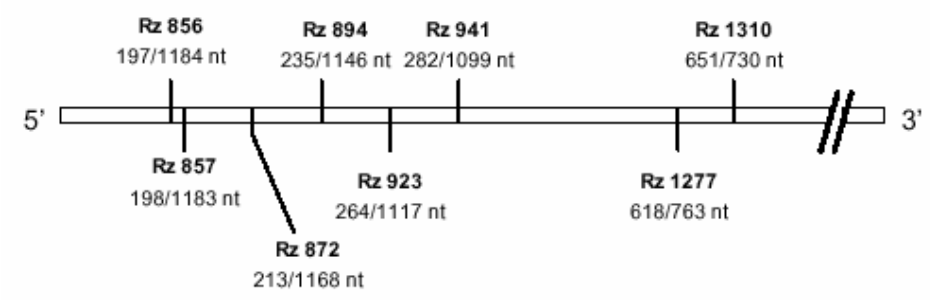


**Figure 5.4**: *In Vitro Cleavage of ODC RNA by Selected Ribozymes*.

Nine ribozymes identified by the SELEX screen were evaluate *in vitro* to determine how effectively each cleaved ODC RNA. The ribozyme and in vitro transcribed ODC RNA were incubated together in 20 mM Tris-HCl, pH 7.4 and 25 mM $MgCl_2$ for 30 min. Full-length ODC RNA and cleavage products were resolved by gel electrophoresis (A). A schematic representation showing the expected size cleavage products for each ribozyme (B).

Pan *et a*l. (*194*) have developed a novel ribozyme expression cassette. The $SNIP_{AA}$ cassette consists of two double internal, *trans*-acting hammerhead ribozymes (dITRZ) that are released from the vector by flanking *cis*-acting ribozymes (A, Figure 5.5). Each dITRZ has several modifications to increase stability. To enhance stability, a 10-bp hairpin loop and 30-nt poly(A)tail were added to the 3' end of each dITRZ. A 26-nt histone binding region was also added to the 3' end to facilitate pre-mRNA processing in the nucleus. A plasmid, SnipA/pVAX which expresses an empty cassette was used as the control in the experiments in cell culture. To create this plasmid, the $SNIP_{AA}$ empty cassette was cloned into pVAX1 expression vector (Invitrogen). Therefore, the *cis*-acting ribozymes from the cassette still release an RNA with the 10-bp hairpin loop, a 26-nt histone binding region and the poly(A) tail, however this RNA does not contain *trans*-acting ribozymes. It only contains a transcript of the sequence from the cassette used to clone the ribozymes into the cassette.

### *Cell Culture Experiments*

Four of the ribozymes (RZ 857, 923, 941, 1310) that exhibited the best activity were cloned into $SNIP_{AA}$. RZ 856 was not used, although it also displayed similar activity to the chosen ribozymes, because it cleaves so close to RZ 856 and we wanted to test ribozymes that target different areas o the ODC mRNA. The four ribozymes were cloned in combinations to make three different dITRZ: A (RZ 941 and 1310), B (RZ 857 and 923) and C (RZ 923 and 923) (B, Figure 5.5). The different dITRZ combinations

A.

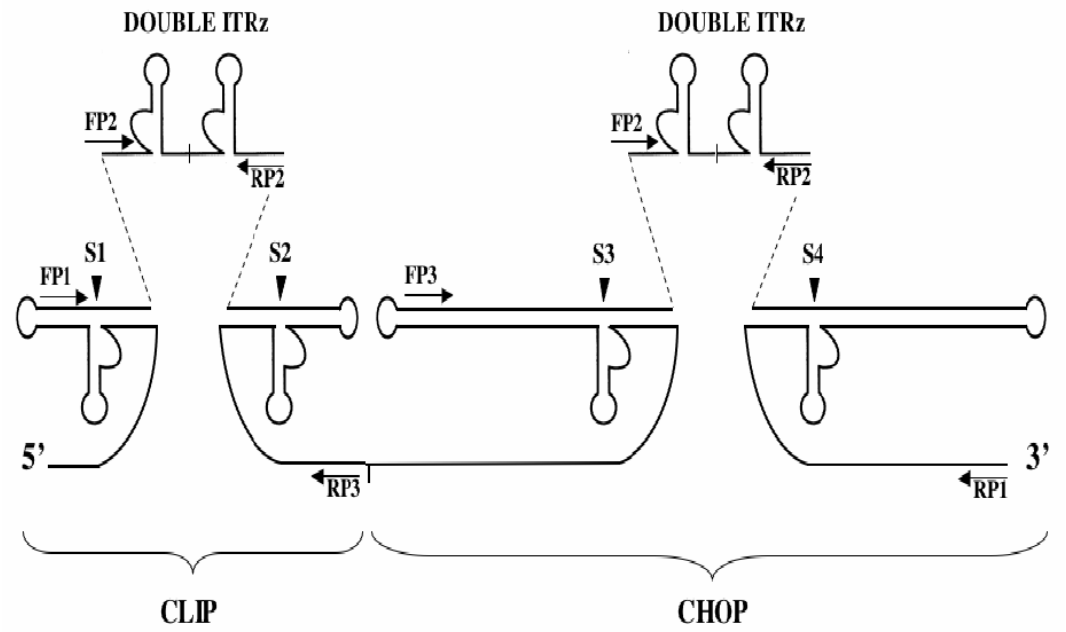


B.

| Double ITRZ | | |
|---|---|---|
| A | RZ 1310 | RZ 941 |
| B | RZ 923 | RZ 857 |
| C | RZ 923 | RZ 923 |

Constructs AA, BB, AB, CC

**Figure 5.5**: *Ribozyme Expression from SNIP$_{AA}$ Cassette*.

The ribozymes were cloned into the SNIPAA cassette. SNIPAA contains two double internal trans-acting ribozymes that are liberated from the vector by flanking cis-acting ribozymes (A, figure supplied by Dr Wei-Hua Pan). Different combinations of ribozymes were cloned into a dITRZ to make three different dITRZs (A, B, C). Then the different dITRZ were cloned into CLIP or CHOP to make four constructs, AA, BB, AB and CC.

were then cloned to make different constructs, AA, BB, AB and CC. For example, construct AA contained two dITRZs with each expressing a contiguous RZ 941 and RZ 1310 (for a total of four ribozymes per construct). From construct AB, two different dITRZs, A (RZs 941 and 1310) and B (RZs 857 and 923), are expressed.

The ribozymes were tested in cell culture in a similar fashion to the testing of the DNAzymes. Each ribozyme or the empty cassette (SnipA/pVAX) were co-transfected into HEK 293 cells along with the plasmid coding for truncated ODC and ODC activity was measured 24 or 48 hr post-transfection. Construct AB reduced ODC activity by 47% at both 24 and 48 hr post-transfection compared to SnipA/pVAX (Figure 5.6). Construct CC lead to a 31% and 40% reduction at 24 and 48 hr respectively. Constructs AA and BB had minimal effect on ODC activity compared to the control.

To determine if a different amount of co-transfected ribozyme would result in a more optimal silencing of ODC, various ribozyme concentrations were co-transfected with pCMV-Zeo-ODCtr. Four different amounts (1, 2, 4, 6 μg) of construct AB, which showed the most complete silencing of all the constructs in the previous experiment (Figure 5.6), were co-transfected into the cells. 4 μg of construct AB lead to a decrease (41%, Figure 5.7) in ODC activity similar to the decrease detected with construct AB in the prior experiment (Figure 5.7). At the other AB concentrations, no significant decrease in ODC activity was measure for AB vs. SnipA/pVAX, and in fact the activity was higher for AB at 1 μg (Figure 5.7).

The modest effect that the ribozymes had on ODC activity together with low absolute ODC activity levels for the control lead us to examine whether the empty

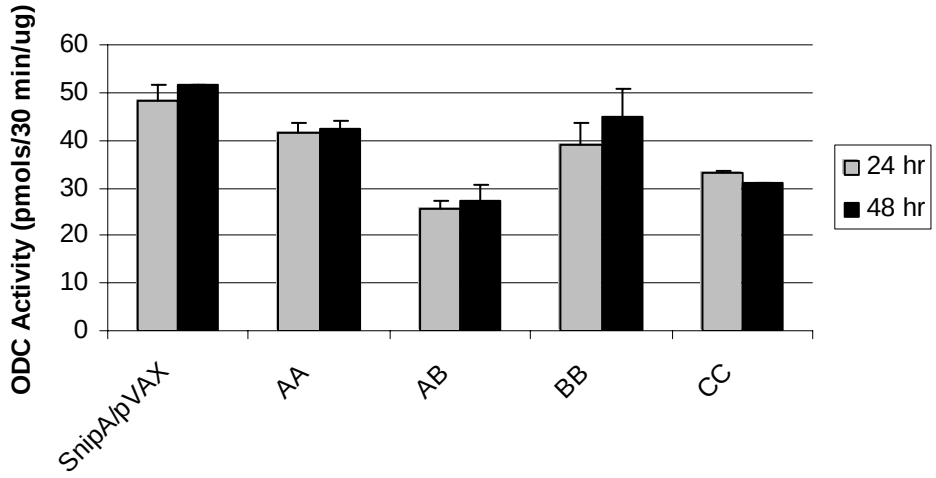


**Figure 5.6***: Evaluation of Selected Ribozymes*.

The empty cassette control (SnipA/pVAX) or RZ AA, AB, BB or CC (3 µg) was co-transfected into HEK 293 cells with 0.1 µg of a plasmid coding for ODC, pCMV-Zeo-ODCtr. The cells were harvested either 24 or 48 hr post-transfection and ODC activity was determined.

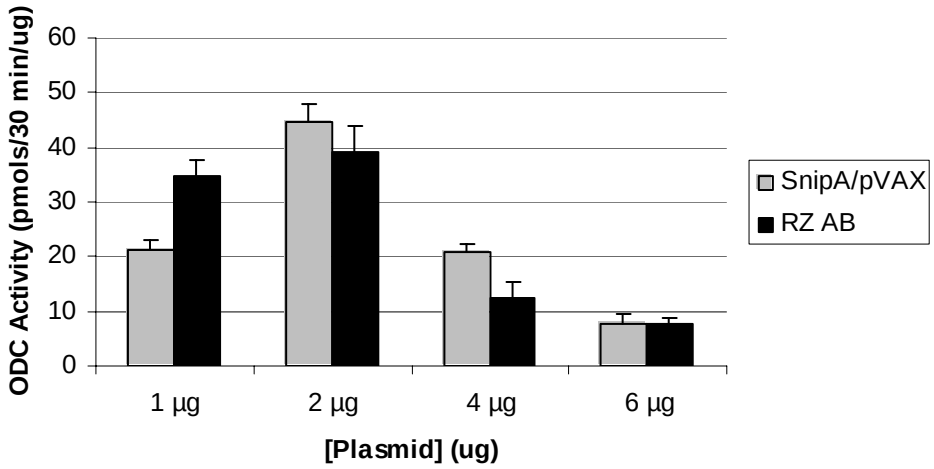


**Figure 5.7***: Effect of Increasing Amounts of Riboyzme on ODC Activity*.

Various amounts of RZ AB or SnipA/pVAX were co-transfected into HEK 293 cells with 0.1 µg of pCMV-Zeo-ODCtr. ODC activity was measured 36 hr after transfection.

cassette control SnipA/pVAX was in someway leading to the reduction in ODC activity. To test this, 2 μg of SnipA/pVAX, AB, or plasmids coding for β-gal or GFP were co-transfected into HEK 293 cells with 0.1 μg of pCMV-Zeo-ODCtr. The β-gal and GFP coding plasmids differ in that β-gal is expressed from this plasmid in mammalian cells, but the GFP plasmid does not have a mammalian promoter (it is designed to be expressed in *E. coli*) and it is not transcribed or translated in HEK 293 cells. The SnipA/pVAX control may lead to a reduction by two means; a passive means in which just transfecting a plasmid interferes with transfection or expression of ODC or an active means in which transcription of the empty SnipA/pVAX cassette affects ODC activity. If in fact SnipA/pVAX was silencing or inhibiting ODC activity, using a plasmid that is expressed and one that is not would allow us to determine if the reduction in ODC activity is unique to SnipA/pVAX or a general problem with the co-transfection method. In fact, ODC activity is elevated >4 and >6-fold respectively when transfected with either the β-gal or GFP plasmid compared to SnipA/pVAX (Figure 5.8). It is therefore clear that transfection of a plasmid alone is not the cause of suppressed ODC activity and that SnipA/pVAX is interfering with ODC activity in some other way.

Cells transfected with 0.1 μg of pCMV-Zeo-ODCtr alone have lower ODC activity (~4 and 2-fold lower activity respectively) than those co-transfected with 0.1 μg of pCMV-Zeo-ODCtr and 2 μg of SnipA/pVAX or RZ AB (Figure 5.9). This suggests that DNA is needed to enhance the transfection efficiency of 0.1 μg pCMV-Zeo-ODCtr. It is likely that the vector SnipA/pVAX is not blocking the transfection of pCMV-Zeo-ODCtr, but interfering with the expression of ODC from the plasmid. The *cis*-acting

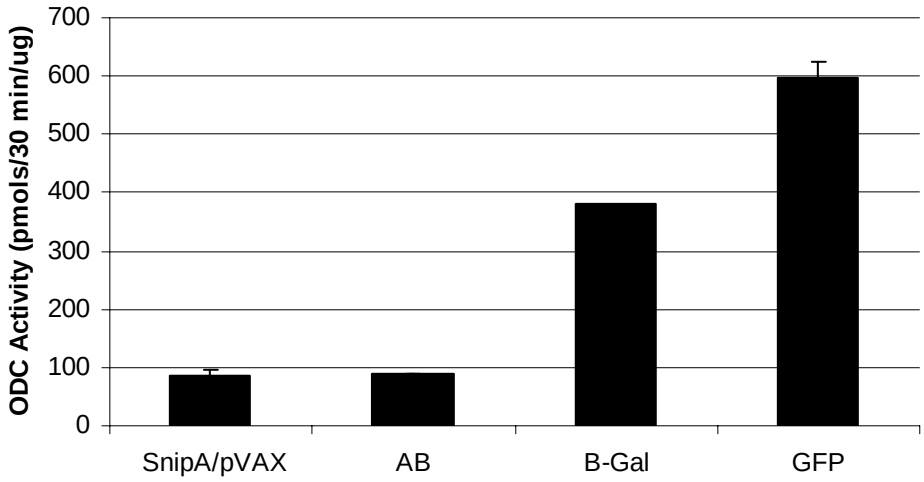


**Figure 5.8*:*** *Determining the Effect of SnipA/pVAX on ODC Activity*.

The effect of co-transfecting 0.1 μg of pCMV-Zeo-ODCtr with 2 μg of SnipA/pVAX, RZ AB, β-gal or GFP on ODC activity was determined. The β-gal and GFP plasmids provided control plasmids to assess whether SnipA/pVAX interfered with ODC activity. β -gal is expressed from the plasmid in mammalian cells; GFP is not expressed from its plasmid in mammalian cells.

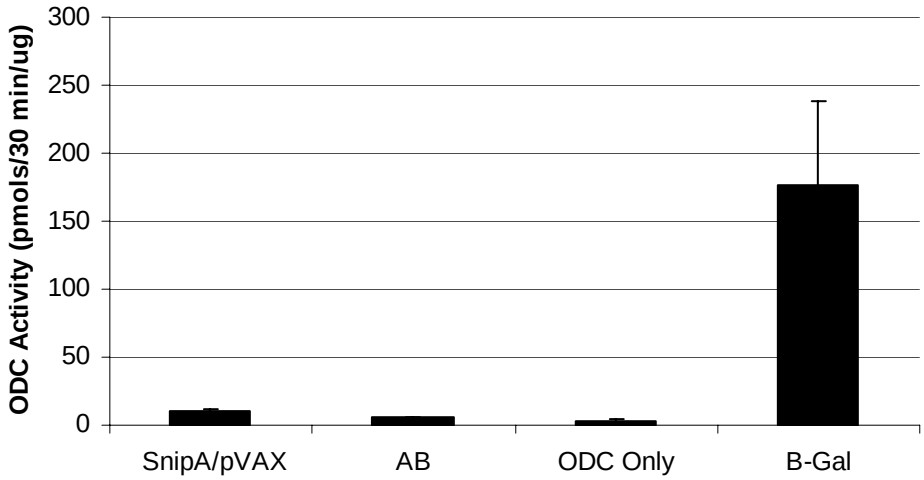


**Figure 5.9**: *Determining the Effect of the Presence of a Co-transfected Plasmid on the Activity of pCMV-Zeo-ODCtr.*

pCMV-Zeo-ODCtr (0.1 μg) was either transfected alone or along with 2 μg of SnipA/pVAX, RZ AB or pSV-β-gal into HEK 293 cells and ODC activity was determined. Additional DNA is necessary to increase the transfection efficiency of the 0.1 μg of pCMV-Zeo-ODCtr.

ribozymes in SnipA/pVAX or the RNA released from the empty cassette could be interfering with the translation of ODC.

**Discussion**

The novel SELEX ribozyme selection screen identified sites within ODC mRNA deemed to be good targets for ribozymes (and likely other methods of gene silencing that require hybridization to the mRNA). Ribozymes targeted to these sites were able to cleave *in vitro* transcribed RNA, and showed very high activity (A, Figure5.4). Interestingly, most of these sites were localized to the same general region of ODC mRNA, suggesting that this is the most accessible region within the mRNA (Figure 5.3). Indeed, two ribozymes (RZ 856 and 857) with good activity against *in vitro* transcribed ODC RNA (Figure 5.4) cleaved at sites within 5-nt from the cleavages site of DZ IV—a DNAzyme that also displayed good activity (Figure 5.3).

RZ AB exhibited the best activity in cell culture leading to an ~50% reduction in ODC activity 24 and 48 hr post-transfection (Figure 5.6). However, a dose-response experiment showed no statistical difference in ODC activity between the control and RZ AB for any of the four concentrations tested (Figure 5.7). Absolute ODC activity for the control was also lower than previously observed for similar experiments. This lead us to test whether the control SnipA/pVAX was interfering with the transfection or expression of the ODC coding plasmid.

To determine if treatment with SnipA/pVAX had an unanticipated effect on ODC activity, two unrelated plasmids were co-transfected into the HEK 293 cells along with ODC. One plasmid, pIVEX-GFP, is not transcribed in mammalian cells. It simply serves as a DNA plasmid control. However, β-gal mRNA is transcribed from pSV-β-gal

in these cells. SnipA/pVAX could cause non-specific reduction in ODC activity because: (1) the presence of a plasmid alters the transfection efficiency of the co-transfected ODC plasmid, (2) the general process of transcription is altered by the co-expression of the co-transfected plasmids and/or (3) the empty cassette transcript coded for by SnipA/pVAX reduces the amount of ODC mRNA available for translation. ODC activity increased ~4 and 6-fold when pCMV-Zeo-ODCtr was co-transfected with pSV-βgal and GFP, respectively, compared to SnipA/pVAX (Figure 5.8). Therefore it is unlikely that ODC activity is decreased in pCMV-Zeo-ODCtr transfected cells because the plasmid is altering transfection efficiency. If this was the reason, then ODC activity would not be higher in cells transfected with pSV-βgal and pIVEX-GFP. To the contrary, a certain amount of co-expressed plasmid enhances the expression of ODC from pCMV-Zeo-ODCtr (Figure 5.9). Nor is it likely the decrease in ODC activity is the result of transcription of the co-transfected plasmid because the activity of pSV-βgal transfected cells is higher than SnipA/pVAX transfected cells (Figure 5.9). The RNA transcribed from the empty cassette of SnipA/pVAX is likely repressing ODC activity or ODC transcription.

It can not be determined from these experiments whether the ribozymes are active or not. The ribozymes substantially silence ODC activity compared to pSV-βgal and pIVEX-GFP, but the change in ODC activity is not statistically significantly different compared to SnipA/pVAX. The ribozymes constructs may be silencing ODC by the same non-specific mechanism as SnipA/pVAX or the ribozymes may very well be active, but the activity is masked by the nonspecific silencing of SnipA/pVAX.

As previously described, SnipA/pVAX is not an empty vector—it is a pVAX vector with the empty $SNIP_{AA}$ cassette cloned into it. Two dITRZ RNAs are still transcribed from this vector, but no *trans*-acting ribozymes have been cloned into the cassette. The transcripts may affect ODC activity in a number of ways. The *cis*-acting internal ribozymes transcribed from SnipA/pVAX may have off-target effects on ODC mRNA. The transcript released by the *cis*-acting internal ribozymes may interfere with the stability or translation of ODC mRNA. This released transcript does contain the stability and pre-mRNA processing enhancing features: a 10-bp hairpin loop, a 30-nt poly(A) tail and a 26-nt histone binding region. This stable RNA could potentially silence ODC mRNA in several ways. High concentrations of siRNA have shown to nonspecifically silence non-targeted genes (*196, 197*). High expression is generally observed from SnipA/pVAX. It has been demonstrated that microRNAs can silence partially matched genes by interfering with translation (*198*). The phenomena of transitive RNAi, although not yet identified in human cells, can also suppress gene expression (*199*). All of these represent potential means by which the RNA transcribed from SnipA/pVAX or the two fragments of the transcript released by the internal *cis*-acting ribozymes could silence ODC or an7 co-transfected plasmid.

Although ribozymes expressed from a $SNIP_{AA}$ cassette have been reported to be active (*194*), nonspecific silencing effects have been observed by others (personal communication with Wei-Hua Pan, Penn State College of Medicine). For future experiments to help assess the viability of the ODC-targeting ribozymes, we could use another plasmid to express the ribozymes. Nawrot *et al*. have demonstrated up to 95% inhibition of β-secretase gene expression in HEK 293 cells using a $tRNA_{Val}$-driven

hammerhead ribozyme (*200*). The effect of SnipA/pVAX on the activity or protein expression of other co-transfected genes could also be studied to determine if this plasmid universally silences gene expression or if it is specific to ODC.

In summary, we have identified sites in ODC mRNA that are efficiently cleaved by hammerhead ribozymes *in vitro*. Two identified sites cleave within 5-nt of the cleavage site for DZ IV, a DNAzyme which has shown good activity. This suggests that this region is most susceptible to targeting. In cell culture, the control plasmid SnipA/pVAX nonspecifically silences ODC, thereby the activity of the ribozymes can not be accurately assessed. The proposed experiments may determine whether the ribozymes are actively or nonspecifically silencing ODC.

# Chapter 6

## Overall Conclusions and Future Perspectives

Polyamines are essential for cell growth, but the role of polyamines in cell growth is not well-understood, in part due to the ubiquitous nature of these polycationic molecules and the complexity of polyamine homeostasis. ODC is an important regulator of polyamine biosynthesis and is known to be one of the most highly regulated enzymes. This tight regulation suggests the importance of this enzyme with only one known function—to decarboxylate ornithine into putrescine. This thesis focused on developing and identifying modulators of ODC activity and to determine a role of ODC in transformation in order to identify downstream targets of ODC.

Two approaches to modulate ODC activity by targeting ODC at the mRNA level using DNAzymes and ribozymes were explored. The development and identification of an effective DNAzyme is detailed in three phases. In the design phase (Chapter 2), six 10-23 DNAzymes successfully cleaved *in vitro* transcribed ODC RNA, which correlated with the percentage of translated ODC protein and ODC activity from the DNAzyme-treated transcripts.

DNAzymes posses an advantage over AS-ODNs in that DNAzymes have catalytic potential. Therefore, if a DNAzyme has poor catalytic activity, the difference in gene silencing between the DNAzyme and an analogous AS-ODN is expected to be attenuated. The length of the hybridization arms of one of the most promising DNAzymes (DZ IV), based on the *in vitro* evaluation, was altered to determine the most

catalytically efficient configuration (Chapter 2). We developed a new method to determine DNAzyme kinetics that permits the reaction product to be more accurately quantified. Using this method, it was established that equal nine nucleotide length arms is the optimal catalytic configuration for DZ IV. This catalytically optimized DNAzyme was used in the subsequent evaluation phases.

Evaluation of the efficacy of the catalytically optimized DNAzyme was determined *in vitro* (Chapter 3) and *in vivo* (Chapter 4). The *in vitro* evaluation studies were conducted to determine whether DZ IV with a 3' inverted T (DZ IV-T) was capable of silencing ODC in a cell culture model in which the DNAzyme would be subjected to a more physiologically relevant environment, yet eliminating complicating factors involved in an *in vivo* model. In summary, these studies demonstrated that the catalytically optimized DZ IV-T indeed silenced ODC more completely than counterparts with scrambled hybridization arms or a catalytically inactive mutant, as well as a corresponding AS-ODN in cell culture.

A DNAzyme that effectively silences ODC potentially has two-fold uses. One, it can be used as a research tool to modulate ODC activity *in vitro* to study ODC and polyamines. The studies referenced above from Chapter 3 established that DZ IV-T could be successfully used for this purpose. Another potential use for this DNAzyme is as a therapeutic agent to reduce ODC activity for the treatment of a disorder. ODC is a proven drug target for the treatment of West African trypanosomiasis (*119*), unwanted facial hair (Vaniqa™) and DFMO has been and is currently under investigation as a chemopreventative/therapeutic agent. Presently, DFMO is undergoing phase II clinical trials for the prevention of nonmelanoma skin cancer in patients with actinic keratosis

(www.fda.gov). In addition, it has been shown in several different models that ODC is involved in skin carcinogenesis (*165-168*) and in the maintenance of hair follicles (*167, 169-171*). Therefore, a topical agent that reduces ODC activity has the potential to be effective for a number of disorders.

Topical application of the catalytically optimized DZ IV-T applied to the skin of mice was used to evaluate this DNAzyme *in vivo*. ODC mRNA and activity was up-regulated in the skin prior to DNAzyme treatment with the application of TPA. DZ IV-T significantly reduced ODC activity, although the vehicle and a scrambled DZ IV-T (DZ IV-SCR-T) did not. Impressively, DZ IV-T was effective despite the massive TPA-induced increase in ODC and the fact that DNA is not efficiently taken-up by cells.

Additionally, using a ribozyme SELEX screen, we identified hammerhead ribozymes with very good *in vitro* activity (Chapter 5). Ribozymes selected by the screen and tested all cleaved *in vitro* transcribed ODC RNA at their targeted site. However, the ribozymes could not be accurately evaluated in cell culture because the novel ribozyme expression vector used in the studies caused non-specific gene silencing. Other ribozyme expression cassettes could be obtained to evaluate the efficacy of these ribozymes to silence ODC.

Together these studies do confirm that targeting ODC mRNA is an effective strategy to reduce ODC activity. DZ IV-T can be used to study ODC and polyamines *in vitro* and in cell culture, but the question as to whether nucleic acid based drug could compete favorably against small molecule compounds is another issue. DNAzymes have a number of distinct advantages over small molecule drug inhibitors. DNAzymes are potentially more effective and would elicit fewer side effects because DNAzymes

intervene in a highly specific manner. Target validation using DNAzyme (and AS-ODN) technology is fast and economical. Once a gene target has been identified, these nucleic acid-base drugs can be used to validate the target in less than 30 days. Thereafter, the design of an AS-ODN lead drug compound only takes approximately 90 days compared to the 2-4 year time period that it can take to design a small molecule therapeutic agent (Isis Pharmaceuticals, www.isip.com). This shortens the drug development process bringing potential therapeutics to the market faster and substantially reducing research and development costs.

Nucleic acid drugs are faced with a number of significant drawbacks that presently limit the potential of these drugs, namely cost and delivery issues. These issues should not deter further research in this field, but in fact promote it because they can be overcome. In general, delivery of nucleic acid based drugs has been thought to be problematic, but it has been shown that they readily distribute to a number of organs including the liver, spleen, bone marrow and fat cells (*201, 202*). Significant enhancements in the potency and specificity of nucleic acid drugs have been brought about by modifying the chemistries of the nucleic acids (e.g. locked nucleic acids, 2'-*O*-methoxyethyl).

Moreover, many companies, as well as academic research groups, are dedicated to the advancement of mRNA targeting strategies (e.g. ISIS Pharmaceuticals, Genta, Hybridon, Antisense Therapeutics, Sirna Therapeutics, CytRx Corporation, Sequitur, Genta, CytoGenix). These companies and groups are actively pursuing research to enhance delivery, reduce cost and to increase the potency and stability of nucleic acid based drugs. For example, Isis has developed a solid oral dosing technology in which the

company has used to achieve sufficient drug plasma concentrations of an antisense inhibitor of tumor necrosis factor-alpha (Orasense™). Recently, siRNA has been successfully delivered systemically by attaching it to cholesterol (*203*). Other significant progress has been made in oral, topical cream, intravenous, subcutaneous, intravitreal, aerosol and enema nucleic acid based drug delivery by these groups as well.

Another approach to regulate ODC activity was pursued and is detailed in the proceeding appendix (Appendix A). In this approach, ODC protein, not mRNA, was targeted. ODC is only active as a homodimer, therefore small molecules that block ODC homodimerization would in theory be effective inhibitors of ODC activity. To identify such inhibitors we sought to develop a high-throughput screen to detect the dimerization state of ODC. After testing a number of strategies, studies suggest that a change in the dimerization state of ODC can be detected by monitoring intrinsic protein fluorescence.

ODC protein exhibits robust intrinsic fluorescence originating from unquenched tryptophan residues. Data obtained from preliminary studies suggest that tryptophan fluorescence is more intense when ODC is dimerized than in the monomeric form. Diluting the protein concentration abates the difference in fluorescence between wild type and dimerizing mutants from non-dimerizing ODC mutants. ODC dimerization is transient—that is dimers dissociate and reassociate (*20*)—therefore dilution of the protein favors a higher percentage of the monomeric form at a given time.

Further validation of this method is needed and can be provided by studying the fluorescence of additional protein preparations and other dimerizing and non-dimerizing mutants. Additionally, fluorescence anisotropy and surface plasmon resonance can also be used to validate the dimerization state of the protein. Using this strategy, we may be

able to identify small molecule ODC inhibitors that mechanistically inhibit ODC by interfering with ODC dimerization.

ODC is a target for chemoprevention/therapeutics, yet little is known about a role of ODC in cancer. In Appendix B, the design of a microarray experiment to better understand the role(s) of ODC in cell transformation is detailed. A dominant-negative ODC mutant reverts the transformed phenotype of Ras-transformed cells. Microarray analysis was used to identify differential gene expression in these cells. Using the gene list generated by this experiment, we may be able to identify genes downstream of ODC that are essential for Ras transformation in these cells, and thereby gain a better understanding of a role of ODC in cancer.

In conclusion, this thesis has detailed the successful development and demonstrated the feasibility of novel methods to reduce ODC activity and to potentially identify inhibitors of ODC protein. In addition, genes were identified which may aid in understanding a role of ODC in cell transformation and cancer.

## Bibliography


1. Cohen, S. S. (1998) *A guide to the polyamines*, Oxford University Press, New York.
2. Fontecave, M., Atta, M., and Mulliez, E. (2004) S-adenosylmethionine: nothing goes to waste, *Trends Biochem. Sci. 29*, 243-9.
3. Pegg, A. E., Xiong, H., Feith, D., and Shantz, L. M. (1998) in *Methionine Metabolisn: Molecular Mechanisms and Clinical Implications* (Mato, J. M., and Cabellero, A., Eds.), Jarpyo Editores, Madrid.
4. Avila, M. A., Garcia-Trevijano, E. R., Lu, S. C., Corrales, F. J., and Mato, J. M. (2004) Methylthioadenosine, *Int J Biochem Cell Biol 36*, 2125-30.
5. Pegg, A. E. (1986) Recent advances in the biochemistry of polyamines in eukaryotes, *Biochem. J. 234*, 249-262.
6. Casero Jr, R. A., and Pegg, A. E. (1993) Spermidine/spermine N1-acetyltransferase: the turning point in polyamine metabolism, *FASEB J. 7*, 653-661.
7. Marton, L. J., and Pegg, A. E. (1995) Polyamines as targets for therapeutic intervention., *Annu. Rev. Pharm. 35*, 55-91.
8. Bolkenius, F. N., and Seiler, N. (1981) Acetyl derivatives as intermediates in polyamine catabolism, *Int. J. Biochem. 13*, 287-292.
9. Chopra, S., and Wallace, H. M. (1998) Induction of spermidine/spermine $N^1$-acetyltransferase in human cancer cells in response to increased production of reactive oxygen species, *Biochem. Pharmacol. 55*, 1119-1123.
10. Wang, Y., Devereux, W., Woster, P. M., Stewart, T. M., Hacker, A., and Casero Jr, R. A. (2001) Cloning and characterization of a human polyamine oxidase that is inducible by polyamine analogue exposure., *Cancer Res. 61*, 5370-5373.
11. Vujcic, S., Diegelman, P., Bacchi, C. J., Kramer, D. L., and Porter, C. W. (2002) Identification and characterization of a novel flavin-containing spermine oxidase of mammalian cell origin, *Biochem. J. 367*, 665-675.
12. Wallace, H. M. (1987) Polyamine catabolism in mammalian cells: excretion and acetylation, *Med. Sci. Res. 15*, 1437-1440.
13. Coffino, P. (2001) Regulation of cellular polyamines by antizyme, *Nature Rev. Mol. Cell. Biol. 2*, 188-194.
14. Mitchell, J. L. A., Judd, G. G., Bareyal-Leyser, A., and Ling, S. Y. (1994) Feedback repression of polyamine transport is mediated by antizyme in mammalian tissue culture cells, *Biochem. J. 299*, 19-22.
15. Suzuki, T., He, Y., Kashiwagi, K., Murakami, Y., Hayashi, S., and Igarashi, K. (1994) Antizyme protects against abnormal accumulation and toxicity of polyamines in ornithine decarboxylase-overproducing cells, *Proc. Natl. Acad. Sci. USA 91*, 8930-8934.
16. Sakata, K., Kashiwagi, K., and Igarashi, K. (2000) Properties of a polyamine transporter regulated by antizyme, *Biochem. J. 347*, 297-303.

17. Wallace, H. M., Fraser, A. V., and Hughes, A. (2003) A perspective of polyamine metabolism, *Biochem. J. 376*, 1-14.
18. Matsufuji, S., Matsufuji, T., Miyazaki, Y., Murakami, Y., Atkins, J. F., Gesteland, R. F., and Hayashi, S. (1995) Autoregulatory frameshifting in decoding mammalian ornithine decarboxylase antizyme, *Cell 80*, 51-60.
19. Kern, A. D., Oliveira, M. A., Coffino, P., and Hackert, M. L. (1999) Structure of mammalian ornithine decarboxylase at 1.6 Å resolution: stereochemical implications of PLP-dependent amino acid decarboxylases, *Structure 7*, 567-581.
20. Coleman, C. S., Stanley, B. A., Viswanath, R., and Pegg, A. E. (1994) Rapid exchange of subunits of mammalian ornithine decarboxylase, *J. Biol. Chem. 269*, 3155-3158.
21. Tobias, K. E., Mamroud-Kidron, E., and Kahana, C. (1993) Gly387 of murine ornithine decarboxylase is essential for the formation of stable homodimers, *Eur. J. Biochem. 218*, 245-250.
22. Shantz, L. M., and Pegg, A. E. (1999) Translational regulation of ornithine decarboxylase and other enzymes of the polyamine pathway, *Int. J. Biochem. Cell Biol. 31*, 107-122.
23. Auvinen, M., Jarvinen, K., Hotti, A., Okkeri, J., Laitinen, J., Janne, O. A., Coffino, P., Bergman, M., Andersson, L. C., Alitalo, K., and Holtta, E. (2003) Transcriptional regulation of the ornithine decarboxylase gene by c-Myc/Max/Mad network and retinoblastoma protein interacting with c-Myc, *Int. J. Biochem. Cell Biol. 35*, 496-521.
24. Nilsson, J. A., Maclean, K. H., Keller, U. B., Pendeville, H., Baudino, T. A., and Cleveland, J. L. (2004) Mnt loss triggers Myc transcription targets, proliferation, apoptosis, and transformation, *Mol. Cell. Biol. 24*, 1560-9.
25. Hurlin, P. J., Zhou, Z. Q., Toyo-oka, K., Ota, S., Walker, W. L., Hirotsune, S., and Wynshaw-Boris, A. (2003) Deletion of Mnt leads to disrupted cell cycle control and tumorigenesis, *Embo J 22*, 4584-96.
26. Willis, A. E. (1999) Translational control of growth factor and proto-oncogene expression, *Int. J. Biochem. Cell. Biol. 31*, 73-86.
27. Pyronnet, S., Pradayrol, L., and Sonenberg, N. (2000) A cell cycle-dependent internal ribosome entry site, *Mol. Cell 5*, 607-616.
28. Persson, L., Holm, I., and Heby, O. (1986) Translational regulation of ornithine decarboxylase by polyamines, *FEBS Lett. 205*, 175-178.
29. Persson, L., Oredsson, S. M., Anehus, S., and Heby, O. (1985) Ornithine decarboxylase inhibitors increase the cellular content of the enzyme: implications for translational regulation, *Biochem. Biophys. Res. Commun. 131*, 239-45.
30. Shantz, L. M., and Pegg, A. E. (1994) Overproduction of ornithine decarboxylase caused by relief of translational repression is associated with neoplastic transformation, *Cancer Res. 54*, 2313-2316.
31. Shantz, L. M., Hu, R.-H., and Pegg, A. E. (1996) Regulation of ornithine decarboxylase in a transformed cell line that overexpresses translation initiation factor eIF-4E., *Cancer Res. 56*, 3265-3269.
32. Shantz, L. M. (2004) Transcriptional and translational control of ornithine decarboxylase during Ras transformation, *Biochem. J. 377*, 257-64.

33. Pegg, A. E. (1988) Polyamine metabolism and its importance in neoplastic growth and as a target for chemotherapy, *Cancer Res. 48*, 759-774.
34. Jänne, J., Alhonen, L., and Leinonen, P. (1991) Polyamines: From molecular biology to clinical applications, *Ann. Med. 23*, 241-259.
35. Bauer, P. M., Buga, G. M., Fukuto, J. M., Pegg, A. E., and Ignarro, L. J. (2001) Nitric oxide inhibits ornithine decarboxylase via S-nitrosylation of cysteine 360 in the active site of the enzyme, *J. Biol. Chem. 276*, 34458-34464.
36. Satriano, J., S., M., Murakami, Y., Lortie, M. J., Schwartz, D., Kelly, C. J., Hayashi, S., and Blantz, R. C. (1998) Agmatine suppresses proliferation by frameshift induction of antizyme and attenuation of cellular polyamine levels., *J. Biol. Chem. 273*, 15313-15316.
37. Coleman, C. S., Hu, G., and Pegg, A. E. (2004) Putrescine biosynthesis in mammalian tissues, *Biochem J 379*, 849-55.
38. Jin, Y., Lee, H., Zeng, S. X., Dai, M. S., and Lu, H. (2003) MDM2 promotes p21waf1/cip1 proteasomal turnover independently of ubiquitylation, *Embo J 22*, 6365-77.
39. Murakami, Y., Matsufuji, S., Nishiyama, M., and Hayashi, S. (1989) Properties and fluctuations in vivo of rat liver antizyme inhibitor, *Biochem. J. 259*, 839-845.
40. Murakami, Y., Ichiba, T., Matsufuji, S., and Hayashi, S. (1996) Cloning of antizyme inhibitor, a highly homologous protein to ornithine decarboxylase, *J. Biol. Chem. 271*, 3340-3342.
41. Koguchi, K., Kobayashi, S., Hayashi, T., Matsufuji, S., Murakami, Y., and Hayashi, S.-i. (1997) Cloning and sequencing of a human cDNA encoding ornithine decarboxylase antizyme inhibitor, *Biochim. Biophys. Acta 1353*, 209-216.
42. Zhu, C., Lang, D. W., and Coffino, P. (1999) Antizyme2 is a negative regulator of ornithine decarboxylase and polyamine transport., *J. Biol. Chem. 274*, 26425-26430.
43. Ivanov, I. P., Rohrwasser, A., Terreros, D. A., Gesteland, R. F., and Atkins, J. F. (2000) Discovery of a spermatogenesis stage-specific ornithine decarboxylase antizyme: Antizyme 3, *Proc. Natl. Acad. Sci. USA 97*, 4808-4813.
44. Hakovirta, H., Keiski, A., Toppari, J., Halmekytö, M., Alhonen, L., Jänne, J., and Parvinen, M. (1993) Polyamines and regulation of spermatogenesis: Selective stimulation of late spermatogonia in transgenic mice overexpressing the human ornithine decarboxylase gene, *Mol. Endocrinol. 7*, 1430-1436.
45. Newman, R. M., Mobascher, A., Mangold, U., Koike, C., Diah, S., Schmidt, M., Finley, D., and Zetter, B. R. (2004) Antizyme targets cyclin D1 for degradation. A novel mechanism for cell growth repression, *J Biol Chem 279*, 41504-11.
46. Auvinen, M., Paasinen, A., Andersson, L. A., and Hölttä, E. (1992) Ornithine decarboxylase activity is critical for cell transformation, *Nature 360*, 355-358.
47. Moshier, J. S., Dosescu, J., Skunca, M., and Luk, G. D. (1993) Transformation of NIH/3T3 cells by ornithine decarboxylase overexpression, *Cancer Res. 53*, 2618-2622.

48. Repasky, G. A., Chenette, E. J., and Der, C. J. (2004) Renewing the conspiracy theory debate: does Raf function alone to mediate Ras oncogenesis?, *Trends Cell Biol 14*, 639-47.
49. Pendeville, H., Carpino, N., Marine, J. C., Takahashi, Y., Muller, M., Martial, J. A., and Cleveland, J. L. (2001) The ornithine decarboxylase gene is essential for cell survival during early murine development, *Mol. Cell Biol. 21*, 6459-6558.
50. Pegg, A. E., Feith, D. J., Fong, L. Y., Coleman, C. S., O'Brien, T. G., and Shantz, L. M. (2003) Transgenic mouse models for studies of the role of polyamines in normal, hypertrophic and neoplastic growth, *Biochem. Soc. Trans. 31*, 356-60.
51. Janne, J., Alhonen, L., Pietila, M., and Keinanen, T. A. (2004) Genetic approaches to the cellular functions of polyamines in mammals, *Eur. J. Biochem. 271*, 877-94.
52. Halmekyto, M., Hyttinen, J. M., Sinervirta, R., Urtrainen, M., Myöhänen, S., Voipio, H. M., Wahlfors, J., Syrjänen, S., Syrjänen, K., Alhonen, L., and Jänne, J. (1991) Transgenic mice aberrantly expressing human ornithine decarboxylase gene, *J. Biol. Chem. 266*, 19746-19751.
53. Halmekytö, M., Alhonen, L., Wahlfors, J., Sinervirta, R., Eloranta, T., and Jänne, J. (1991) Characterization of a transgenic mouse line over-expressing the human ornithine decarboxylase gene, *Biochem. J. 278*, 895-898.
54. Halmekytö, M., Alhonen, L., Alakuijala, L., and Jänne, J. (1993) Transgenic mice over-producing putrescine in their tissues do not convert the diamine into higher polyamines, *Biochem. J. 291*, 505-508.
55. Auvinen, M., Laine, A., Paasinen-Sohns, A., Kangas, A., Kangas, L., Saksela, O., Andersson, L. C., and Hölttä, E. (1997) Human ornithine decarboxylase-overproducing NIH3T3 cells induce rapidly growing, highly vascularized tumors in nude mice, *Cancer Res. 57*, 3016-3025.
56. Lan, L., Trempus, C., and Gilmour, S. K. (2000) Inhibition of ornithine decarboxylase (ODC) decreases tumor vascularization and reverses spontaneous tumors in ODC/Ras transgenic mice, *Cancer Res. 60*, 5696-5703.
57. Heby, O., Luk, G. D., and Schindler, J. (1987) in *Inhibition of Polyamine Metabolism. Biological Significance and Basis for New Therapies* (McCann, P. P., Pegg, A. E., and Sjoerdsma, A., Eds.) pp 165-186, Academic Press, Orlando, FL.
58. Fredlund, J. O., Johansson, M. C., Dahlberg, E., and Oredsson, S. M. (1995) Ornithine decarboxylase and S-adenosylmethionine decarboxylase expression during the cell cycle of Chinese hamster ovary cells, *Exp. Cell Res. 216*, 86-92.
59. Kaczmarek, L., Calabretta, B., Ferrari, S., and de Riel, J. K. (1987) Cell-cycle-dependent expression of human ornithine decarboxylase., *J Cell Physiol 132*, 545-551.
60. Kramer, D. L., Vujcic, S., Diegelman, P., Alderfer, J., Miller, J. T., Black, J. D., Bergeron, R. J., and Porter, C. W. (1999) Polyamine analogue induction of the p53-p21 $^{WAF1/CIP1}$-Rb pathway and $G_1$ arrest in human melanoma cells, *Cancer Res. 59*, 1278-1286.
61. Heby, O. (1981) Role of polyamines in the control of cell proliferation and differentiation, *Differentiation 19*, 1-20.

62. Fredlund, J. O., and Oredsson, S. M. (1996) Impairment of DNA replication within one cell cycle after seeding of cells in the presence of a polyamine-biosynthesis inhibitor, *Eur. J. Biochem. 237*, 539-544.
63. Fredlund, J. O., and Oredsson, S. M. (1996) Normal $G_1$/S transition and prolonged S phase within one cell cycle after seeding cells in the presence of an ornithine decarboxylase inhibitor, *Cell Prolif. 29*, 457-465.
64. Charollais, R. H., and Mester, J. (1988) Resumption of cell cycle in BALB/c-3T3 fibroblasts arrested by polyamine depletion: relation with "competence" gene expression., *J. Cell. Physiol. 137*, 559-564.
65. Ray, R. M., Zimmerman, B. J., McMormack, S. A., Patel, T. B., and Johnson, L. R. (1999) Polyamine depletion arrests cell cycle and induces inhibitors $p21^{Waf1/Cip1}$, $p27^{Kip1}$, and p53 in IEC-6 cells, *Am. J. Physiol. 276*, C684-C691.
66. Wagner, A. J., Meyers, C., Laimins, L. A., and Hay, N. (1993) c-Myc Induces the expression and activity of ornithine decarboxylase, *Cell Growth & Differentiation 4*, 879-883.
67. Bello-Fernandez, C., Packham, G., and Cleveland, J. L. (1993) The ornithine decarboxylase gene is a transcriptional target of c-Myc, *Proc. Natl. Acad. Sci. USA 90*, 7804-7808.
68. Peña, A., Wu, S., Hickok, N. J., Soprano, D. R., and Soprano, K. J. (1995) Regulation of human ornithine decarboxylase expression following prolonged quiescence: Role for the c-Myc/Max protein complex, *J. Cell. Physiol. 162*, 234-245.
69. Packham, G., and Cleveland, J. L. (1995) c-Myc and apoptosis, *Biochim. Biophys. Acta 1242*, 11-28.
70. Packham, G., Porter, C. W., and Cleveland, J. L. (1996) c-Myc induces apoptosis and cell cycle progression by separable, yet overlapping, pathways, *Oncogene 13*, 461-9.
71. Frostejö, L., and Heby, O. (1999) Polyamine depletion up-regulates Myc expression, yet induces $G_1$ arrest and terminal differentiation of F9 teratocarcinoma stem cells, *J. Cell. Biochem. 76*, 143-152.
72. Kramer, D. L., Vujcic, S., Diegelman, P., Alderfer, J., Miller, J. T., Black, J. D., Bergeron, R. J., and Porter, C. W. (1999) Polyamine analogue induction of the p53-p21WAF1/CIP1-Rb pathway and G1 arrest in human melanoma cells, *Cancer Res 59*, 1278-86.
73. Harada, J. J., and Morris, D. R. (1981) Cell cycle parameters of Chinese hamster ovary cells during exponential, polyamine-limited growth, *Mol Cell Biol 1*, 594-9.
74. Seidenfeld, J., Block, A. L., Komar, K. A., and Naujokas, M. F. (1986) Altered cell cycle phase distributions in cultured human carcinoma cells partially depleted of polyamines by treatment with difluoromethylornithine, *Cancer Res 46*, 47-53.
75. Ray, R. M., McCormack, S. A., and Johnson, L. R. (2001) Polyamine depletion arrests growth of IEC-6 and Caco-2 cells by different mechanisms, *Am J Physiol Gastrointest Liver Physiol 281*, G37-43.
76. Nemoto, T., Kamei, S., Seyama, Y., and Kubota, S. (2001) p53 independent G(1) arrest induced by DL-alpha-difluoromethylornithine, *Biochem Biophys Res Commun 280*, 848-54.

77. Kramer, D. L., Chang, B. D., Chen, Y., Diegelman, P., Alm, K., Black, A. R., Roninson, I. B., and Porter, C. W. (2001) Polyamine depletion in human melanoma cells leads to $G_1$ arrest associated with induction of $p21^{WAF1/CIWAF1P1/SDI1}$, changes in the expression of p21-regulated genes, and a senescence-like phenotype[1], *Cancer Res. 61*, 7754-7762.
78. Gartel, A. L., and Tyner, A. L. (1999) Transcriptional regulation of the p21((WAF1/CIP1)) gene., *Exp Cell Res. 246*, 280-289.
79. Ray, R. M., Zimmerman, B. J., McCormack, S. A., Patel, T. B., and Johnson, L. R. (1999) Polyamine depletion arrests cell cycle and induces inhibitors p21(Waf1/Cip1), p27(Kip1), and p53 in IEC-6 cells, *Am J Physiol 276*, C684-91.
80. Nemoto, T., Kamei, S., Seyama, Y., and Kubota, S. (2001) p53 Independent $G_1$ arrest induced by DL-a-difluoromethylornithine, *Biochem. Biophys. Res. Comm. 280*, 848-854.
81. Gartel, A. L., Ye, X., Goufman, E., Shianov, P., Hay, N., Najmabadi, F., and Tyner, A. L. (2001) Myc represses the p21(WAF1/CIP1) promoter and interacts with Sp1/Sp3, *Proc Natl Acad Sci U S A 98*, 4510-5.
82. Bauer, P. M., Buga, G. M., and Ignarro, L. J. (2001) Role of p42/p44 mitogen-activated-protein kinase and p21waf1/cip1 in the regulation of vascular smooth muscle cell proliferation by nitric oxide, *Proc Natl Acad Sci U S A 98*, 12802-7.
83. Bauer, P. M., Fukuto, J. M., Buga, G. M., Pegg, A. E., and Ignarro, L. J. (1999) Nitric oxide inhibits ornithine decarboxylase by S-nitrosylation, *Biochem Biophys Res Commun 262*, 355-8.
84. Gartel, A. L., and Tyner, A. L. (1999) Transcriptional regulation of the p21((WAF1/CIP1)) gene, *Exp Cell Res 246*, 280-9.
85. Li, L., Rao, J. N., Guo, X., Liu, L., Santora, R., Bass, B. L., and Wang, J. Y. (2001) Polyamine depletion stabilizes p53 resulting in inhibition of normal intestinal epithelial cell proliferation, *Am J Physiol Cell Physiol 281*, C941-53.
86. Kramer, D. L., Chang, B. D., Chen, Y., Diegelman, P., Alm, K., Black, A. R., Roninson, I. B., and Porter, C. W. (2001) Polyamine depletion in human melanoma cells leads to G1 arrest associated with induction of p21WAF1/CIP1/SDI1, changes in the expression of p21-regulated genes, and a senescence-like phenotype, *Cancer Res 61*, 7754-62.
87. Mitchell, J. L., Leyser, A., Holtorff, M. S., Bates, J. S., Frydman, B., Valasinas, A., Reddy, V. K., and Marton, L. J. (2002) Antizyme induction by polyamine analogues as a factor of cell growth inhibition, *Biochem. J. 366*, 663-671.
88. Gilmour, S. K., Birchler, M., Smith, M. K., Rayca, K., and Mostochuk, J. (1999) Effect of elevated levels of ornithine decarboxylase on cell cycle progression in skin, *Cell Growth & Differentiation 10*, 739-748.
89. Seiler, N. (2003) Thirty years of polyamine-related approaches to cancer therapy. Retrospect and prospect. Part 1. Selective enzyme inhibitors, *Curr Drug Targets 4*, 537-64.
90. Seiler, N. (2003) Thirty years of polyamine-related approaches to cancer therapy. Retrospect and prospect. Part 2. Structural analogues and derivatives, *Curr Drug Targets 4*, 565-85.

91. Poulin, R., Lu, L., Ackermann, B., Bey, P., and Pegg, A. E. (1992) Mechanism of the irreversible inactivation of mouse ornithine decarboxylase by α-difluoromethylornithine, *J. Biol. Chem. 267*, 150-158.
92. McCann, P. P., and Pegg, A. E. (1992) Ornithine decarboxylase as an enzyme target for therapy, *Pharmacol. Ther. 54*, 195-215.
93. Bacchi, C. J., and Yarlett, N. (1993) Effects of antagonists of polyamine metabolism on African trypanosomes, *Acta Tropica 54*, 225-236.
94. Levin, V. A., Jochec, J. L., Shantz, L. M., Koch, P. E., and Pegg, A. E. (2004) Tissue-based assay for ornithine decarboxylase (ODC) to identify patients likely to respond to difluoromethylornithine (DFMO). *J. Histochem. Cytochem.*
95. Hickok, N. J., Seppänen, P. J., Gunsalus, G., and Jänne, O. A. (1987) Complete amino acid sequence of human ornithine decarboxylase deduced from complementary DNA, *DNA 6*, 179-187.
96. Guo, Y., Harris, R. B., Rosson, D., Boorman, D., and O'Brien, T. G. (2000) Functional analysis of human ornithine decarboxylase, *Cancer Res. 60*, 6314-6317.
97. Martinez, M. E., O'Brien, T. G., Fultz, K. E., Babbar, N., Yerushalmi, H., Qu, N., Guo, Y., Boorman, D., Einspahr, J., Alberts, D. S., and Gerner, E. W. (2003) Pronounced reduction in adenoma recurrence associated with aspirin use and a polymorphism in the ornithine decarboxylase gene, *Proc. Natl. Acad. Sci. U S A 100*, 7859-7864.
98. Rimmele, M. (2003) Nucleic acid aptamers as tools and drugs: recent developments, *Chembiochem 4*, 963-71.
99. Breaker, R. R. (2000) Tech.Sight. Molecular biology. Making catalytic DNAs, *Science 290*, 2095-6.
100. Scherer, L. J., and Rossi, J. J. (2003) Approaches for the sequence-specific knockdown of mRNA, *Nat. Biotechnol. 21*, 1457-65.
101. Kurreck, J. (2003) Antisense technologies. Improvement through novel chemical modifications, *Eur. J. Biochem. 270*, 1628-44.
102. Baker, B. F., and Monia, B. P. (1999) Novel mechanisms for antisense-mediated regulation of gene expression, *Biochim. Biophys. Acta 1489*, 3-18.
103. Meister, G., and Tuschl, T. (2004) Mechanisms of gene silencing by double-stranded RNA, *Nature 431*, 343-9.
104. Joyce, G. F. (2004) Directed evolution of nucleic acid enzymes, *Annu. Rev. Biochem. 73*, 791-836.
105. Sun, L. Q., Cairns, M. J., Saravolac, E. G., Baker, A., and Gerlach, W. L. (2000) Catalytic nucleic acids: from lab to applications, *Pharmacol Rev 52*, 325-47.
106. Puerta-Fernandez, E., Romero-Lopez, C., Barroso-delJesus, A., and Berzal-Herranz, A. (2003) Ribozymes: recent advances in the development of RNA tools, *FEMS Microbiol Rev 27*, 75-97.
107. Breaker, R. R. (1999) Catalytic DNA: in training and seeking employment, *Nat. Biotechnol. 17*, 422-3.
108. Breaker, R. R., and Joyce, G. F. (1994) A DNA enzyme that cleaves RNA, *Chem. Biol. 1*, 223-9.

109. Santoro, S. W., and Joyce, G. F. (1997) A general purpose RNA-cleaving DNA enzyme, *Proc. Natl. Acad. Sci. U S A 94*, 4262-6.
110. Santoro, S. W., and Joyce, G. F. (1998) Mechanism and utility of an RNA-cleaving DNA enzyme, *Biochemistry 37*, 13330-42.
111. Sioud, M., and Leirdal, M. (2000) Therapeutic RNA and DNA enzymes, *Biochem Pharmacol 60*, 1023-6.
112. Chen, Y., Wang, M., and Mao, C. (2004) An autonomous DNA nanomotor powered by a DNA enzyme, *Angew Chem Int Ed Engl 43*, 3554-7.
113. Sando, S., Sasaki, T., Kanatani, K., and Aoyama, Y. (2003) Amplified nucleic acid sensing using programmed self-cleaving DNAzyme, *J Am Chem Soc 125*, 15720-1.
114. Wallace, H. M. (1998) Polyamines: specific metabolic regulators or multifunctional polycations?, *Biochem. Soc. Trans. 26*, 569-71.
115. Pendeville, H., Carpino, N., Marine, J. C., Takahashi, Y., Muller, M., Martial, J. A., and Cleveland, J. L. (2001) The ornithine decarboxylase gene is essential for cell survival during early murine development, *Mol. Cell. Biol. 21*, 6549-58.
116. Shantz, L. M., and Pegg, A. E. (1998) Ornithine decarboxylase induction in transformation by H-Ras and RhoA, *Cancer Res. 58*, 2748-53.
117. Auvinen, M., Paasinen, A., Andersson, L. C., and Holtta, E. (1992) Ornithine decarboxylase activity is critical for cell transformation, *Nature 360*, 355-8.
118. Coffino, P. (2001) Regulation of cellular polyamines by antizyme, *Nat. Rev. Mol. Cell. Biol. 2*, 188-94.
119. Pepin, J., and Milord, F. (1994) The treatment of human African trypanosomiasis, *Adv. Parasitol. 33*, 1-47.
120. Pegg, A. E. (1988) Polyamine metabolism and its importance in neoplastic growth and a target for chemotherapy, *Cancer Res. 48*, 759-74.
121. Janne, J., Alhonen, L., and Leinonen, P. (1991) Polyamines: from molecular biology to clinical applications, *Ann. Med. 23*, 241-59.
122. Shantz, L. M., and Pegg, A. E. (1999) Translational regulation of ornithine decarboxylase and other enzymes of the polyamine pathway, *Int. J. Biochem. Cell. Biol. 31*, 107-22.
123. Persson, L., Holm, I., and Heby, O. (1986) Translational regulation of ornithine decarboxylase by polyamines, *FEBS Lett. 205*, 175-8.
124. Shantz, L. M., and Pegg, A. E. (1994) Overproduction of ornithine decarboxylase caused by relief of translational repression is associated with neoplastic transformation, *Cancer Res. 54*, 2313-6.
125. Shantz, L. M., Hu, R. H., and Pegg, A. E. (1996) Regulation of ornithine decarboxylase in a transformed cell line that overexpresses translation initiation factor eIF-4E, *Cancer Res. 56*, 3265-9.
126. Madhubala, R., and Pegg, A. E. (1992) Inhibition of ornithine decarboxylase and S-adenosylmethionine decarboxylase synthesis by antisense oligodeoxynucleotides, *Mol Cell Biochem 118*, 191-5.
127. Lu, L., Stanley, B. A., and Pegg, A. E. (1991) Identification of residues in ornithine decarboxylase essential for enzymatic activity and for rapid protein turnover, *Biochem. J. 277 ( Pt 3)*, 671-5.

128. Coleman, C. S., and Pegg, A. E. (1998) Assay of mammalian ornithine decarboxylase activity using [14C]ornithine, *Methods Mol. Biol. 79*, 41-4.
129. Cairns, M. J., King, A., and Sun, L. Q. (2003) Optimisation of the 10-23 DNAzyme-substrate pairing interactions enhanced RNA cleavage activity at purine-cytosine target sites, *Nucleic Acids Res. 31*, 2883-9.
130. Ghoda, L., van Daalen Wetters, T., Macrae, M., Ascherman, D., and Coffino, P. (1989) Prevention of rapid intracellular degradation of ODC by a carboxyl-terminal truncation, *Science 243*, 1493-5.
131. Schubert, S., Gul, D. C., Grunert, H. P., Zeichhardt, H., Erdmann, V. A., and Kurreck, J. (2003) RNA cleaving '10-23' DNAzymes with enhanced stability and activity, *Nucleic Acids Res. 31*, 5982-92.
132. Sun, L. Q., Cairns, M. J., Gerlach, W. L., Witherington, C., Wang, L., and King, A. (1999) Suppression of smooth muscle cell proliferation by a c-myc RNA-cleaving deoxyribozyme, *J. Biol. Chem. 274*, 17236-41.
133. Kurreck, J., Bieber, B., Jahnel, R., and Erdmann, V. A. (2002) Comparative study of DNA enzymes and ribozymes against the same full-length messenger RNA of the vanilloid receptor subtype I, *J. Biol. Chem. 277*, 7099-107.
134. Cairns, M. J., Hopkins, T. M., Witherington, C., Wang, L., and Sun, L. Q. (1999) Target site selection for an RNA-cleaving catalytic DNA, *Nat. Biotechnol. 17*, 480-6.
135. Warashina, M., Kuwabara, T., Nakamatsu, Y., and Taira, K. (1999) Extremely high and specific activity of DNA enzymes in cells with a Philadelphia chromosome, *Chem. Biol. 6*, 237-50.
136. Pan, W. H., Xin, P., Bui, V., and Clawson, G. A. (2003) Rapid identification of efficient target cleavage sites using a hammerhead ribozyme library in an iterative manner, *Mol. Ther. 7*, 129-39.
137. Cairns, M. J., Hopkins, T. M., Witherington, C., and Sun, L. Q. (2000) The influence of arm length asymmetry and base substitution on the activity of the 10-23 DNA enzyme, *Antisense Nucleic Acid Drug Dev. 10*, 323-32.
138. Thomson, J. B., Tuschl, T., and Eckstein, F. (1996) in *Catalytic RNA* (F., E., and D.M.J., L., Eds.) pp 173-196, Spring-Verlag, Berlin, Germany.
139. He, Q. C., Zhou, J. M., Zhou, D. M., Nakamatsu, Y., Baba, T., and Taira, K. (2002) Comparison of metal-ion-dependent cleavages of RNA by a DNA enzyme and a hammerhead ribozyme, *Biomacromolecules 3*, 69-83.
140. Cieslak, M., Niewiarowska, J., Nawrot, M., Koziolkiewicz, M., Stec, W. J., and Cierniewski, C. S. (2002) DNAzymes to beta 1 and beta 3 mRNA down-regulate expression of the targeted integrins and inhibit endothelial cell capillary tube formation in fibrin and matrigel, *J. Biol. Chem. 277*, 6779-87.
141. Heidenreich, O., and Eckstein, F. (1992) Hammerhead ribozyme-mediated cleavage of the long terminal repeat RNA of human immunodeficiency virus type 1, *J. Biol. Chem. 267*, 1904-9.
142. Scarabino, D., and Tocchini-Valentini, G. P. (1996) Influence of substrate structure on cleavage by hammerhead ribozyme, *FEBS Lett. 383*, 185-90.

143. Lazaris-Karatzas, A., Montine, K. S., and Sonenberg, N. (1990) Malignant transformation by a eukaryotic initiation factor subunit that binds to mRNA 5' cap, *Nature 345*, 544-547.
144. Koromilas, A. E., Lazaris-Karatzas, A., and Sonenberg, N. (1992) mRNAs containing extensive secondary structure in their 5' non-coding region translate efficiently in cells overexpressing initiation factor eIF-4E, *EMBO J. 11*, 4153-4158.
145. Lu, L., Stanley, B. A., and Pegg, A. E. (1991) Identification of residues in ornithine decarboxylase essential for enzymatic activity and for rapid protein turnover, *Biochem. J. 277*, 671-675.
146. Zhang, M., Pickart, C. M., and Coffino, P. (2003) Determinants of proteasome recognition of ornithine decarboxylase, a ubiquitin-independent substrate, *Embo J. 22*, 1488-96.
147. Dass, C. R., Saravolac, E. G., Li, Y., and Sun, L. Q. (2002) Cellular uptake, distribution, and stability of 10-23 deoxyribozymes, *Antisense Nucleic Acid Drug Dev 12*, 289-99.
148. Marcusson, E. G., Bhat, B., Manoharan, M., Bennett, C. F., and Dean, N. M. (1998) Phosphorothioate oligodeoxyribonucleotides dissociate from cationic lipids before entering the nucleus, *Nucleic Acids Res 26*, 2016-23.
149. Zelphati, O., and Szoka, F. C., Jr. (1996) Intracellular distribution and mechanism of delivery of oligonucleotides mediated by cationic lipids, *Pharm Res 13*, 1367-72.
150. Kato, Y., Kuwabara, T., Warashina, M., Toda, H., and Taira, K. (2001) Relationships between the activities in vitro and in vivo of various kinds of ribozyme and their intracellular localization in mammalian cells, *J Biol Chem 276*, 15378-85.
151. O'Brien, T. G., Lewis, M. A., and Diamond, L. (1979) Ornithine decarboxylase activity and DNA synthesis after treatment of cells in culture with 12-O-tetradecanoylphorbol-13-acetate, *Cancer Res 39*, 4477-80.
152. Unwalla, H., and Banerjea, A. C. (2001) Novel mono- and di-DNA-enzymes targeted to cleave TAT or TAT-REV RNA inhibit HIV-1 gene expression, *Antiviral Res. 51*, 127-39.
153. Sriram, B., and Banerjea, A. C. (2000) In vitro-selected RNA cleaving DNA enzymes from a combinatorial library are potent inhibitors of HIV-1 gene expression, *Biochem. J. 352 Pt 3*, 667-73.
154. Chakraborti, S., and Banerjea, A. C. (2003) Inhibition of HIV-1 gene expression by novel DNA enzymes targeted to cleave HIV-1 TAR RNA: potential effectiveness against all HIV-1 isolates, *Mol. Ther. 7*, 817-26.
155. Chen, Y., Ji, Y. J., Roxby, R., and Conrad, C. (2000) In vivo expression of single-stranded DNA in mammalian cells with DNA enzyme sequences targeted to C-raf, *Antisense Nucleic Acid Drug Dev. 10*, 415-22.
156. Chen, Y., and McMicken, H. W. (2003) Intracellular production of DNA enzyme by a novel single-stranded DNA expression vector, *Gene Ther. 10*, 1776-80.

157. Tan, X. X., Rose, K., Margolin, W., and Chen, Y. (2004) DNA enzyme generated by a novel single-stranded DNA expression vector inhibits expression of the essential bacterial cell division gene ftsZ, *Biochemistry 43*, 1111-7.
158. Shantz, L. M., Coleman, C. S., and Pegg, A. E. (1996) Expression of an ornithine decarboxylase dominant-negative mutant reverses eukaryotic initiation factor 4E-induced cell transformation, *Cancer Res. 56*, 5136-40.
159. Schubert, S., Furste, J. P., Werk, D., Grunert, H. P., Zeichhardt, H., Erdmann, V. A., and Kurreck, J. (2004) Gaining target access for deoxyribozymes, *J Mol Biol 339*, 355-63.
160. White, P. J., Atley, L. M., and Wraight, C. J. (2004) Antisense oligonucleotide treatments for psoriasis, *Expert Opin Biol Ther 4*, 75-81.
161. Arora, V., Hannah, T. L., Iversen, P. L., and Brand, R. M. (2002) Transdermal use of phosphorodiamidate morpholino oligomer AVI-4472 inhibits cytochrome P450 3A2 activity in male rats, *Pharm Res 19*, 1465-70.
162. Wingens, M., Pfundt, R., van Vlijmen-Willems, I. M., van Hooijdonk, C. A., van Erp, P. E., and Schalkwijk, J. (1999) Sequence-specific inhibition of gene expression in intact human skin by epicutaneous application of chimeric antisense oligodeoxynucleotides, *Lab Invest 79*, 1415-24.
163. Nestle, F. O., Mitra, R. S., Bennett, C. F., Chan, H., and Nickoloff, B. J. (1994) Cationic lipid is not required for uptake and selective inhibitory activity of ICAM-1 phosphorothioate antisense oligonucleotides in keratinocytes, *J Invest Dermatol 103*, 569-75.
164. Cserhalmi-Friedman, P. B., Panteleyev, A. A., and Christiano, A. M. (2004) Recapitulation of the hairless mouse phenotype using catalytic oligonucleotides: implications for permanent hair removal, *Exp. Dermatol. 13*, 155-62.
165. Soler, A. P., Gilliard, G., Megosh, L., George, K., and O'Brien, T. G. (1998) Polyamines regulate expression of the neoplastic phenotype in mouse skin, *Cancer Res. 58*, 1654-1659.
166. O'Brien, T. G., Megosh, L. C., Gilliard, G., and Peralta Soler, A. (1997) Ornithine decarboxylase overexpression is a sufficient condition for tumor promotion, *Cancer Res. 57*, 2630-2637.
167. Megosh, L., Gilmour, S. K., Rosson, D., Peralta Soler, A., Blessing, M., Sawicki, J. A., and O'Brien, T. G. (1995) Increased frequency of spontaneous skin tumors in transgenic mice which overexpresses ornithine decarboxylase, *Cancer Res. 55*, 4205-4209.
168. Fischer, S. M., Conti, C. J., Viner, J., Aldaz, C. M., and Lubet, R. A. (2003) Celecoxib and difluoromethylornithine in combination have strong therapeutic activity against UV-induced skin tumors in mice, *Carcinogenesis 24*, 945-52.
169. Wheeler, D. L., Ness, K. J., Oberley, T. D., and Verma, A. K. (2003) Inhibition of the development of metastatic squamous cell carcinoma in protein kinase C epsilon transgenic mice by alpha-difluoromethylornithine accompanied by marked hair follicle degeneration and hair loss, *Cancer Res. 63*, 3037-42.
170. Hynd, P. I., and Nancarrow, M. J. (1996) Inhibition of polyamine synthesis alters hair follicle function and fiber composition, *J Invest Dermatol 106*, 249-53.

171. Malhotra, B., Noveck, R., Behr, D., and Palmisano, M. (2001) Percutaneous absorption and pharmacokinetics of Eflornithine Hcl 13.9% cream in women with unwanted facial hair, *J. Clin. Pharmacol. 41*, 972-978.
172. Verma, A. K., Erickson, D., and Dolnick, B. J. (1986) Increased mouse epidermal ornithine decarboxylase activity by the tumour promoter 12-O-tetradecanoylphorbol 13-acetate involves increased amounts of both enzyme protein and messenger RNA, *Biochem J 237*, 297-300.
173. Kennard, M. D., Kang, D. C., Montgomery, R. L., and Butler, A. P. (1995) Expression of epidermal ornithine decarboxylase and nuclear proto-oncogenes in phorbol ester tumor promotion-sensitive and -resistant mice, *Mol Carcinog 12*, 14-22.
174. Megosh, L. C., Hu, J., George, K., and O'Brien, T. G. (2002) Genetic control of polyamine-dependent susceptibility to skin tumorigenesis, *Genomics 79*, 505-512.
175. Chen, Y., Hu, J., Boorman, D., Klein-Szanto, A., and O'Brien, T. G. (2004) Therapy of murine squamous cell carcinomas with 2-difluoromethylornithine, *J Carcinog 3*, 10.
176. Feith, D. J., Shantz, L. M., and Pegg, A. E. (2001) Targeted antizyme expression in the skin of transgenic mice reduces tumor promoter induction of ornithine decarboxylase and decreases sensitivity to chemical carcinogenesis., *Cancer Res. 61*, 6073-6081.
177. Einspahr, J. G., Bowden, G. T., and Alberts, D. S. (2003) Skin cancer chemoprevention: strategies to save our skin, *Recent Results Cancer Res 163*, 151-64; discussion 264-6.
178. Einspahr, J. G., Nelson, M. A., Saboda, K., Warneke, J., Bowden, G. T., and Alberts, D. S. (2002) Modulation of biologic endpoints by topical difluoromethylornithine (DFMO), in subjects at high-risk for nonmelanoma skin cancer, *Clin. Cancer. Res. 8*, 149-55.
179. Alberts, D. S., Dorr, R. T., Einspahr, J. G., Aickin, M., Saboda, K., Xu, M. J., Peng, Y.-M., Goldman, R., Foote, J. A., Warneke, J. A., Salasche, S., Roe, D. J., and Bowden, G. T. (2000) Chemoprevention of human actinic keratoses by topical 2-(difluoromethyl)-dl-ornithine, *Cancer Epidemiol. Biomarkers & Prevention 9*, 1281-1286.
180. Ahmad, N., Gilliam, A. C., Katiyar, S. K., O'Brien, T. G., and Mukhtar, H. (2001) A definitive role of ornithine decarboxylase in photocarcinogenesis, *Am. J. Pathol. 159*, 885-892.
181. Fischer, S. M., Lee, M., and Lubet, R. A. (2001) Difluoromethylornithine is effective as both a preventive and therapeutic agent against the development of UV carcinogenesis in SKH hairless mice, *Carcinogenesis 22*, 83-88.
182. Tang, X., Kim, A. L., Feith, D. J., Pegg, A. E., Russo, J., Zhang, H., Aszterbaum, M., Kopelovich, L., Epstein Jr., E. H., Bickers, D. R., and Athar, M. (2004) Ornithine Decarboxylase is a target for chemoprevention of basal and squamous cell carcinomas in *Ptch*$^{+/-}$ mice, *J. Clin. Invest. 113*, 867-875.
183. Rebel, H., van Steeg, H., Beems, R. B., Schouten, R., de Gruijl, F. R., and Terleth, C. (2002) Suppression of UV carcinogenesis by difluoromethylornithine

in nucleotide excision repair-deficient Xpa knockout mice, *Cancer Res. 62*, 1338-1342.
184. Muller-Rover, S., Handjiski, B., van der Veen, C., Eichmuller, S., Foitzik, K., McKay, I. A., Stenn, K. S., and Paus, R. (2001) A comprehensive guide for the accurate classification of murine hair follicles in distinct hair cycle stages, *J Invest Dermatol 117*, 3-15.
185. Soler, A. P., Gilliard, G., C., M. L., and O'Brien, L. G. (1996) Modulations of murine hair follicle function by alterations in ornithine decarboxylase activity, *J. Invest. Dermatol. 106*, 1108-1113.
186. Grosshans, E., Henry, M., Tell, G., Schechter, P. J., Bohlen, P., Grove, J., and Koch-Weser, J. (1980) [Polyamines in psoriasis], *Ann Dermatol Venereol 107*, 377-87.
187. O'Brien, T. G., Simsiman, R. C., and Boutwell, R. K. (1975) Induction of the polyamine-biosynthetic enzymes in mouse epidermis and their specificity for tumor promotion, *Cancer Res 35*, 2426-33.
188. van Erp, P. E., and Wingens, M. (2001) Does antisense make sense in dermatology?, *Acta Derm Venereol 81*, 385-91.
189. Vlassov, V. V., Balakireva, L. A., and Yakubov, L. A. (1994) Transport of oligonucleotides across natural and model membranes, *Biochim Biophys Acta 1197*, 95-108.
190. Lochmann, D., Jauk, E., and Zimmer, A. (2004) Drug delivery of oligonucleotides by peptides, *Eur J Pharm Biopharm 58*, 237-51.
191. Laktionov, P. P., Dazard, J. E., Vives, E., Rykova, E. Y., Piette, J., Vlassov, V. V., and Lebleu, B. (1999) Characterisation of membrane oligonucleotide-binding proteins and oligonucleotide uptake in keratinocytes, *Nucleic Acids Res 27*, 2315-24.
192. Mehta, R. C., Stecker, K. K., Cooper, S. R., Templin, M. V., Tsai, Y. J., Condon, T. P., Bennett, C. F., and Hardee, G. E. (2000) Intercellular adhesion molecule-1 suppression in skin by topical delivery of anti-sense oligonucleotides, *J Invest Dermatol 115*, 805-12.
193. Turner, P. C. (2000) in *Cancer Gene Therapy: Past Achievements and Future Challenges* (Academic, H. K., Ed.) pp 303-318, Plenum Publishers, New York.
194. Pan, W. H., Xin, P., Morrey, J. D., and Clawson, G. A. (2004) A self-processing ribozyme cassette: utility against human papillomavirus 11 E6/E7 mrna and hepatitis B virus, *Mol Ther 9*, 596-606.
195. Gao, Z., Fields, J. Z., and Boman, B. M. (1999) Tumor-specific expression of anti-mdr1 ribozyme selectively restores chemosensitivity in multidrug-resistant colon-adenocarcinoma cells, *Int J Cancer 82*, 346-52.
196. Myers, J. W., Jones, J. T., Meyer, T., and Ferrell, J. E., Jr. (2003) Recombinant Dicer efficiently converts large dsRNAs into siRNAs suitable for gene silencing, *Nat Biotechnol 21*, 324-8.
197. Persengiev, S. P., Zhu, X., and Green, M. R. (2004) Nonspecific, concentration-dependent stimulation and repression of mammalian gene expression by small interfering RNAs (siRNAs), *Rna 10*, 12-8.

198. Bartel, D. P. (2004) MicroRNAs: genomics, biogenesis, mechanism, and function, *Cell 116*, 281-97.
199. Sijen, T., Fleenor, J., Simmer, F., Thijssen, K. L., Parrish, S., Timmons, L., Plasterk, R. H., and Fire, A. (2001) On the role of RNA amplification in dsRNA-triggered gene silencing, *Cell 107*, 465-76.
200. Nawrot, B., Antoszczyk, S., Maszewska, M., Kuwabara, T., Warashina, M., Taira, K., and Stec, W. J. (2003) Efficient inhibition of beta-secretase gene expression in HEK293 cells by tRNAVal-driven and CTE-helicase associated hammerhead ribozymes, *Eur J Biochem 270*, 3962-70.
201. Geary, R. S., Leeds, J. M., Fitchett, J., Burckin, T., Truong, L., Spainhour, C., Creek, M., and Levin, A. A. (1997) Pharmacokinetics and metabolism in mice of a phosphorothioate oligonucleotide antisense inhibitor of C-raf-1 kinase expression, *Drug Metab Dispos 25*, 1272-81.
202. Yu, R. Z., Geary, R. S., Leeds, J. M., Watanabe, T., Moore, M., Fitchett, J., Matson, J., Burckin, T., Templin, M. V., and Levin, A. A. (2001) Comparison of pharmacokinetics and tissue disposition of an antisense phosphorothioate oligonucleotide targeting human Ha-ras mRNA in mouse and monkey, *J Pharm Sci 90*, 182-93.
203. Soutschek, J., Akinc, A., Bramlage, B., Charisse, K., Constien, R., Donoghue, M., Elbashir, S., Geick, A., Hadwiger, P., Harborth, J., John, M., Kesavan, V., Lavine, G., Pandey, R. K., Racie, T., Rajeev, K. G., Rohl, I., Toudjarska, I., Wang, G., Wuschko, S., Bumcrot, D., Koteliansky, V., Limmer, S., Manoharan, M., and Vornlocher, H. P. (2004) Therapeutic silencing of an endogenous gene by systemic administration of modified siRNAs, *Nature 432*, 173-8.
204. Almrud, J. J., Oliveira, M. A., Kern, A. D., Grishin, N. V., Phillips, M. A., and Hackert, M. L. (2000) Crystal structure of human ornithine decarboxylase at 2.1 Å resolution: structural insights to antizyme binding, *J. Mol. Biol. 295*, 7-16.
205. Liu, J., Dehbi, M., Moeck, G., Arhin, F., Bauda, P., Bergeron, D., Callejo, M., Ferretti, V., Ha, N., Kwan, T., McCarty, J., Srikumar, R., Williams, D., Wu, J. J., Gros, P., Pelletier, J., and DuBow, M. (2004) Antimicrobial drug discovery through bacteriophage genomics, *Nat Biotechnol 22*, 185-91.
206. Kane, S. A., Fleener, C. A., Zhang, Y. S., Davis, L. J., Musselman, A. L., and Huang, P. S. (2000) Development of a binding assay for p53/HDM2 by using homogeneous time-resolved fluorescence, *Anal Biochem 278*, 29-38.
207. Leblanc, V., Delaunay, V., Claude Lelong, J., Gas, F., Mathis, G., Grassi, J., and May, E. (2002) Homogeneous time-resolved fluorescence assay for identifying p53 interactions with its protein partners, directly in a cellular extract, *Anal Biochem 308*, 247-54.
208. Whitfield, J., Harada, K., Bardelle, C., and Staddon, J. M. (2003) High-throughput methods to detect dimerization of Bcl-2 family proteins, *Anal Biochem 322*, 170-8.
209. Lakowicz, J. R. (1999) *Principles of Fluorescence Spectroscopy*, 2 ed., Kluwer Academic/Plenum Publishers, New York.

210. Suzuki, Y., Yasunaga, T., Ohkura, R., Wakabayashi, T., and Sutoh, K. (1998) Swing of the lever arm of a myosin motor at the isomerization and phosphate-release steps, *Nature 396*, 380-3.
211. Murakami, H., Hohsaka, T., Ashizuka, Y., Hashimoto, K., and Sisido, M. (2000) Site-directed incorporation of fluorescent nonnatural amino acids into streptavidin for highly sensitive detection of biotin, *Biomacromolecules 1*, 118-25.
212. Cohen, S. L., Ferre-D'Amare, A. R., Burley, S. K., and Chait, B. T. (1995) in *Protein Sci* pp 1088-99.
213. Churchich, J. E. (1986) in *Vitamin B6 Pyridoxal Phosphate: Chemical, Biochemical, and Medical Aspects* (Dolphin, D., Poulson, R, Avramovic, O, Ed.) pp 545-568, John Wiley & Sons, New York.
214. Sacchetti, A., Subramaniam, V., Jovin, T. M., and Alberti, S. (2002) Oligomerization of DsRed is required for the generation of a functional red fluorescent chromophore, *FEBS Lett 525*, 13-9.
215. Shayovits, A., and Bachrach, U. (1995) Ornithine decarboxylase: an indicator for growth of NIH 3T3 fibroblasts and their c-Ha-ras transformants, *Biochim Biophys Acta 1267*, 107-14.
216. Holtta, E., Sistonen, L., and Alitalo, K. (1988) The mechanisms of ornithine decarboxylase deregulation in c-Ha-ras oncogene-transformed NIH 3T3 cells, *J. Biol. Chem. 263*, 4500-7.
217. Tabib, A., and Bachrach, U. (1998) Polyamines induce malignant transformation in cultured NIH 3T3 fibroblasts, *Int. J. Biochem. Cell Biol. 30*, 135-146.
218. Peric, M., Bozdogan, B., Galderisi, C., Krissinger, D., Rager, T., and Appelbaum, P. C. (2004) Inability of L22 ribosomal protein alteration to increase macrolide MICs in the absence of efflux mechanism in Haemophilus influenzae HMC-S, *J Antimicrob Chemother 54*, 393-400.
219. Feinstein, E. (2004) Ral-GTPases: good chances for a long-lasting fame, *Oncogene*.

# Appendix A

## Development of a High-Throughput Assay to Detect ODC Dimerization

### Specific Aim

To develop an assay for use as a high-throughput screen to detect ODC inhibitors that mechanistically inhibit ODC by interfering with ODC homodimerization.

## Introduction

As discussed in Chapter 1, active ODC is formed by homodimerization of two monomers. Two monomers bind in a head to tail orientation so that the C-terminal domain of one interacts with the N-terminal domain of the other. This brings together residues in the N-terminus involved in PLP binding and residues in the C-terminus that have been implicated in substrate binding to form two active sites per homodimer (*204*). Point mutations have been identified which prevent ODC homodimerization and subsequently abolish ODC activity ((*21*), personal communication with David Feith, Penn State College of Medicine). Antizyme also binds to the ODC monomer thus blocking ODC activity by preventing the formation of ODC homodimers. Based on the fact that homodimerization is necessary for ODC activity, we set out to develop an assay that could rapidly determine the state of ODC dimerization and could subsequently be developed as the basis for a high-throughput screen to detect compounds that mechanistically inhibit ODC activity by blocking homodimerization.

A number of reports have been published that describe methods to detect protein dimerization *in vitro* and *in vivo* (*205-208*). Several methods, and variations thereof, have been utilized, but many are based on resonance energy transfer (RET). FRET (fluorescence resonance energy transfer) is often used in reference to RET, but FRET is a misnomer because the resonance energy transfer does not involve emission and reabsorption of a photon. RET is a technique well suited to detect protein-protein interactions and can be adapted for high throughput applications. In RET, a donor

fluorophore is excited and instead of emitting a photon, the energy is transferred to the acceptor via long-range dipole-dipole interactions. RET is often detected by exciting the donor and monitoring the decrease in donor emission if the RET acceptor is within an acceptable range of the donor (typically <100 Å). The acceptor does not have to emit fluorescence—it only has to quench the energy of the donor; if the donor does emit fluorescence then a ratio of increase in acceptor fluorescence to decrease in donor emission can be used to measure RET. The efficiency of RET is determined by the spectral overlap of the donor's emission spectrum and the acceptor's excitation spectrum (i.e. the dipoles have similar resonance frequencies), the distance between the acceptor and donor, the quantum yield of the donor and the relative orientation of the donor and acceptor transition dipoles (*209*). The Förster distance, defined as the distance where RET is 50% efficient (between 20-60 Å), is similar in size to biomacromolecules, thus making RET useful to study the interactions of proteins.

RET screens to detect protein dimerization of various molecules have been successfully established. One such example was developed to investigate the interaction of p53 and HDM2. HDM2 is a negative regulator of the tumor suppressor p53. It interacts with p53 and traffics it out of the nucleus into the cytoplasm where p53 is targeted for degradation. Recombinant HDM2 and p53 proteins tagged with GST or biotin respectively were expressed and purified. HDM2-GST was prebound to an anti-GST antibody containing a conjugated fluorescent donor (europium cryptate) and p53-biotin was similarly conjugated to streptavidin labeled with a RET acceptor (XL665). Both the HDM2 and p53 complexes were incubated in microtiter plates and RET was detected by time-resolved fluorescence. Preventing the interaction of the two complexes

blocked the transfer of energy from europium cryptate to XL665 (*206*). A similar strategy was used to detect heterodimerization between Bcl-2 family members, which are critical regulators of apoptosis (*208*).

A number of strategies exist to label proteins with fluorophores. Fluorescent conjugated antibodies were used in the experiment described above and others (*206, 207*). Fusion proteins can be engineered in which a fluorescent protein is fused to the protein of interest (*210*). Amine and thiol reactive fluorescent probes are commercially available. Synthetic fluorescent amino acids can be incorporated into proteins (*211*, *212*). Some proteins do not need to be labeled at all if they contain an unquenched aromatic amino acid, particularly tryptophan.

In this chapter, three approaches to develop a screen to rapidly detect the dimerization state of ODC are described. The first two approaches are based on RET and differ in the method used to label ODC. In one approach, recombinant ODC proteins were engineered with one of two different fluorescent proteins fused to the C-terminus. In the second, recombinant ODC was labeled with extrinsic fluorescent probes. The third approach, which was not based on RET, attempted to take advantage of the intrinsic fluorescence of ODC. ODC exhibits significant fluorescence from tryptophan residues. With the aid of non-dimerizing mutants, we sought to determine whether there is a discernable difference in the intrinsic fluorescence of ODC in the monomer and dimer form.

## Methods

### *Cloning of ODC Fluorescent Fusion Proteins*

The sequence for two fluorescent proteins, DsRed and ECFP, were cloned into pQE30-ODC so that the resulting ODC protein has either fluorescent protein fused to its C-terminus. The stop codon in pQE30-ODC was removed by PCR. The sense primer (5'-CATGGCAACAGAAGTTGGTTTCAGC-3') targeted a sequence upstream of the *Sph*I site in the ODC coding region of pQE30-ODC. The antisense primer (5'-GCAACCTTGG*GTCGACGCGGCCGCGC*ATCTGAAC*ACCGGT*GCTCCCACATTGATCCTAGCAGAAGCACAG-3') changed the ODC stop codon into a glycine and added *Age*I, *Not*I and *Sal*I sites, respectively, to the 3' end of the PCR product. The PCR product was gel purified, digested with *Sph*I and *Sal*I and ligated into *Sph*I/*Sal*I digested pQE30-ODC to make pQE30-ODC-ns (no stop).

The region coding for ECFP was amplified by PCR from the pECFP-Nuc (Clontech, Palo Alto, CA) vector using primers that encompass a 5' *Age*I site from the multiple cloning site of the vector and add a *Not*I site 3' to the coding region. ECFP was PCR amplified out of pECFP-Nuc using the sense primer, TTAGTGAACCGTCAGATCCGCTAGC, and antisense primer, 5'-GGTCTGACAT*GCGGCCGC*TTACTTGTACAGCTCGTCCATGCCGAG-3'. The antisense primer adds a stop codon and a downstream *Not*I site 3' to the region coding for ECFP. The region coding for DsRed in pDsRed-N1 (Clontech) is flanked by a 5' *Age*I site and 3' *Not*I site, therefore no additional engineering was needed.

The ECFP PCR product and pDsRed-N1 were digested with *Age*I and *Not*I and ligated into pQE30-ODCns after digestion with the same restriction enzymes. The resulting apparent constructs, pQE30-ODC-DsRed and pQE30-ODC-ECFP, were transformed into XL-Blue subcloning-grade competent cells (Stratagene, La Jolla, CA) and DNA preps of each were purified. The constructs were verified by sequence analysis and confirmed that the correct constructs were engineered.

***Protein Purification***

The plasmids pQE30-ODC, pQE30-ODC-DsRed and pQE30-ODC-ECFP were transformed into XL1-Blue *E. coli* strain (Stratagene, La Jolla, CA). Frozen stocks of bacteria were grown-up in LB containing 100 μg/ml ampicillin and synthesis of ODC-DsRed or ODC-ECFP was induced upon addition of 270 μM IPTG at either 30° or 37° C. The bacterial cultures were pelleted 2-5 hr after the addition of IPTG. The pelleted bacteria was lysed by sonication in Sonication Buffer (25 mM Tris-HCl, pH 8.0; 400 mM NaCl; 5 mM imidazole) and the supernatant was separated from the pellet by centrifugation (20,000xg, 30 min. 4°C). The supernatant was further clarified by high speed centrifugation (35,000xg, 30 min, 4°C). Note that several figures in the chapter refer to the "pellet" and "supernatant" samples from the purification. These samples refer to the supernatant and pellet obtained at this step. The 6x-His tagged ODC-DsRed and ODC-ECFP proteins were purified from the supernatant on a column with a metal affinity resin (Talon, Clontech, Palo Alto, CA). After loading the supernatant onto the column, the column was washed with Wash Buffer (25 mM Tris-HCl, pH 8.0; 400 mM

NaCl; 10 mM imidazole) and eluted in Elution Buffer (25 mM Tris-HCl, pH 8.0; 400 mM NaCl; 200 mM Imidazole). The protein was eluted in separate fraction each containing 2.5 mM DTT to stabilize the protein. Fractions containing protein were dialyzed in ODC Buffer (25 mM Tris-HCl, pH 7.5; 2.5 mM DTT; 0.1 mM EDTA) and the protein was concentrated with a Centriprep YM-10 centricon (Micron Bioseparations, Millipore). Samples from different steps in the purification protocol were analyzed by SDS-PAGE to evaluate the purification.

The fusion proteins proved to be very insoluble with most of the protein remaining in the pellet after sonication. To increase solubility, ODC-ECFP was also purified under denaturing conditions. The purification procedure was carried out as described above except that it was done under denaturing conditions on a bacterial pellet from which the soluble protein was already extracted. To denature the fusion protein, 8M urea was added to the Sonication, Wash and Elution Buffers. The purified protein was dialyzed in ODC Buffer containing diminished urea concentrations (5, 2.5, 1 and 0 M urea) with every change in buffer to assist in protein refolding.

***Western Blotting***

Western blotting was performed on the purified fusion proteins. A known amount of protein obtained from the purification of ODC, ODC-DsRed and ODC-ECFP was resolved by SDS-PAGE and transferred to a PVDF membrane (Pall Corporation, Pensacola, FL, USA). The membrane was probed with a RGS His antibody (0.1 μg/ml, Qiagen, Valencia, CA) or an affinity-purified ODC polyclonal antibody (0.5 μg/ml) (*116*)

and detected using a chemiluminescent detection system (Cell Signaling Technology, Beverly, MA). Images were obtained using a fluorimager (Molecular Dynamics, Sunnyvale, CA).

***Fluorescence Readings of Fusion Proteins***

Purified ODC-DsRed or ODC-ECFP was diluted in ODC Buffer to 0.8 μM of total fusion protein (of which 0.25 μM represents the fluorescent protein portion of the fusion protein). Fluorescent excitation and emission spectrums were obtained for each protein. Excitation spectra were determined by measuring changes in the intensity of the emission fluorescence at a fixed emission wavelength (the emission maxima, 582 nm DsRed, 474 ECFP) while exciting the protein over a range of excitation wavelengths. Conversely, emission spectra were obtained by exciting the protein at a fixed wavelength (560 nm DsRed, 435 nm ECFP) and measuring the emission fluorescence over a range of emission wavelengths. All fluorescence measurements were done on a Spex FluoroMax scanning fluorometer. The data was plotted as a ratio of the maxima for each curve. For example, the emission max for DsRed occurred at 583 nm. The fluorescence intensity for the other wavelengths measured in the emission curve for DsRed were divided by the fluorescence intensity of DsRed at 583 nm.

***Assay for ODC Activity***

ODC activity was determined as described previously in Chapter 2. Different amounts (50-300 ng) of protein from purified 6xHis-tagged WT-ODC, ODC-DsRed or ODC-ECFP were assayed for ODC activity. Equivalent stoichiometric concentrations of ODC were used (i.e. concentrations were normalized to account for the larger size of the fusion proteins). ODC activity was calculated in pmols $^{14}C$/ 30 min/ng protein and then plotted as a percentage of WT-ODC activity. The plotted data represents at least three different concentrations of protein determined in duplicate for one or two different protein preps.

***Conjugation of Fluorescent Dyes to ODC***

Purified 6xHis-tagged ODC , initially in ODC Buffer, was dialyzed against Fluorescent Labeling Buffer (25 mM sodium phosphate, pH 7.5; 2.5 mM DTT) to remove the Tris and EDTA which could react with the amine-reactive fluorescent dyes. ODC (0.2 mg per reaction) was incubated with an excess dye (Oregon green [OG] or tetramethylrhodamine [TMR], Molecular Probes, Eugene, Oregon) to ODC molar ratio (MR) of 15, 20, 40 (TMR only), 100 (OG only) in the presence of 100 mM sodium bicarbonate, pH 8.3 (succinimidyl esters react most efficiently with primary amines at slightly alkaline pH) at room temp for one hour in the dark. Free unreacted dye was removed from the labeled protein using a spin column containing 30,000 MW size exclusion resin.

The recovery of the resulting proteins (referred to as ODC-OG or ODC-TMR) was estimated to be 85% (manufacturer reports yields typically are 80-90%). Dye per protein molecule was calculated by dividing the absorbance of ODC-TMR or ODC-OG by the product of the molecular extinction coefficient of the dye at 555 nm multiplied by the protein concentration. The three preps (MR 15, 20, and 40 or 100) were pooled for subsequent experiments.

### *Fluorescent Readings of ODC-OG and ODC-TMR*

ODC-OG and ODC-TMR were diluted in fluorescence labeling buffer to 50 ng/mL and 50 ng was read on a scanning fluorometer (Spex FluoroMax ) at the excitation and emission maxima for the respective proteins (OG = 511/530 nm; TMR = 555/580 nm).

### *Resonance Energy Transfer Studies for ODC-OG and ODC-TMR*

ODC-OG and ODC-TMR (100 ng each) were incubated together at 37°C for 10 or 45 min either in fluorescence labeling buffer or ODC reaction mix (40 μM PLP, 2.5 mM DTT, 400 μM ornithine, and 50 mM Tris-HCl pH 7.5 at 25°C). Incubations without either ODC-OG or ODC-TMR were also performed in the same manner. After the 10 or 45 min incubation, the samples were read on the fluorometer.

The spectrums were obtained by exciting the mixes at 508 nm (excitation max of the OG donor) and monitoring emission over a 520-650 nm interval. The mixes

contained both ODC-OG or ODC-TMR alone (to provide a baseline of expected fluorescence in the absence of the donor or acceptor) or ODC-OG and ODC-TMT.. In addition, the mix containing ODC-OG and ODC-TMR was excited at 555 nm (the excitation max of the TMR acceptor) to provide a reference point for TMR emission.

### *Cloning ODC Mutants into pQE30*

The three ODC mutants, G387D, F397E and F397Y, used for the intrinsic fluorescence studies were cloned from a pGEM plasmid (gift from David Feith, Penn State College of Medicine) into a pQE30 vector (Qiagen). This vector adds a 6xHis tag and allows the protein to be expressed in bacteria. pGEM-ODC-G387D, pGEM-ODC-F397E and pGEM-ODC-F397Y were digested with *Sph*I and *Bst*XI and ligated into pQE30-ODC digested with the same restriction enzymes in order to clone the point mutations into pQE30. The constructs were transformed into bacteria and purified following the same procedure used for the fusion proteins.

### *Fluorescent Readings of Intrinsic ODC Fluorescence*

Purified wild-type (WT) ODC, ODC-G387D, ODC-F397E and ODC-F397Y were diluted to 20 and 50 μg/ml in ODC Buffer and fluorescence was determined using an excitation wavelength at 290 nm and monitoring the emission from 300-400 nm.

## Results

### Resonance Energy Transfer Approaches

Two different approaches were pursued to develop a RET screen for ODC dimerization. In one approach recombinant fusion proteins were engineered that contained one of two different fluorescent proteins at the C-terminus. Extrinsic fluorescent dyes were conjugated to ODC in the second approach. Although the means of labeling ODC differed, the principle of the screen was the same. This principle is depicted in Figure A.1 using the fusion proteins ODC-DsRed and ODC-ECFP as the example. ODC containing one tag has spectral properties that differ from ODC containing the other tag. By monitoring the change in donor emission and increase in acceptor emission, a change in the state of dimerization should be detectable. Antizyme, which binds to the ODC monomer, and non-dimerizing ODC mutants can be used to validate the approach once it is established that energy transfer does occur.

#### *Purification of Fusion Proteins*

Two constructs were engineered, pQE30-ODC-DsRed and pQE30-ODC-ECFP, so that when transcribed and translated in bacteria the product of these plasmids would be a truncated ODC (425 of 461 amino acids) containing a 6xHis tag at the N-terminus and C-terminal fluorescent protein (DsRed or ECFP). The fusion proteins have predicted molecular weights approximately 1.5 times the size of ODC (51 kD ODC, 78 kD ODC-

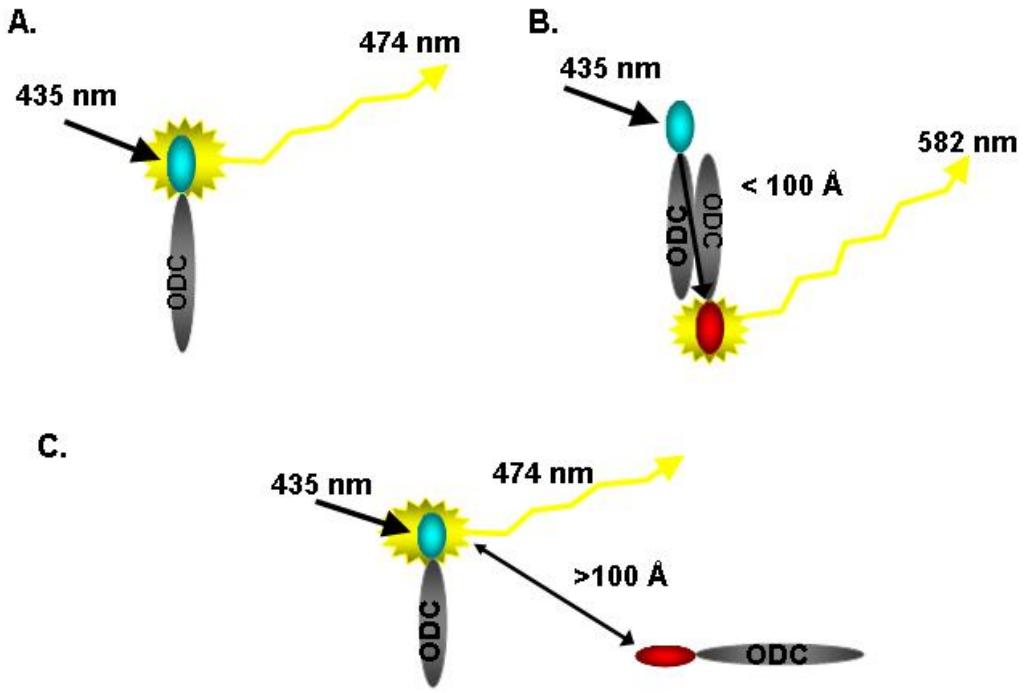


**Figure A.1**: *Theory of RET for ODC Dimerization Screen.*

The donor, ODC-ECFP, when excited at 435 nm emits fluorescence at 474 nm (A). Upon excitation at 435 nm, resonance energy from ODC-ECFP is transferred to ODC-DsRed when in a dimerized form. The emission of ODC-ECFP at 474 nm decreases and the excitation of ODC-DsRed increases (B). If the dimerization is disrupted then energy is not transferred from ODC-ECFP to ODC-DsRed (C). The state of dimerization is determined by the ratio of fluorescence emitted at 582 nm versus 474 nm. In practice, the wavelengths used for excitation and emission, when monitoring RET, may not be taken at max wavelength in order to avoid exciting the acceptor or recording overlapping emissions.

DsRed and 80 kD ODC-ECFP). ECFP (enhanced cyan fluorescent protein) and DsRed (red fluorescent protein isolated from an IndoPacific sea anemone-relative, *Discosoma sp*.) were chosen based on their spectral properties. ECFP (the donor fluorophore) can be excited near its maxima with minimal excitation of DsRed (the acceptor fluorophore), yet the emission of ECFP overlaps considerably with the excitation of DsRed making for good RET partners. Both plasmids were successfully engineered. When expressed in XL1 Blue strain of *E. coli*, the fusion proteins were very insoluble and found mostly in the pellet fraction after sonication and centrifugation (Figure A.2, A.3). In Figure A.2, samples taken from a purification of the 80 kD ODC-ECFP after the cells had been lysed and centrifuged were resolved by SDS-PAGE. Lane 2 and 3 represent samples taken from the pellet (insoluble fraction) and supernatant (soluble fraction) respectively. A high percentage of the total protein in the pellet fraction is ODC-ECFP, whereas very little soluble ODC-ECFP is present in the supernatant. Little full-length ODC-ECFP is present in the eluted purified protein fractions (lanes 4-7) and 11 and 6 μg (lanes 8, 9) of the concentrated, pooled purified protein also showed that only a portion of the protein corresponded to full-length ODC-ECFP. Protein purification regularly yielded <0.5 mg of protein per L of bacterial culture and it is apparent that only a portion of this protein is full-length fusion protein. Purification of the 78 kD ODC-DsRed yielded similar results (Figure A.3). ODC-DsRed is clearly induced and it represents the major protein in the induced cells (A, lane 2), but it remains insoluble in the pellet (A, lane 4) with little protein representing ODC-DsRed visible in the supernatant (A, lane 3 and 5). As a result, little ODC-DsRed is obtained

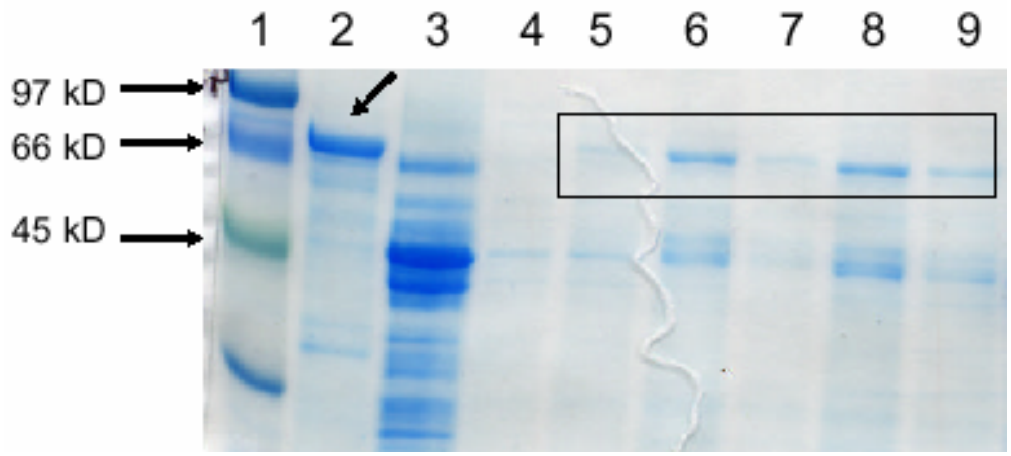


**Figure A.2:** *Purification of ODC-ECFP*.

Samples from different steps of ODC-ECFP protein purification were resolved by gel electrophoresis, resolved on a polyacrylamide gel and stained with commassie dye. Lane: (1) marker, (2) bacterial pellet, (3) supernatant, (4) fraction 1 (F1), (5) F2, (6) F3, (7) F4, (8) 11 µg purified protein, (9) 6 µg purified protein. The bacterial pellet (lane 2) and supernatant (lane 3) samples are after the sonication and centrifugation and thereby lane 2 represents the insoluble fraction. The different fractions (lanes 4-7) represent different fractions collected during elution of the 6xHis-tagged ODC-ECFP from the Talon resin. Purified protein is the pooled fractions containing protein that has been dialyzed and concentrated. The arrow in lane 2 and the box (lanes 5-9) designate the bands representing the 80 kD ODC-ECFP fusion protein.

A.

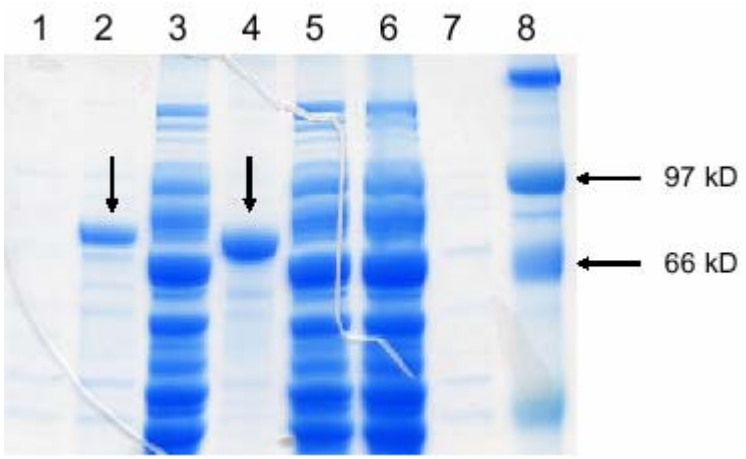


B.

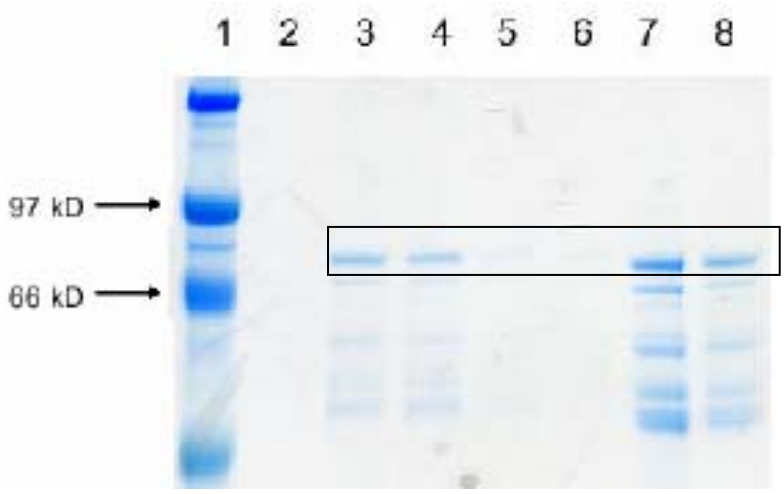


**Figure A.3**: *Purification of ODC-DsRed*.

Samples from different steps of ODC-DsRed protein purification were analyzed as stated in Figure A.2. A. Lane: (1) uninduced cells, (2) induced cells, (3) 1st spin supernatant, (4) 1st spin pellet, (5) 2nd spin supernatant, (6) flow through, (7) wash, (8) marker. B. Lane (1) marker, (2) F1, (3) F2, (4) F3, (5) F4, (6) F5, (7) 10 µg purified protein, (8) 5 µg purified protein. The designations of the samples are as noted in Figure A.2. Uninduced and induced cells represent samples taken from bacterial culture before and after (4 hr after), respectively, IPTG was added to the bacterial culture to induce synthesis of ODC-DsRed. Flow through was taken from the solution that flowed through the metal affinity column when the bacterial lysate was passed through. The wash sample would contain protein that was eluted by the wash step. The arrows in lanes 2 and 4 (A) and the box (B) denote the bands representing the 78 kD ODC-DsRed protein.

from the purification and only a portion of the purified protein is full-length ODC-DsRed (B, lanes 3-8).

Purification of the 78 kD ODC-DsRed yielded similar results (Figure A.3). ODC-DsRed is clearly induced and it represents the major protein in the induced cells (A, lane 2), but it remains insoluble in the pellet (A, lane 4) with little protein representing ODC-DsRed visible in the supernatant (A, lane 3 and 5). As a result, little ODC-DsRed is obtained from the purification and only a portion of the purified protein is full-length ODC-DsRed (B, lanes 3-8).

***Characterization of ODC-DsRed and ODC-ECFP***

The purified proteins were characterized by Western blotting, the fluorescent spectrum analysis and ODC activity assay. Western blots of the purified proteins with antibodies directed against the His tag and ODC reveal more detail as to whether the fusion protein is degraded. The commassie stained gels in Figure A.2 and Figure A.3 show a number of bands smaller than the fusion protein. These bands could be either degradation products of the fusion protein or polypeptides of ODC in which translation was prematurely terminated. Alternatively, these bands could also represent background proteins eluted during the purification that normally are not detected when higher levels of the His-tagged protein are obtained. Blotting with either the His-tagged antibody or ODC antibody shows similar results (A, Figure A.4). Major bands are present around the expected sizes for both ODC-DsRed and ODC-ECFP, however smaller bands are also apparent. Purified 6xHis-ODC (referred to as ODC or wild type ODC in this chapter)

always runs as a doublet at ~51 kD. A prominent doublet similar in size to the ODC doublet is present in the ODC-DsRed lane. There is a third unidentified major band between the bands representing ODC-DsRed and ODC. A similar band also appears in the ODC-ECFP lane, but the distinct ODC doublet is not detected on these blots. In a different ODC-ECFP protein prep, a Western blot with the ODC antibody shows three clear, distinct bands—ODC-ECFP and the ODC doublet (B, Figure A.4). Therefore it appears that the full-length fusion protein is translated, but the protein is cleaved by a protease where ODC and the fluorescent protein are fused or it is degraded. It is also possible that the small protein products result from premature translation or nuclease degradation of the transcript for the fusion protein.

In order to confirm that the band on the Western blots, presumed to be the fusion protein, is in fact ODC-DsRed or ODC-ECFP, the fluorescence of the purified proteins was analyzed. Both ODC-DsRed and ODC-ECFP show the prototypical fluorescent spectrums for the respective protein (Figure A.5). The excitation and emission maximums agree with the reported values and the shape of the peaks and the appearance of the shoulders coincide with the manufacturer's spectrums. No fluorescence above background was detected for ODC or ODC Buffer when analyzed under the same excitation and emission wavelengths as ODC-DsRed and ODC-ECFP (data not shown). These experiments prove that the purified preps do contain the fluorescent proteins.

The purified proteins were assayed for ODC activity to determine whether the fused fluorescent protein interfered with ODC activity. Both ODC-DsRed and ODC-ECFP exhibited decreased ODC activity (86 % and 59 % decrease respectively)

A.

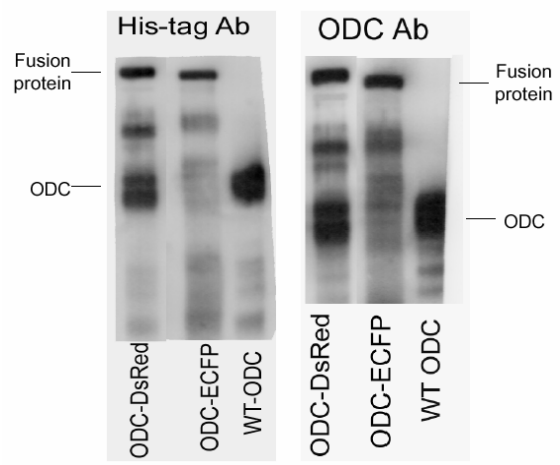


B.

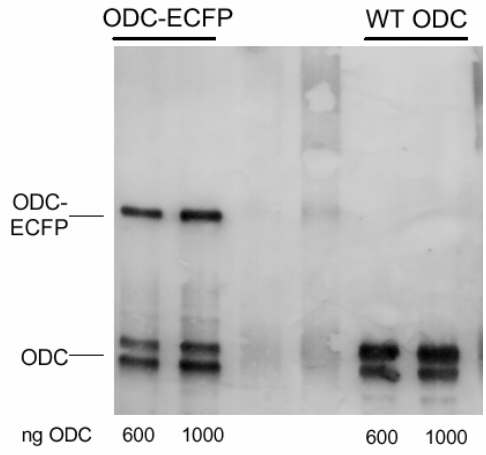


**Figure A.4**: *Western Blots of Purified Fusion Proteins.*

Western blotting was performed on 500 ng of ODC, ODC-DsRed and ODC-ECFP using an antibody to the His tag or to ODC (A). Another Western blot of 600 or 1000 ng ODC-ECFP or ODC, probed with the ODC antibody, is shown in B.

Note: The amount of protein loaded represents the amount of ODC and not the total amount of protein (i.e. ODC-DsRed and ODC-ECFP are approximately 1.5x the size of ODC so 1.5x more protein was loaded for these samples). Therefore, equimolar amounts of ODC were resolved.

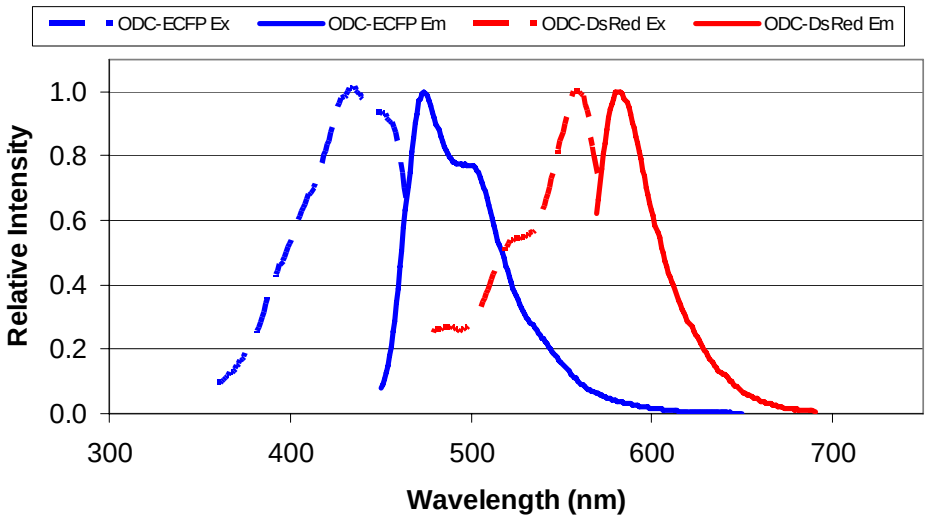


**Figure A.5**: *Fluorescent Spectrums for ODC-DsRed and ODC-ECFP*.

The fluorescent spectrums for purified ODC-DsRed and ODC-ECFP were determined by scanning fluorometry. 0.8 µM total fusion protein (0.25 µM of fluorescent protein portion of fusion protein) was measured. The dotted lines represent the excitation spectrums; the solid lines represent emission spectrums. ODC-DsRed is depicted in red; ODC-ECFP in blue. The intensity for each curve is expressed as a ratio of the maxima for that particular curve so that the scales are the same.

compared to WT-ODC (Figure A.6). However it can not be determined whether the decrease in ODC activity is due to decreased ODC activity of the fusion protein or it may be that the fusion protein has no activity at all and that the ODC activity from these preps is from the species of protein that lacks the fluorescent protein (i.e. the doublet band that runs with WT-ODC). The decrease activity may also be due to the impurity of the preps.

### *Alternative Strategies to Purify Fusion Proteins*

It was clear that it would be difficult to use the protein from the preps characterized above to develop a high-throughput RET screen. The two main limitations with the fusion proteins are that only a percentage of the purified fusion proteins are intact and that they are insoluble. The bacteria express ample fusion protein and if the proteins were more soluble then the purification would yield increased amounts of protein. If enough protein would be obtained by increasing the yield, then the full-length fusion protein could be separated from the contaminating protein.

One attempt to increase protein solubility was to purify the fusion protein under denaturing conditions. ODC-ECFP was grown up in bacteria and purified as described (soluble ODC-ECFP). The soluble material in the pellet was sonicated again and repurified in the presence of 8M urea. The solubility of ODC-ECFP was enhanced (Figure A.7). Although some protein still remained in the pellet (lane 5), ODC-ECFP was the major band detected in the supernatant (lane 4 and 6). This is in contrast to the purification of ODC-ECFP under non-denaturing conditions (Figure A.2). .

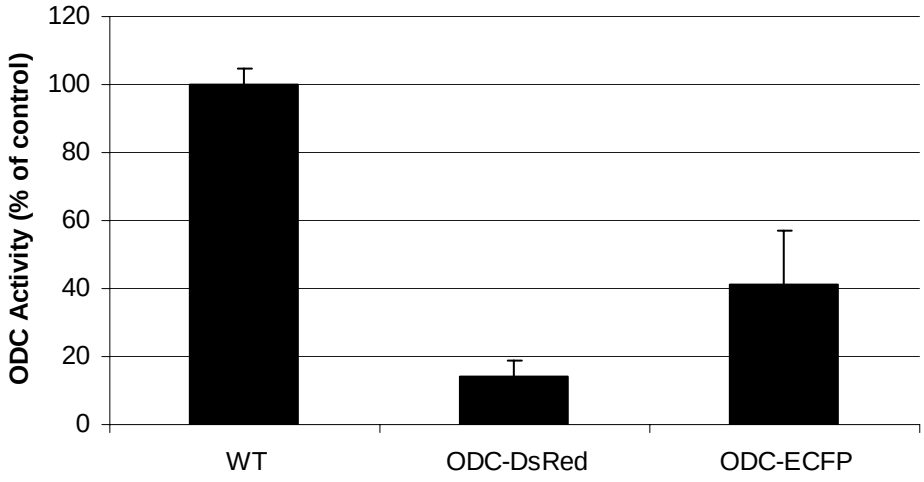


**Figure A.6***: ODC Activity of ODC-DsRed and ODC-ECFP.*

ODC activity of purified protein preps was determined for WT-ODC, ODC-DsRed and ODC-ECFP. WT-ODC was designated the control and the activity of ODC-DsRed and ODC-ECFP are expressed as a percentage of WT-ODC activity.

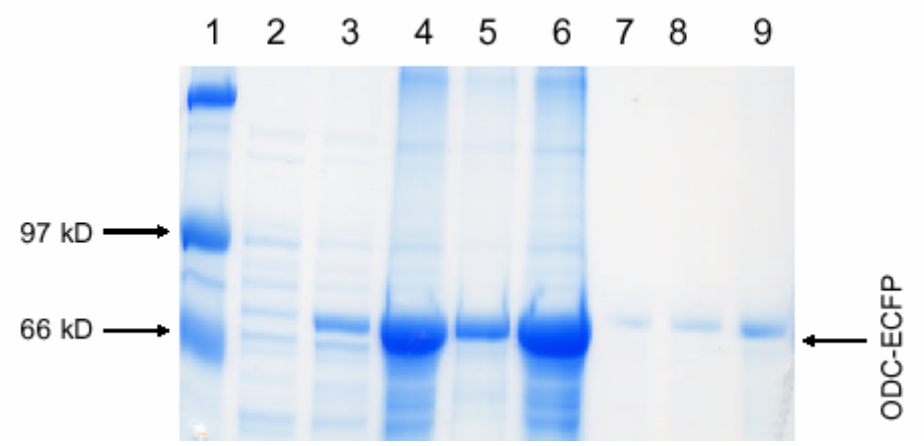


**Figure A.7**: *Purification of Denatured ODC-ECFP*.

Samples from different steps of ODC-ECFP protein purification were analyzed as in Figure A.2. However, ODC-ECFP was purified under denaturing conditions—in the presence of 8 M urea. Lane: (1) marker, (2) uninduced cells, (3) induced cells, (4) first spin supernatant, (5) pellet, (6) second spin supernatant, (7) 2.5 µg purified protein, (8) 5 µg purified protein, (9) 10 µg purified protein. The arrow indicates the band representing ODC-ECFP.

A total of 0.2 µg of soluble ODC-ECFP was extracted from the pellet under native conditions. When ODC-ECFP was extracted from the same pellet, 0.4 µg was obtained. Therefore, purification of denatured ODC-ECFP does increase protein yield.

An attempt to restore the native structure of ODC-ECFP was made by dialyzing out the urea from the purified protein in a step-wise manner. The fluorescence spectra and ODC activity were determined for ODC-ECFP purified under denaturing conditions (and then dialyzed) and compared to ODC-ECFP purified under native conditions (soluble ODC-ECFP). ODC-ECFP purified under denaturing conditions was not fluorescent (A, Figure A.8) nor did it have ODC activity (B, Figure A.8). Although the protein yield was improved, the protein could not be renatured to restore fluorescence or enzyme activity.

A number of other attempts to increase protein yield were also tried. The bacteria were grown at reduced temperature (30°C vs. 37°C) which has been shown to increase protein solubility. Shorter protein induction times were used because it has been reported that some proteins become more insoluble when produced in larger quantities. The fusion proteins were expressed in another strain of *E. coli*, JM109. The cells were lysed by chemical disruption instead of sonication to help improve protein solubility. A protease inhibitor cocktail set was added during the purification to prevent protease-mediated degradation of the fusion proteins. The fusion proteins were cloned into expression vectors to express the proteins in an *E. coli in vitro* transcription/translation kit (Roche) which claimed high yields of proteins as large as 120 kD. However, none of these strategies significantly improved protein yield or quality.

A.

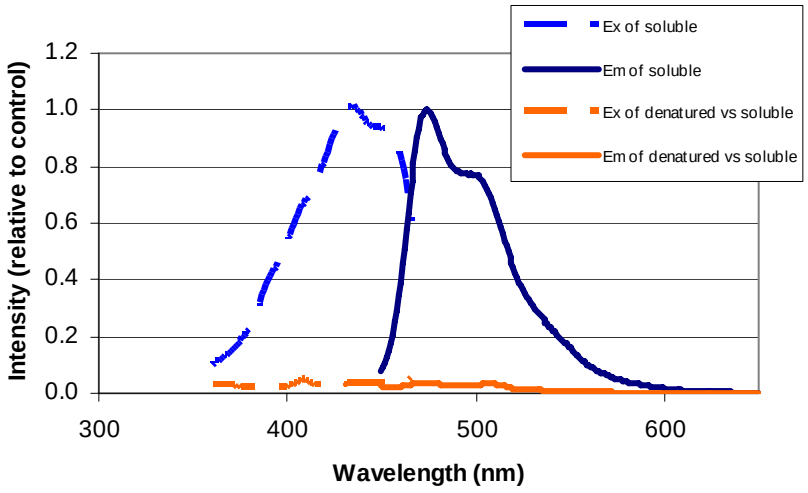


B.

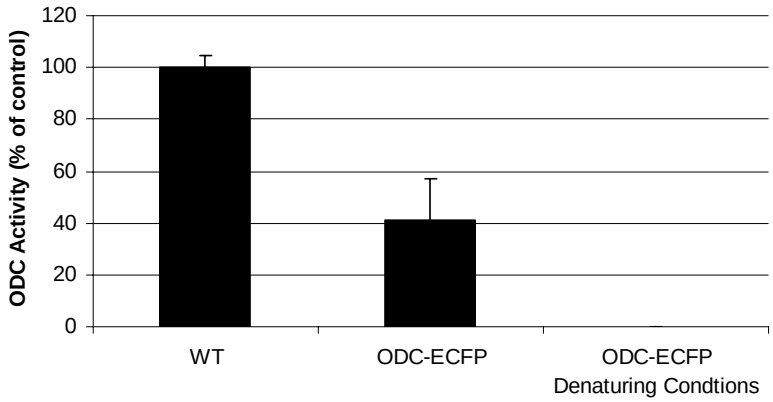


**Figure A.8:** *Characterization of ODC-ECFP Purified Under Denaturing Conditions.*

Soluble ODC-ECFP was extracted from a bacterial pellet and insoluble ODC-ECFP was re-extracted from the same pellet. Fluorescence spectra and ODC activity were determined for both preps. A. Equal amounts of protein (0.8 µM total fusion protein or 0.25 µM of fluorescent protein portion of fusion protein) were assayed for fluorescence. The fluorescence intensity is expressed relative to the intensity of native ODC-ECFP. B. ODC activity was determined for the different protein preps and expressed as a percentage of control WT-ODC protein activity.

### *Labeling ODC with Extrinsic Fluorescent Dyes*

One alternative to using ODC fused to a fluorescent protein for use in resonance energy transfer (RET) studies is to label purified ODC with fluorescent dyes. Extrinsic fluorescent amine or thiol-reactive dyes are commercially available. Two fluorescent dyes, Oregon green (OG) and tetramethylrhodamine (TMR), were chosen for the RET experiment based upon several criteria, including; the spectral overlap between the emission of the donor (OG) and excitation of the acceptor (TMR), the shift in excitation wavelengths between the pair, the dyes' affinity for photobleaching, and the dyes' linear relative fluorescence as a function of fluorophores attached per protein. Both dyes have a reactive succinimidyl ester moiety, which reacts with primary amines (ODC contains 29 lysines) to form stable dye-protein conjugates.

### *Fluorescence Characterization of ODC-OG and ODC-TMR*

Both amine reactive fluors successfully conjugated to ODC. Analysis of 50 ng ODC-OG or ODC-TMR on the scanning fluorometer revealed the characteristic peaks for the respective dyes (Figure A.9). Out of 30 potential conjugation sites (29 lysines and the amino terminus), the dyes bound to ODC at an approximately 1:1 stoichiometric ratio. Labeling efficiency generally increased when the molar ratio of dye to protein molecule was increased.

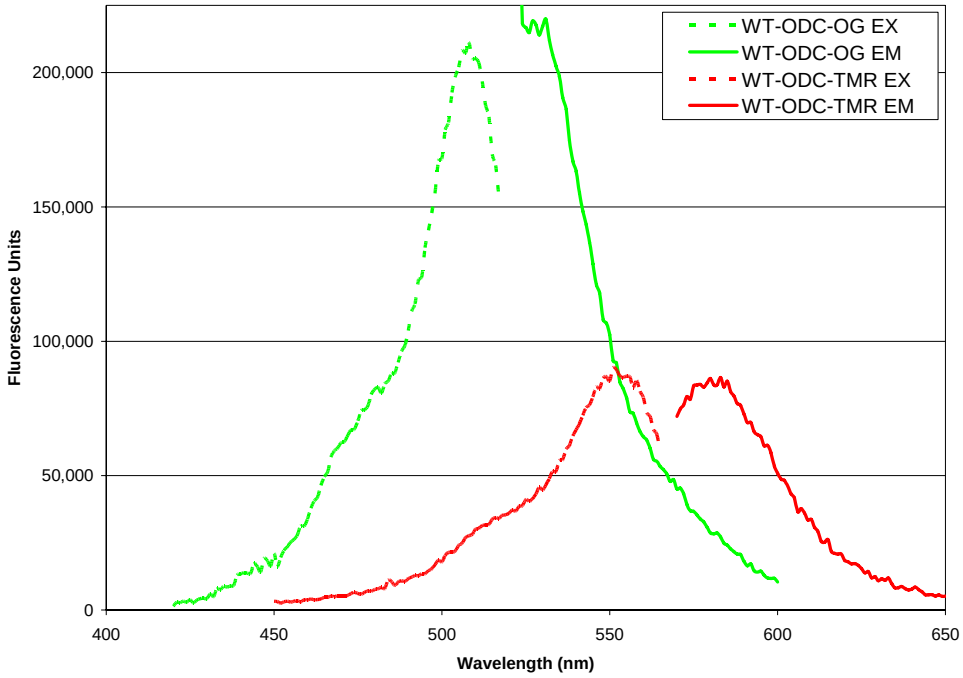


**Figure A.9**: *Fluorescent Spectrums for ODC-OG and ODC-TMR*.

Fluoresecent spectrums for 50 ng of ODC-OG and ODC-TMR were scanned. The dotted lines represent the excitation spectrums; the solid lines represent emission spectrums. ODC-OG is displayed in green; ODC-TMR in red. The intensity for each curve is expressed in arbitrary fluorescence units.

***Resonance Energy Transfer Experiments with ODC-OG and ODC-TMR***

ODC-OG and ODC-TMR incubated together for either 10 or 45 min in Fluorescence Labeling Buffer or ODC reaction mix did not show transfer of energy between the two fluors (Figure A.10). The increase in emission at 580 nm when ODC-OG and ODC-TMR are mixed and excited at 508 nm (black vs. red lines) is the result of overlapping fluorescence from ODC-OG (green line) and excitation (albeit sub-optimal) of TMR's broad excitation shoulder at 508 nm. Only the spectrum for the proteins in fluorescence labeling buffer is shown, however the spectrums were very similar for the mixes in ODC reaction mix.

Replotting the data from Figure A.10 to compare the fluorescence spectra for the 10 min and 45 min samples suggests RET may have occurred. For the 45 min samples, the emission at 530 nm (OG donor emission max) slightly decreases while the emission at 580 nm (TMR acceptor emission max) increases when excited at 508 nm (OG donor excitation max, A, Figure A.11). Replotting the controls, in which only ODC-OG (green lines) or ODC-TMR (red lines) were included in the mix, shows that the change in the spectra is not due to RET (B, Figure A.11)**.** The 45 min controls compared to the 10 min controls displayed a decrease in OG emission (dark green versus lime green, B) and an increase in TMR emission (dark red versus red, B) that coincides with the differences observed between the ODC-OG/ODC-TMR mixes at 10 and 45 minutes (black and yellow lines, A).

A.

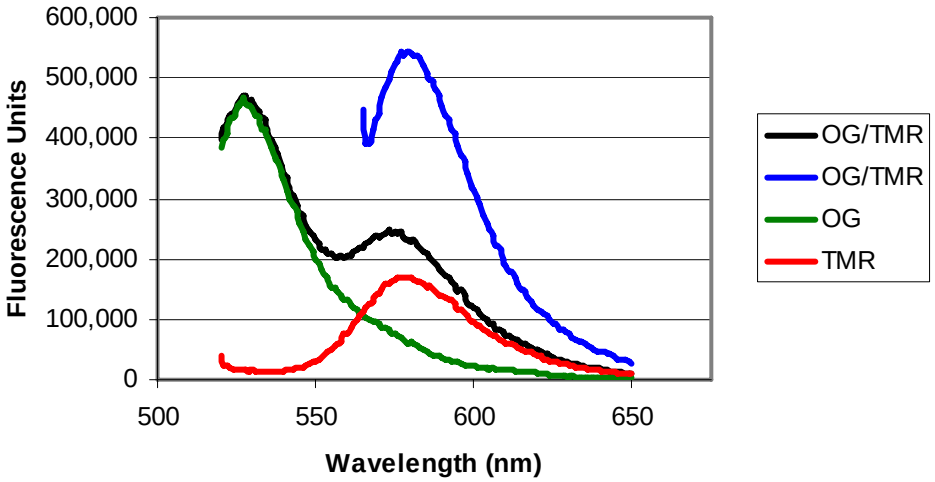


B.

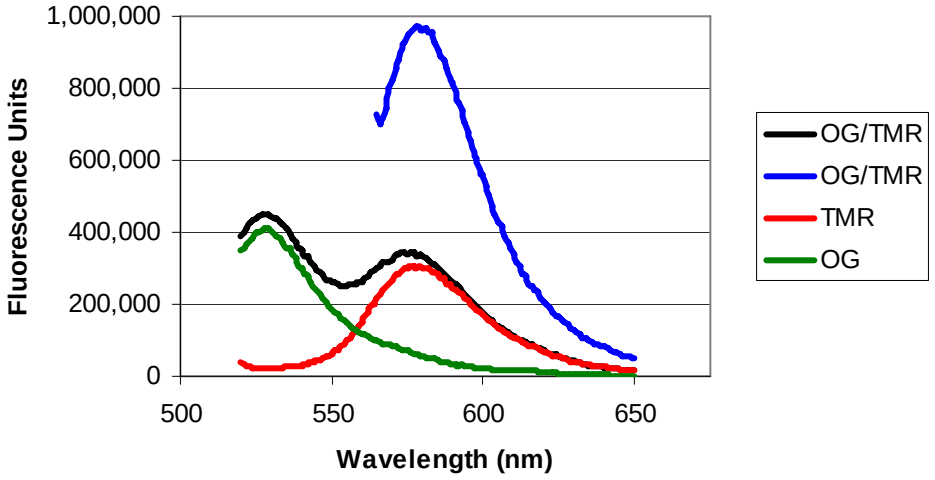


**Figure A.10**: *RET Experiments with ODC-OG and ODC-TMR.*

ODC-OG and ODC-TMR (100 ng each) were incubated alone or together at 37ºC for 10 min (A) or 45 min (B) in Fluorescence Labeling Buffer. The mixtures were excited either at 508 nm (excitation max for OG) and fluorescence was monitored from 520-560 nm. A mixture containing both ODC-OG and ODC-TMR was also excited at 555 nm (excitation max for TMR) to provide a reference point for TMR fluorescence (blue line).

A.

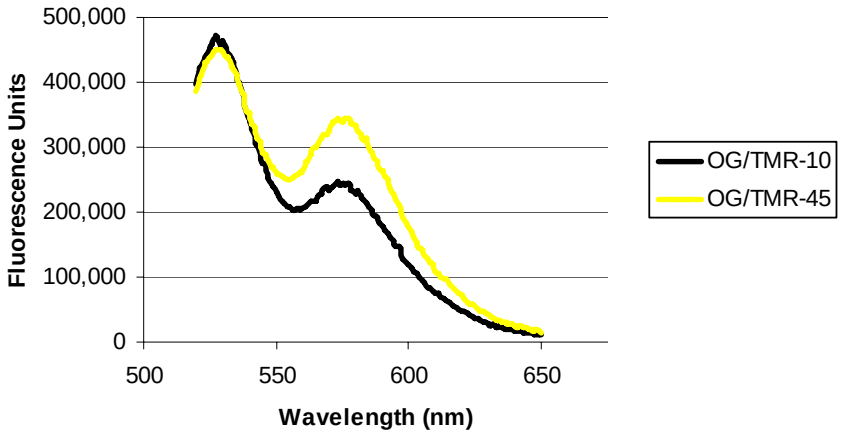


B.

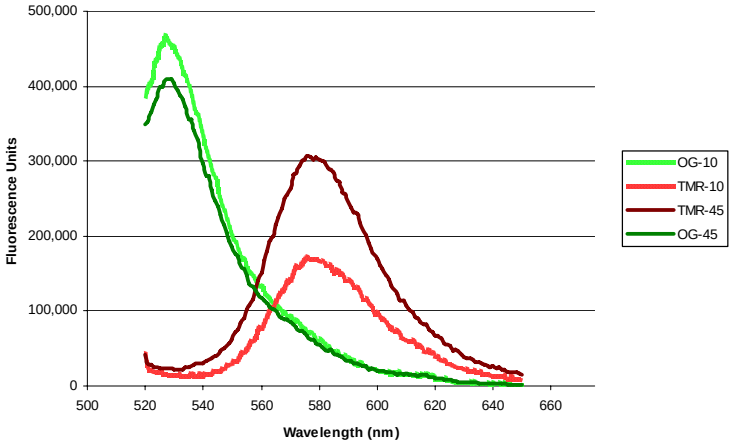


**Figure A.11**: *Fluorescence of ODC-OG and ODC-TMR Changes Over Time*.

The spectra in this figure are the data from Figure A.10 replotted to show the differences between the 10 and 45 min incubations. In comparing the fluorescence for ODC-OG and ODC-TMR at 10 min to 45 min, there is a slight decrease at 530 nm and an increase at 580 nm when excited at 508 nm (A). A similar trend is expected in RET. However when only one protein is present, there is a decrease in the fluorescence of ODC-OG at 530 nm and an increase is ODC-TMR at 580 nm for the 45 min samples.

***Intrinsic ODC Fluorescence***

The indole group of tryptophan residues is a major source of UV absorbance and emission in proteins (*209*). Phenylalanine and tyrosine can also contribute to the fluorescence of a protein but for the most part fluorescence from these residues is not significant. Phenylalanine has a low quantum yield and the emission of tyrosines is often quenched in native proteins, possibly due to energy transfer to tryptophan or interaction with the peptide chain. Fluorescence analysis of ODC shows that at least 1 of the 16 tryptophans emits fluorescence. We sought to investigate whether a change in dimerization state of ODC could be detected by monitoring the intrinsic fluorescence of ODC.

WT-ODC displays robust absorbance when excited at 290 nm (A, Figure A.12). This is the fluorescence associated with the homodimer. Single point mutations in ODC that prevent dimerization have been identified ((*21*), personal communication with David Feith). Both G387D and F397E mutations to ODC block dimerization, however a mutation of F397 to tyrosine does not affect dimerization (although it does abolish ODC activity). The fluorescence intensity of the dimerizing forms of ODC (WT and F397Y) exhibit greater intensity than the non-dimerizing mutants (G387D and F397E). Since mutation of F397 to glutamic acid decreases fluorescence intensity but a mutation to tyrosine does not, it is unlikely that the change in fluorescence is caused by a conformational change induced by altering F397 and more likely to a change in the state of dimerization. The change in conformation upon dimerization may expose a tryptophan that was previously buried or quenched in the monomer.

A.

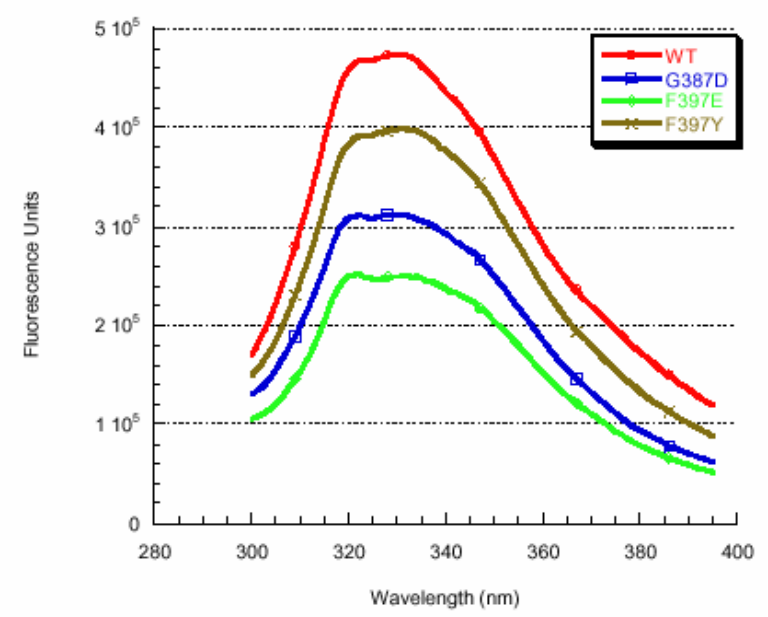


B.

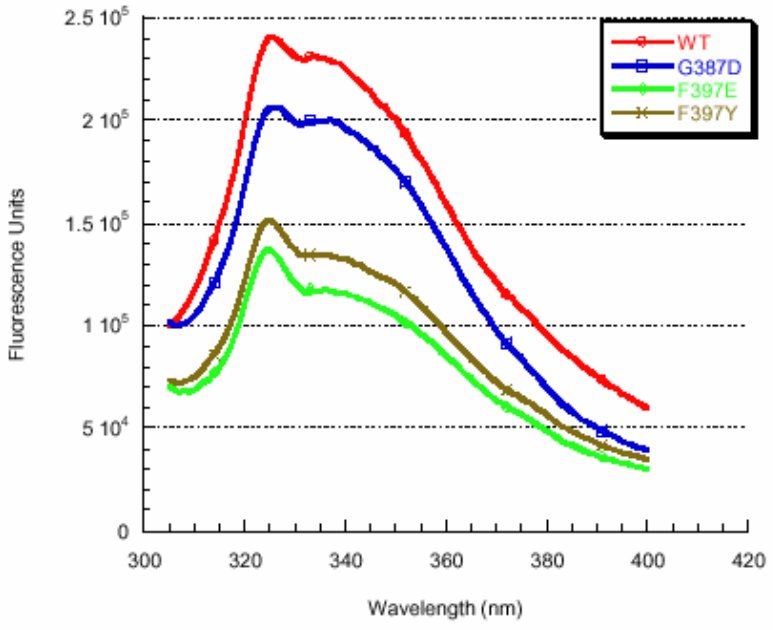


**Figure A.12**: *Intrinsic Fluorescence of ODC and ODC Mutants.*

Either 50 ug/ml (A) or 20 ug/ml (B) of each protein was excited at 290 nm in ODC Buffer.

WT-ODC (truncated wild-type ODC, 425 of 461 amino acids).

G387D, F397E and F397Y are point mutations of ODC. G387D and F397E are nondimerizing mutants. F397Y mutation does not affect ODC dimerization.

If dimerization enhances fluorescence, it would be expected that diluting the protein would minimize the difference in fluorescence between the dimerizing and non-dimerizing mutants. The interaction of ODC monomers is rapid and transient—the dimers dissociate and reassociate (*20*). At any given time, the percentage of ODC in the monomer form would be expected to be greater for the diluted protein. Diluting the protein from 50 μg/ml to 20 μg/ml does reduce the fluorescence of both WT and F397Y so that the intensity for these proteins approaches that of the non-dimerizing mutants (B, Figure A.12).

**Discussion**

Two strategies were pursued to detect ODC dimerization that could be incorporated into a high-throughput screening method used to detect ODC inhibitors. The first strategy was based on RET; the second, on a change in intrinsic fluorescence as ODC changes from the monomer to dimer state. Two methods of labeling the protein were used for the RET studies. Fusion proteins were constructed to add one of two fluorescent proteins to the C-terminus of ODC or ODC was labeled with extrinsic dyes. Full-length fusion proteins were successfully purified (Figure A.2 – Figure A.4) and each exhibited the characteristic spectrums for the respective fluorescent protein (Figure A.5), but full-length fusion proteins could not be purified to homogeneity and were largely insoluble.

The impurity of the protein preps has the potential to cause a number of problems. It is not clear whether the proteins smaller than ODC-DsRed or ODC-ECFP are degradation products of the full-length protein or the result of premature termination of ODC translation. The major "degradation" product was a protein the size of WT-ODC that was recognized by the His-tag and ODC antibodies (Figure A.4). Therefore, this protein represents the N-terminal portion of the fusion protein. It appeared that the fusion protein was cleaved at the junction between ODC and the fluorescent protein. Possibly the fusion protein was cleaved by a protease. The proteins were purified in the presence of a protease inhibitor cocktail but this did not improve the proportion of full-length fusion protein. Either the protease inhibitor cocktail was not effective (e.g. did not contain the appropriate protease inhibitor) or the fusion protein was not being degraded

by a protease. The protein preps do show the characteristic fluorescence for DsRed and ECFP (Figure A.5) and they do have ODC activity, albeit reduced (Figure A.6). The full-length fusion proteins are fluorescent and may have limited activity, but the activity could also be from the "degraded" protein that corresponds to WT-ODC. However, the fluorescence is from the full-length fusion proteins because even if the fluorescent protein was released from the fusion protein by a protease, the fluorescent protein does not have a His-tag and therefore would be lost during the purification.

The different size protein products presents a problem for determining RET. If RET was determined with full-length fusion proteins, then three species of dimers could form; ODC-DsRed:ODC-DsRed, ODC-ECFP:ODC-ECFP and ODC-ECFP:ODC-DsRed. The latter is the desired heterodimer and ODC-ECFP:ODC-ECFP (the donor) would actually contribute to background fluorescence (because it is excited but not quenched. When measuring RET, the acceptor ODC-DsRed is titrated in to a higher final molar ratio than ODC-ECFP for this reason). If degraded or truncated fusion proteins are added into the mix then the background fluorescence at 474 nm (emission of ECFP) would be even higher (because other heterodimer species could form like ODC-ECFP and a C-terminal truncated ODC lacking the fluorescent protein). Experiments to determine RET were attempted but RET could not be detected (data not shown).

A better protein yield would allow us to purify the full-length fusion protein from the contaminating proteins (e.g. using a sizing column) but this is not feasible with such poor protein solubility. Purifying the fusion proteins under denaturing conditions improved protein yield, however the purified protein could not be renatured (Figures A.7, A.8). It was not in our interest to work out a repurification procedure that would restore

the fusion protein to its native state because this purification still did not yield a significant improvement in the amount of purified protein. A number of modifications were made to the protein purification method to increase protein solubility and to increase the yield of full-length protein—but to no avail. An attempt to express the fusion proteins in a high yield *in vitro* coupled transcription/translation system did not improve upon the purification results obtained from expressing the proteins in bacteria.

After encountering the difficulties with the fusion protein-based RET method, an alternative strategy in which ODC protein was labeled with extrinsic dyes was pursued. We attempted the fusion protein strategy first because of the uncertainty associated with labeling a protein with an extrinsic dye. Extrinsic dyes are coupled to a reactive group, usually a thiol or amine reactive group. We used dyes coupled to an amine reactive group. A potential problem is that any of the 29 lysines plus the N-terminus of ODC could be labeled. If ten lysines are labeled, but only one is capable of transferring energy to an acceptor of the other monomer of ODC, then RET would not be detectable due to the background fluorescence of the other lysines. Nonuniform labeling represents another potential problem—one monomer could be labeled on one lysine and another monomer on a different lysine. Specific labeling can sometimes be achieved using thiol reactive dyes. Cysteines, which contain a thiol group, have a low average occurrence in proteins (<2 cysteines per protein). If the protein of interest only has two cysteines, then nonuniform labeling is less of a concern. One of the two cysteines could even by changed to a different amino acid or both could be changed and a strategically placed cysteine could be introduced. However, ODC contains 12 cysteines. Purified ODC was successfully labeled with either OG or TMR (Figure A.10), but RET was not detected.

Less than two dye molecules were estimated to react with each mole of ODC. Increasing the molar ratio of dye to protein from 20 to 100 did not significantly increase labeling of the ODC.

After encountering difficulties with the RET approach, we attempted to take advantage of the intrinsic fluorescence of ODC. ODC has significant intrinsic fluorescence from tryptophans. Studies comparing WT ODC to non-dimerizing mutants suggest that the intrinsic fluorescence of ODC as a dimer is greater than that of monomeric ODC (Figure A.12). It has also been reported that the fluorescence of PLP is enhanced when bound to proteins that use it as a cofactor (*213*). PLP fluorescence may then be different unbound, bound to a monomer and bound to a dimer and could be monitored to corroborate the tryptophan fluorescence results. However, there was no enhancement or change in fluorescence of free PLP from ODC bound PLP (data not shown).

Detecting dimerization by monitoring the intrinsic fluorescence of ODC appears to be the most promising strategy. The problems encountered with the RET strategies could inevitably be worked out. The fusion proteins could be expressed in a higher yield system, like in baculovirus- infected insect cells. However, it is still not guaranteed that the RET would occur with the fusion proteins. The addition of the fluorescent protein to ODC may prevent dimerization or one fluorescent tag may need to be on the C-terminus and the other fluorescent tag on the N-terminus of ODC for RET to occur. There have been reports published that the DsRed protein forms aggregates (*214*). Oligomerization of DsRed is required for protein fluorescence. This may have exaggerated the insolubility problems but ECFP was also insoluble and has not been reported to form

aggregates. Labeling ODC with an extrinsic probe would also likely be a viable way to detect RET. It would require identifying residues on each monomer that would be within Förster distance when the protein dimerizes but do not affect protein structure and dimerization and that could be labeled efficiently and reproducibly. Detecting dimerization by monitoring the intrinsic fluorescence of ODC appears promising, but needs more validation. The availability of other non-dimerizing mutants could provide stronger evidence that ODC dimerization enhances ODC intrinsic fluorescence. Other point mutations are known to prevent ODC dimerization and could be cloned into the appropriate vector and used for these studies. Fluorescence anisotropy could also possibly be used to monitor ODC dimerization, but this technique is more suited for smaller macromolecules than the 102 kD ODC dimer because the fluorescence lifetime of the fluor has to be comparable to the rotational correlation time of the protein. In summary, although the RET strategy would likely work with more time invested in it, detecting the dimerization state of ODC by monitoring tryptophan fluorescence is a promising strategy.

# Appendix B

## Identification of Genes Involved in ODC-Mediated Ras Transformation

### Specific Aim

To identify genes downstream of ODC that are essential for Ras transformation in NIH/3T3 cells.

## Introduction

Despite the numerous clinical trials that have investigated DFMO as a chemopreventative or chemotherapeutic, the role(s) of ODC in cell transformation is not well-understood. Identifying how ODC is involved in transformation would assist in identifying other potential drug targets—possibly targets downstream of ODC that would be more effective than targeting ODC.

A number of cell culture and animal models have shown that functional ODC is necessary for Ras-mediated transformation. ODC has been reported to be up-regulated in Ras-transformed NIH/3T3 cells (*116, 215-217*) and the transformed phenotype can be reverted with DFMO treatment (*217*) or expression of a dominant-negative ODC (*116, 217*) in the cells. Studies have provided evidence that Ras-mediated up-regulation of ODC can occur at least through the Raf/MEK/ERK (*32, 116*) and phosphoinositide 3-kinase (PI3K) (*32*) pathways downstream of Ras.

ODC induction has been shown to be necessary for oncogenic Ras transformation in several mouse models. A transgenic mouse line overexpressing a constitutively active mutant of mitogen-activated protein kinase/extracellular-signal-regulated protein kinase (ERK) kinase (MEK) in the skin from a K14 promoter were generated (K14/MEK mice) to study carcinogenesis in a pathway downstream of Ras (reviewed in (*50*)). Activation of the Raf/ERK pathway on an ICR background moderately increased hyperplasia, but by 5 weeks of age the mice developed spontaneous tumors with elevated ODC activity. Crossing the K14/MEK mice with transgenic mice overexpressing antizyme from either a

K5 or K6 promoter onto the carcinogenesis sensitive DBA/2J or resistant C57BL/6J background significantly delayed tumor incidence and reduced tumor multiplicity. Beside inhibiting and targeting ODC for degradation, antizyme does block polyamine uptake and has recently been proposed to target cyclin D1 for degradation (*45*). However, similar results were obtained when the K14/MEK mice were administered DFMO in the drinking water, suggesting that it was the effect of antizyme on ODC that was reducing susceptibility to tumor development.

The three isogenic cell lines used for these experiments, WT, HRas(61L) and ODC-dn, all are derived from NIH/3T3 mouse fibroblasts (*116*). HRas(61L) are NIH/3T3 cells stably transfected with a plasmid coding for HRas(61L)—an activated form of HRas that remains in the GTP bound state. ODC-dn cells are the HRas(61L) cells transfected with a plasmid coding for dominant-negative form of ODC which have greatly reduced ODC activity. WT cells are NIH/3T3 cells stably transfected with an empty vector.

## Methods

### *Cell Culture*

NIH/3T3, NIH/3T3 + HRas(61L) and NIH/3T3 + HRas(61L) + ODC (K69A/C360A) (referred to as WT (wild-type), HRas(61L) and ODC-dn (dominant-negative)(*116*) were cultured in complete growth medium (Dulbecco's modified Eagle's medium supplemented with 10% (v/v) fetal calf serum), 500 μg/ml geneticin (G418, Life Technologies Inc., Gaithersberg, MD) and 100 μg/ml penicillin and streptomycin and at 37 °C with 5% $CO_2$. In addition, 375 μg/ml zeocin (Invitrogen) was also added to the ODC-dn cells.

### *Growth Curves*

WT, HRas(61L) and ODC-dn cells were plated in 24-well plates (2000 cells/well) and maintained as described above. The cells were plated (time = 0 hr) and harvested at various times up to 250 hr. The cells were maintained in the same complete growth media until harvested. The cell density of the harvested cells was determined.

***Preparation of RNA for Microarray***

Cells were plated were plated in 75 cm2 flasks so that ~96 hr post-plating the cell density would be 60% of confluency at which the cells were harvested. Total RNA was harvested from the cells using a RNAqueous-Midi (Ambion, Austin, TX).

***Microarray Analysis***

Microarray analysis was performed at the Penn State Functional Genomics Core Facility (Hershey, PA). The procedure for cDNA labeling, hybridization and analysis has been previously described (*218*). Briefly, the cDNA was labeled indirectly with AlexaFluor dyes (Molecular Probes, Eugene, OR) and hybridized to epoxysilane slides (MWG Biotech, High Point, NC) spotted with a 10K Mouse Oligo Set (MWG Biotech). Data were analyzed using GeneSpring software (Silicon Genetics, Redwood City, CA). The experiment were set-up to use a direct design in which each cell line was directly analyzed by competitive hybridization against the others (i.e. HRas(61L) vs. WT, HRas(61L) vs. ODC-dn, ODC-dn vs. WT). All conditions were run in triplicate.

**Results**

Gene expression changes in the same cell as that cell progresses through the cell cycle. Therefore, gene expression would be different for a cell in linear-log growth phase than near confluency. Growth curves were determined for the three cell lines (Figure B.1). Two growth curve experiments were performed (Figure B.1 shows one representative curve) and the average doubling times were determined for the linear-log growth phase. The growth curves are consistent with expected results; the transformed HRas(61L) cells have a shorter doubling time (27 hr) than the WT (29 hr) and ODC-dn (31 hr) cells which correlates with the higher ODC activity of the HRas(61L) cells (*116*). The HRas(61L) cells are capable of growing to a higher density than the untransformed cells—likely because transformed cells are not contact inhibited.

The phenotype of these cell lines have been previously characterized based on morphology and anchorage independent growth (*116*). Expression of the activated HRas(61L) transformed the NIH/3T3 cells, but co-expression of the dominant-negative ODC reversed the transformed phenotype. The change in phenotype is easily observed by viewing the cells under a microscope. The HRas(61L) cells form foci and are not contact inhibited (Figure B.2). The WT and ODC-dn cells appear flat and spread out on the plate.

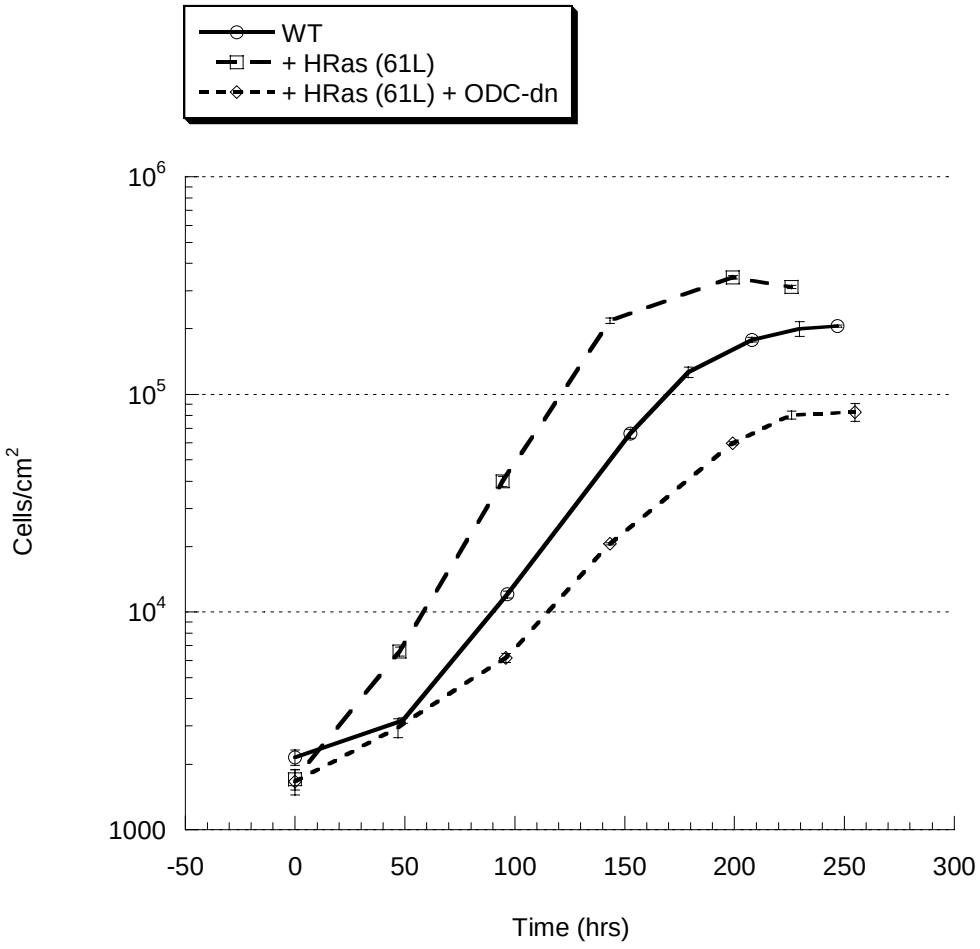


**Figure B.1***: Growth Curves.*

Cells were plated at the same density and allowed to grow for up to 250 hr without a change of media. Error bars represent standard deviation. $n \geq 3$.

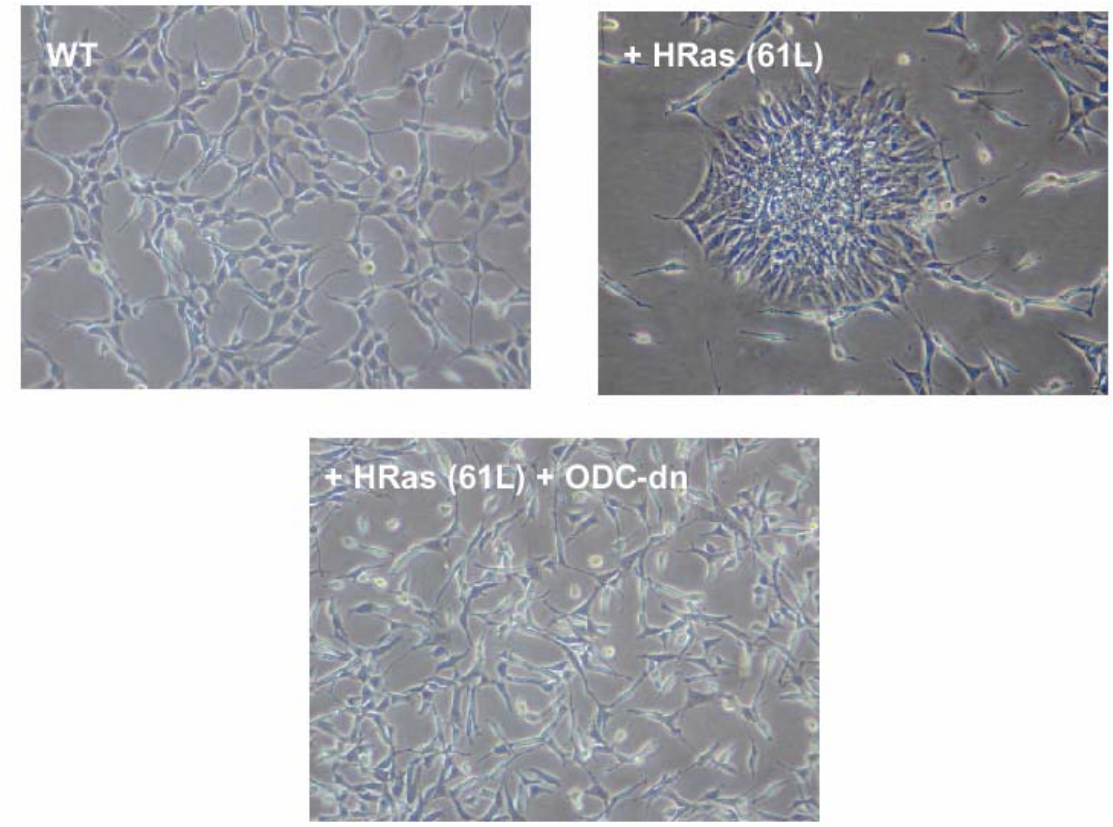


**Figure B.2***: Light Micrographs of the Cell.*

WT NIH/3T3 cells grow normally, but the HRas(61L) cells form foci, a trait of transformed cells. The dominant-negative ODC [+HRas (61L) + ODC-dn] reverts the transformed phenotype back to a phenotype similar to WT NIH/3T3 cells..

All three cell lines were grown for ~94 hr and the cells were harvested at ~60% confluency. Total RNA used for the generating labeled cDNA was of very high quality with no detectable degradation. The labeled cDNA derived from each cell line were directly hybridized against each other in triplicate to increase the statistical power of the data. There are many ways and levels to analyze the microarray results. The data was initially sorted to search for genes that fit a trend. Figures B3 and B4 show genes that are either up-regulated or down-regulated by HRas(61L) relative to both WT and ODC-dn cells, but where there was no change in expression of these genes between ODC-dn and WT cells. In other words, these are the genes that were changed in HRas(61L) transformed cells but in ODC-dn cells, these genes reverted back to the same expression level of WT cells. The three labels on the x-axis designate the two cell lines that were compared to one another (in a X vs. Y format where X is the numerator and Y is the denominator). The ratio of gene expression for each comparison is displayed on the y-axis. For example, Ral-Interacting Protein 1 (RIP1) was up-regulated 1.23-fold in the HRas (61L) cells versus WT cells. There was no change in RIP1 in ODC-dn cells versus WT cells (ratio = 1.02) and RIP1 was up-regulated 1.21-fold in HRas(61L) cells versus ODC-dn cells. Therefore, expressing the activated HRas mutant (61L) in the WT 3T3 cells induces RIP1 gene expression and RIP1 expression can be returned to WT levels by expressing the dominant-negative ODC.

Twenty-one and 10 genes were found to be up-regulated and down-regulated, respectively, by HRas (61L) that were reverted to levels similar to WT cells in the ODC-dn cells (Figure B.3, B.4). The change in gene expression level for all listed genes is statistically significant based upon the data obtained from the three replicate microarrays.

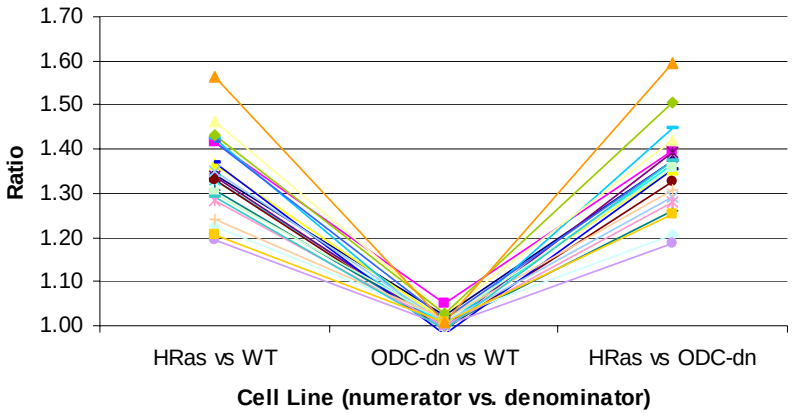


| HRas vs WT | ODC-dn vs WT | HRas vs ODC-dn | Gene |
|---|---|---|---|
| 1.34 | 1.02 | 1.38 | BREAST CANCER ANTI-ESTROGEN RESISTANCE 3 |
| 1.42 | 1.05 | 1.40 | HOMOLOG TO DJ202I21.1 (NOVEL PROTEIN) (CDNA FLJ11101 FIS |
| 1.37 | 1.01 | 1.35 | U1 SMALL NUCLEAR RIBONUCLEOPROTEIN 1C |
| 1.33 | 1.01 | 1.37 | RIKEN CDNA 1110036H21 |
| 1.34 | 0.99 | 1.39 | HYPOTHETICAL PROTEIN |
| 1.33 | 0.99 | 1.33 | CALPASTATIN |
| 1.31 | 1.00 | 1.26 | VASODILATOR-STIMULATED PHOSPHOPROTEIN |
| 1.37 | 0.98 | 1.35 | MANNOSIDASE 2 |
| 1.42 | 0.99 | 1.45 | ACETYLCHOLINE RECEPTOR BETA 2 NEURAL |
| 1.23 | 1.02 | 1.21 | RAL-INTERACTING PROTEIN 1 |
| 1.30 | 1.01 | 1.36 | MYOMESIN 2 |
| 1.46 | 1.03 | 1.42 | UNCLASSIFIABLE |
| 1.35 | 1.01 | 1.29 | DROSOPHILA NK2 TRANSCRIPTION FACTOR RELATED |
| 1.28 | 1.00 | 1.28 | DATA SOURCE:SPTR |
| 1.19 | 1.00 | 1.19 | EXPRESSED SEQUENCE AA408026 |
| 1.24 | 1.01 | 1.31 | NIDOGEN 2 |
| 1.42 | 1.02 | 1.37 | SIMILAR TO MDGL-1 |
| 1.29 | 0.99 | 1.37 | HYPOTHETICAL PROTEIN |
| 1.43 | 1.03 | 1.51 | TUMOR NECROSIS FACTOR RECEPTOR SUPERFAMILY |
| 1.21 | 1.01 | 1.25 | OLIGODENDROCYTE TRANSCRIPTION FACTOR 1 |
| 1.56 | 1.01 | 1.60 | STAUFEN (RNA BINDING PROTEIN) HOMOLOG 1 (DROSOPHILA) |

**Figure B.3**: *Microarray Analysis: HRas(61L) Up-Regulated Genes.*
Genes up-regulated by HRas(61L) that revert to WT levels in ODC-dn cells.

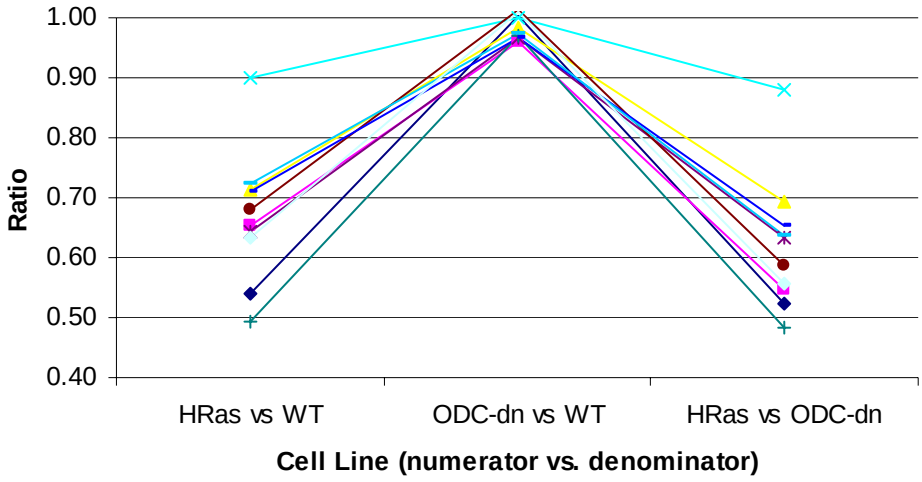


| HRas vs WT | ODC-dn vs WT | HRas vs ODC-dn | Gene |
|---|---|---|---|
| 0.54 | 1.00 | 0.52 | TESTIS EXPRESSED GENE 261 |
| 0.65 | 0.96 | 0.55 | G PROTEIN-COUPLED RECEPTOR 35 |
| 0.71 | 0.98 | 0.69 | NEUROPEPTIDE Y RECEPTOR Y1 |
| 0.90 | 1.00 | 0.88 | RIKEN CDNA 2610524G09 |
| 0.64 | 0.97 | 0.63 | TISSUE-TYPE VOMERONASAL NEURONS PUTATIVE PHEROMONE RECEPTOR V2 |
| 0.68 | 1.01 | 0.59 | CARBOXYLESTERASES TYPE-B CONTAINING PROTEIN DATA SOURCE:INTERPRO |
| 0.49 | 0.97 | 0.48 | ANK REPEAT CONTAINING PROTEIN DATA SOURCE:PFAM |
| 0.71 | 0.97 | 0.65 | HOMOLOG TO HSPC219 |
| 0.72 | 0.97 | 0.64 | MEMBRANE PROTEIN |
| 0.63 | 1.01 | 0.56 | PROTOCADHERIN 7 |

**Figure B.4**: *Microarray Analysis: HRas(61L) Down-Regulated Genes.*
Genes down-regulated by HRas(61L) that revert to WT levels in ODC-dn cells.

**Discussion**

Genes that may potentially cooperate with Ras and ODC to transform cells were identified by this initial microarray analysis. For example, RIP1 (Ral-Interacting Protein 1) is upregulated in HRas(61L) cells and reverts to WT level in ODC-dn cells. RAL is a Ras-like GTPase, and although initially not believed to be as instrumental in cancer as Ras, more recent data establishes a unique role of RAL-A in Ras-mediated metastasis (*219*). The parameters for filtering the data were very stringent and likely excluded other genes that may potentially be involved in ODC-mediated Ras transformation. The data was filtered for genes that were expressed at the same level in WT and ODC-dn cells relative to HRas(61L). For example, if a gene X was up-regulated 1.5-fold in HRas(61L) cells relative to WT and up-regulated 3-fold in HRas(61L) cells relative to ODC-dn (i.e. ODC-dn reverted the expression of that gene), then this gene would not show up in this analysis. Because the relative expression of gene Y is the same for WT and ODC-dn cells relative to HRas does not make gene Y a stronger candidate than gene X to be involved in ODC-mediated Ras transformation. Likewise, genes that change expression in HRas(61L) relative to ODC-dn but do not change in HRas(61L) relative to WT should not be overlooked.

The strength of this experiment lies in the set-up. First, isogenic cell lines were used. This minimizes differential gene expression due to different cell types. Secondly, triplicates were performed. Thirdly, we used a direct design—that is, all possible combinations were competitively hybridized against each other (i.e. A vs. B, B vs. C, A vs. C) so no indirect comparisons were made. This lowers the average variance thereby

increasing the statistical power of the results. Comparison of genes in the ODC-dn cells that revert back to toward WT levels may provide clues to genes that are important in transformation. But as mentioned above, genes that do not meet this criteria may be important in mediating transformation and will not be excluded from the analysis.

Future analysis will include a more thorough examination of the data and a comparison of the data to the previous microarray experiment that we performed on samples from the same cell lines. Differential gene expression in gene families or pathways may lend insight into identifying relevant genes. Genes deemed mostly likely to be differentially expressed, based on statistics, and most interesting, based on gene function, will be validated by quantitative real-time PCR. Differential protein expression can then be assessed by western blotting (if antibodies are available). To determine whether the identified genes play a role in ODC-mediated Ras transformation, the HRas(61L) cells could be transfected with an siRNA against select genes to determine if knockdown of the gene could revert the transformation similar to ODC-dn.

## Appendix C

## LIST OF ABBREVIATIONS

| | |
|---|---|
| AcSpd | $N^1$-acetylspermidine |
| AcSpm | $N^1$-acetylspermine |
| AdoMet | *S*-adenosylmethionine |
| AdoMetDC | *S*-adenosylmethionine decarboxylase |
| AG | anaplastic gliomas |
| Ago | arogonaute |
| AK | actinic keratosis |
| AS-ODNs | antisense oligodeoxynucleotides |
| BCC | basal cell carcinomas |
| b-HLH-Zip | basic helix-loop-helix-leucine zipper |
| CMV | cytomegalovirus |
| dcAdoMet | decarboxylated *S*-adenosylmethionine |
| DETA/NO | (Z)-1-[N-(2-aminoethyl)-N-(2-aminoethyl)-amino]-diazen-1-ium-1,2-diolate |
| DFMO | α-difluoromethylornithine |
| dITRZ | double internal, *trans*-acting hammerhead ribozymes |
| DMBA | 7,12-dimethylbenz(*a*)anthracene |
| ds | double-stranded |
| DsRed | red fluorescent protein isolated from an IndoPacific sea anemone-relative, *Discosoma sp* |

| | |
|---|---|
| ECFP | enhanced cyan fluorescent protein |
| eflornithine | α-difluoromethylornithine (DFMO) |
| ERK | extracellular-signal-regulated protein kinase |
| FRET | fluorescence resonance energy transfer |
| GBM | glioblastoma multiforme |
| HDV | hepatitis delta virus |
| HEK 293 cells | human embryonic kidney cells |
| K5, 6 or 14 | human cytokeratin 5, 6 or 14 promoter |
| KIR | inwardly rectifying $K^+$ |
| LNA | locked nucleic acids |
| LSCM | laser scanning confocal microscopy |
| *MDR-1* | multidrug resistance |
| MEK | mitogen-activated protein kinase/extracellular-signal-regulated protein kinase kinase |
| miRNA | micro RNA |
| miRNP | miRNA-containing effector complex |
| MR | molar ratio |
| MTA | 5'-methyl thioadenosine |
| NER | nucleotide excision repair |
| NMBA | *N*-nitrosomethylbenzylamine |
| NMDA | *N*-methyl-D-aspartate channel |
| NMSC | nonmelanoma skin cancers |
| NO | nitric oxide |

| | |
|---|---|
| ODC | ornithine decarboxylase |
| ODNs | oligodeoxynucleotides |
| ODQ | 1H-(1,2,4)oxadiazolo[4,3-α]quinoxalin-1-one |
| OG | Oregon green |
| ORF | open reading frame |
| P2 cells | NIH/3T3 + pMV7eIF4E cells |
| PAO | polyamine oxidase |
| PGA | physician's global assessment |
| PI3K | phosphoinositide 3-kinase |
| PKCε | protein kinase Cε |
| PLP | pyridoxal-5'-phosphate |
| *PTCH* | tumor suppressor gene patch |
| RET | resonance energy transfer |
| RISC | RNA-induced silencing complex |
| SELEX | Systematic Evolution of Ligands by EXponential enrichment |
| SCC | squamous cell carcinomas |
| siRNA | small interfering RNA |
| SNAP | *S*-nitroso-*N*-acetylpenicillamine |
| SSAT | spermidine-spermine $N^1$-acetyltransferase ( |
| ß-galactosidase | ß-galactosidase |
| $t_{1/2}$ | half-life |
| TMR | tetramethylrhodamine |

| | |
|---|---|
| TPA | 12-*O*-tetradecanoylphorbol-13-acetate |
| UTR | untranslated region |
| Vaniqa | α-difluoromethylornithine HCl, 13.9% |
| Vitravene | formiversen |
| VS | *Neurospora* Varkud satellite |
| WT | wild-type |
| XP | Xeroderma pigmentosum |

# VITA

## Joseph M. Ackermann

## Education

| | |
|---|---|
| 2005 | **Doctor of Philosophy**, Department of Pharmacology<br>Pennsylvania State University College of Medicine, Hershey, PA |
| 2002 | **Master of Business Administration**<br>Pennsylvania State University, Middletown, PA |
| 1997 | **Bachelor of Science**, Department of Biology and Biotechnology<br>Worcester Polytechnic Institute, Worcester, MA |

## Publications

**Ackermann, J. M.**, Kanugula, S., and Pegg, A. E. (2005) DNAzyme-Mediated Silencing of Ornithine Decarboxylase, *Biochemistry 44*, 2143-52.

**Ackermann, J. M.,** Pegg, A. E., and McCloskey, D. E. (2003) Drugs affecting the cell cycle via actions on the polyamine metabolic pathway, *Prog. Cell Cycle Res. 5*, 461-8.

Chauret, N., Dobbs, B., Lackman, R. L., Bateman, K., Nicoll-Griffith, D. A., Stresser, D. M., **Ackermann, J. M.**, Turner, S. D., Miller, V. P., and Crespi, C. L. (2001) The use of 3-[2-(N,N-diethyl-N-methylammonium)ethyl]-7-methoxy-4-methylcoumarin (AMMC) as a specific CYP2D6 probe in human liver microsomes, *Drug Metab. Dispos. 29*, 1196-200.

Busby, W. F., Jr., **Ackermann, J. M.**, and Crespi, C. L. (1999) Effect of methanol, ethanol, dimethyl sulfoxide, and acetonitrile on *in vitro* activities of cDNA-expressed human cytochromes P-450, *Drug Metab. Dispos. 27*, 246-9.